Improving the spatial representation of basin hydrology and flow processes in the SWAT model

Dissertation

zur Erlangung des Doktorgrades
der Mathematisch-Naturwissenschaftlichen Fakultät
der Christian-Albrechts-Universität zu Kiel

vorgelegt von

Hendrik Rathjens

Kiel, 2014

Erste Gutachterin: Prof. Dr. Natascha Oppelt

Zweiter Gutachter: PD Dr. Martin Volk

Tag der mündlichen Prüfung: 04.02.2014

Zum Druck genehmigt: 04.02.2014

gez. Prof. Dr. Wolfgang J. Duschl, Dekan

Absctract

Hydrologic models are essential tools for examining the impact of land use on hydrology and water quality. These models are used for watershed management and have proven to be effective tools for assessing water resource and nonpoint-source pollution problems for a wide range of scales and environmental conditions. Modeling efforts to assess the effectiveness of management practices and conversion measures on water quality and attempts to assess the impacts of global change on water processes have put increasing pressure on the accuracy of hydrologic models. Currently, identifiable barriers to the use of such models are the quality and spatial resolution of the input data, as well as the accuracy of the physical representation of the hydrologic processes within the model. The recurring problem is the discretization of the watershed to best represent watershed processes while, at the same time, not exceeding the limitation of available data and computational time requirements. However, integrated river basin models should provide a spatially distributed representation of basin hydrology and transport processes to allow for spatially implementing specific management and conservation measures.

The currently insufficient implementation of spatially varying processes in many hydrologic models indicates a strong need for research to better represent these processes. Therefore, this dissertation aims at the incorporation of greater spatial detail regarding the spatial distribution of processes and data into the publicly available eco-hydrologic watershed model SWAT (Soil and Water Assessment Tool). To achieve this, the model was enhanced with focus on (1) developing an interface for setting up SWAT in a grid-based discretization scheme, (2) developing spatially distributed routing capabilities between grid cells, and (3) improving the availability and quality of spatial SWAT input data.

The enhanced model was tested by examining SWAT hydrology response at the watershed and grid scale. Also, the most important sources of model error were identified and changes in the temporal resolution and spatial accuracy of land use input data were quantified. To this end, the new model was applied to the Lake Fork catchment (556 km^2, Texas, USA), the Bünzau catchment (210 km^2, Schleswig-Holstein, Germany), and the Little River watershed (334 km^2, Georgia, USA). Results indicate that the new model performs well with regard to streamflow and water balance at the watershed and grid scale.

The results of this dissertation suggest that the incorporation of more spatial detail into the SWAT model by using a grid-based discretization scheme, routing capabilities between grid cells, and temporally and spatially more accurate data will provide a more realistic basis for water quantity and quality simulations. By developing spatially distributed hydrologic algorithms, testing the applicability of the enhanced model, and identifying the main sources of uncertainty, this dissertation laid the groundwork for further research in spatially distributed hydrologic simulations required for water basin management (e.g. identifying non-point source pollutions).

Kurzfassung

Die Qualität von Gewässern unterliegt einer Vielzahl unterschiedlicher Einflüsse. Um die Auswirkungen menschlichen Handelns auf die Wassermenge und -qualität abschätzen zu können, werden Wasserhaushaltsmodelle als Unterstützungswerkzeuge für ein integriertes und nachhaltiges Management von Wasserressourcen genutzt. Belastungen von Gewässern ergeben sich zum einen aus Punktquellen (z.B. industrielle Einleitungen) und zum anderen aus diffusen Quellen (z.B. landwirtschaftliche Tätigkeiten). Während Punktquellen leicht zu lokalisieren sind, erfordert die Identifikation diffuser Eintragspfade eine detaillierte und räumlich differenzierte Betrachtung.

Um solch eine räumlich differenzierte Betrachtung mit Modellen zu gewährleisten, ist es erforderlich, die in den verschiedenen Landschaften auftretenden hydrologischen Prozesse und Stofftransportmechanismen zu berücksichtigen. Die Herausforderung bei der Entwicklung geeigneter Modelle besteht in der Findung eines Kompromisses zwischen einer möglichst realistischen räumlichen Prozessbeschreibung, einer limitierten Menge an zur Verfügung stehenden Modelleingabedaten und einer möglichst geringen Rechenzeit. Modellergebnisse sind generell mit hohen Unsicherheiten verknüpft. Das lässt sich zum einen auf die nur unzulänglich verfügbaren Messdaten, die zur Parametrisierung, Kalibrierung und Validierung des Modells benötigt werden, zurückführen. Zum anderen trägt die häufig stark vereinfachte und ungenaue Beschreibung der hydrologischen Prozesse zu den Modellunsicherheiten bei. Die vorliegende Dissertation beschäftigt sich daher sowohl mit der Verbesserung der geographischen Datenbasis als auch mit der Weiterentwicklung der räumlichen Abbildung von Prozessen für das öko-hydrologische Modell SWAT (Soil and Water Assessment Tool). Dazu wurde eine auf Rasterzellen basierte Version von SWAT entwickelt, welche hydrologische Transport- und Austauschprozesse zwischen den Rasterzellen beinhaltet. Außerdem werden methodische Ansätze vorgestellt, die die Qualität und zeitliche Verfügbarkeit von räumlichen Landnutzungsdaten verbessert.

Das im Rahmen der Dissertation modifizierte Modell wurde im Lake Fork Einzugsgebiet (556 km^2, Texas, USA), im Einzugsgebiet der Bünzau (210 km^2, Schleswig-Holstein, Deutschland) und im Little River Einzugsgebiet (334 km^2, Georgia, USA) angewandt, um Abfluss und Wasserbilanzen abzubilden und die wichtigsten Ursachen für Unsicherheiten in den Modellergebnissen zu identifizieren. Die Ergebnisse zeigen, dass die Weiterentwicklungen des Modells gute Simulationsergebnisse in den untersuchten Einzugsgebieten liefern. Die wesentlichen Verbesserungen des Modells ergeben sich dabei aus einer räumlich detaillieren Beschreibung der hydrologischen Prozesse in SWAT.

Die Ergebnisse dieser Arbeit deuten darauf hin, dass eine verbesserte geographische Datenbasis und eine auf Rasterzellen basierte Version von SWAT, in der Wasser- und Stoffflüsse zwischen den Rasterzellen berücksichtigt werden, zu einer realistischeren räumlichen Prozessbeschreibung führen. Die vorliegende Dissertation stellt somit die Grundlage zur räumlich differenzierten hydrologischen Modellierung mit SWAT dar und leistet einen Beitrag zur Entwicklung eines integrierten Ansatzes zum effizienten und nachhaltigen Management von Wasserressourcen in Flussgebietseinheiten.

Contents

List of Figures

List of Tables

Chapter 1

Introduction

1.1 Motivation

During the past decades the awareness of the value of water increased, which is reflected in a growing competition for limited fresh water resources among agriculture, urban and industrial uses, fisheries and recreation (Sabatier et al., 2005). The increasing governmental and public awareness of water pollution and environmental problems led to the passage of the Clean Water Act (CWA) in the USA in 1972 and the Water Framework Directive (WFD) in the European Union in 2000, both of which aim at watershed-based restoration of water quality. The CWA as well as the WFD stimulated substantial reductions in point-source pollution of lakes, rivers, wetlands, estuaries, coastal waters, and groundwater (e.g., Hering et al., 2010; Copeland, 2012). However, efforts to control pollution from diffuse (i.e. non-point) sources are still ongoing. Data reported by the European Commission and the U.S. Environmental Protection Agency indicate the demand for substantial efforts in restoration: 60 % of European (Hering et al., 2013) and 44 % of U.S. rivers (U.S. Environmental Protection Agency, 2006) do not meet the specified water quality standards.

Both the CWA and the WFD require an integrated river basin management plan to reduce non-point source pollution. They aim at the process of creating and implementing plans, programs, and projects to sustain and enhance watershed functions that affect the plant, animal and human communities within a watershed (Copeland, 2010; Hering et al., 2010). Therefore, integrated river basin management should include water supply, water quality, drainage, stormwater runoff and flood protection, and the overall planning and utilization of watersheds. Landowners, government agencies, and environmental scientists play an integral part in the management of a watershed (e.g., Sabatier et al., 2005).

A key component of integrated and sustainable watershed programs is the identification of pollutants and possible remedies. While point sources are easy to locate, diffuse sources are more difficult to assess due to their extensive spatial occurrence and their temporal variability depending on a number of factors including climate and land use (Carpenter et al., 1998; Ouyang et al., 2010b). Strategies to reduce non-point source pollution are mostly identified by examining the feasibility of implementing various best management practices (BMPs) and assessing their impact on pollutant loading (Bosch et al., 2004). European and U.S. projects accomplished this assessment through environmental monitoring and modeling of the physical processes within a watershed (e.g., Volk et al., 2009; White et al., 2010). Field experiments and observations are time-consuming and costly. The use of models facilitates timely and cost-effective quantification of the impacts of land use and management practices on water quantity and quality. Also, models can help to identify Critical Source Areas (CSA) within a watershed where the implementation of BMPs to improve the state of water resources needs to focus on (Arabi et al., 2006; White et al., 2009).

Watershed based models that take possible land use and management scenarios into account can be helpful in determining measures to achieve a target ecological status of a catchment (e.g., Born and Sonzogni, 1995; Krause et al., 2008; Prodanovic and Simonovic, 2010). They are valuable tools for examining the impact of land use on hydrology and water quality. Examples of such watershed models are AGNPS (Young et al., 1989), HSPF (Bicknell et al., 1996), GWLF (Haith and Shoenaker, 1987), MIKE-SHE (Refsgaard, 1997), SWAT (Arnold et al., 1998), SWIM (Krysanova et al., 2005), and WaSiM (Schulla, 2012). Overviews of different eco-hydrological models are given in Volk and Steinhardt (2001), Krysanova and Haberlandt (2002), Horn et al. (2004), and Arnold and Fohrer (2005). Models used in the context of integrated river basin management are required to provide information on a wide range of hydrologic aspects, which cannot be achieved by using individual groundwater, water quality, or erosion models (e.g., Seppelt et al., 2009). Therefore, water basin management requires spatially distributed and process-oriented models. These models typically need more data, are more sophisticated in structure, but allow more insight into the system behavior than simple conceptual approaches (Blöschl and Sivapalan, 1995). However, Volk et al. (2009) stated that experiences of different European and national projects dealing with the model-supported implementation of the WFD revealed that the available models are "still far from being suitable for operational applications".

A key task of integrated river basin management is the identification of CSAs and assessing the impact of BMPs on pollutant loading within a watershed (e.g., White et al., 2009), which is mainly accomplished through monitoring and modeling hydrologic processes. The primary transport mechanism of many environmental contaminants is

through water flow. Therefore, the accurate simulation of the hydrology of a watershed is a prerequisite for accurate contaminant transport modeling. Rinaldo et al. (1991) and Saco and Kumar (2002) demonstrated that it is more realistic to use spatially varying parameters to represent the different flow processes. In this context Volk (2010) stated that from the management perspective, a landscape with a defined extent represents the suitable scale for the planning of sustainable development. Integrated river basin models should represent landscape processes to allow for implementing specific management and conservation measures. For this, they require accurate spatial and temporal data. Ideally, processes should be observed and modeled at the temporal and spatial scale they occur. In practice, however, process, observation, and model scale do not match; the modeling scale is often orders of magnitude larger or smaller than the observation or management scale (Blöschl and Sivapalan, 1995). Each scale level has specific dominant processes, data requirements, and controlling factors. Hence, the accuracy of the physical representation of the hydrological processes within the model at the scales relevant for planning should be evaluated carefully, before recommendations for conservation measures or land use options are given based on model results. The question, however, remains whether data necessary to describe these processes are available. Hence, consideration of the accuracy of the methods and data used for modeling as well as examination of the sensitivity of the methods used to input data variation is required (e.g., Jha et al., 2004; Romanowicz et al., 2005; Volk, 2010).

Reliable model simulations at multiple scales and locations can be obtained only if the model was validated and conceptualized for the scale at which it is applied and if a scale-specific, robust parameterization method is employed (Kumar et al., 2013). Klemeš (1983) and Blöschl and Sivapalan (1995) give a detailed framework for scaling and scale issues in hydrology. They demonstrate that hydrologic processes occur over a wide range of scales of approximately eight orders of magnitude in space and time. The processes range from unsaturated flow in a 1 m soil profile to floods in river systems of a million square kilometers, from flashfloods of several minutes duration to flow in aquifers over hundreds of years. Runoff generation associated with rainfall intensities exceeding infiltration capacities (i.e. infiltration excess overland flow) is a point phenomenon that is related to very small spatial scales. Saturation excess runoff is an integrating process that is dependent on topographic, land use and soil characteristics and thus needs a certain area to occur. Channel flow operates at scales ranging from a channel initiation area up to the extent of large river basins (Jaeger et al., 2007). The time delay of hydrologic processes increases as the water passes through the subsurface and the main temporal scale of a basin clearly depends on the dominant runoff mechanisms (Blöschl and Sivapalan, 1995). Infiltration excess overland flow response is very fast (< 30 minutes), while saturation excess overland flow responds typically slower because

the soil has to be saturated before runoff occurs. Subsurface flow is often significantly slower, with response times of a day or longer for the same catchment size. Finally, groundwater-controlled flows are associated with time scales from months to hundreds of years (e.g., Dunne et al., 1975). There is, however, a relationship between spatial and temporal scales of hydrologic processes. Small spatial scales tend to be related to small temporal scales and the same applies to large spatial and temporal scales. According to Dooge (1986) and Blöschl and Sivapalan (1995) typical modeling scales in space are the local scale or 'point' scale (1 m), the hillslope scale (100 m), the catchment scale (10 km) and the regional scale (1000 km). Common scales in time are the event scale (1 day), the seasonal scale (1 year), and the long-term scale (100 years).

As hydrologic processes relevant for river basin management act at multiple scales in space and time, modelers have to make compromises between the accuracy desired, the computation time, and the availability of data. Simulating non-linear processes such as precipitation, infiltration, and runoff requires hourly or daily time steps, whereas for seasonal or annual predictions monthly steps are appropriate. The possible degree of spatial resolution ranges from highly aggregating approaches in which the study area is divided into a few sub-units with similar properties (lumped models) to models which take as much variability of spatial characteristics into account as possible (distributed models). The scope of distributed models has increased during the past years in accordance with the requirements for river basin management, the development of faster computers, and the increasing availability of geographic data sets (Volk et al., 2001; Volk, 2010). The appropriate spatial resolution and discretization method depends, however, on the purpose of modeling and the availability of data sources (Bennett et al., 2013). If the modeler's aim is the simulation of aggregated events (e.g., monthly values at the watershed outlet) in a data scarce area a lumped approach may be adequate. But if the modeler's scope is a spatial description of a hydrologic system (e.g., detection of critical source areas) a spatially distributed model is recommended, because spatial patterns of topography and subsurface characteristics often exert significant control over hydrological processes within a watershed (Schulz et al., 2006). Therefore, integrated river basin management requires models that are able to represent runoff and infiltration processes that occur in different parts of the landscape. Despite their wide range of scales, hydrologic processes that are crucial for river basin management are typically related in response to precipitation. These processes can be accounted for by eco-hydrologic models that operate at the landscape or hillslope scale and use a daily time step.

Currently identifiable barriers for the use of models for river basin management are the quality and spatial resolution of the input data, and the accuracy of the physical representation of the hydrological processes within the model (Arnold et al., 2010). In river basin management, models are required to contribute information on a wide

range of processes related to hydrology and water quality, which cannot be provided by individual groundwater, water quality or erosion models (Volk et al., 2009). The eco-hydrological watershed-based Soil and Water Assessment Tool (SWAT, Arnold et al., 1998) was found to be suitable for simulating hydrologic processes in the context of integrated river basin management, even though further testing and improvement is necessary (e.g., Horn et al., 2004; Volk et al., 2009). In particular, model revision is required by (1) enhancing the spatial representation of hydrology and flow transport processes within a watershed (Gassman et al., 2007), and (2) providing model input data in the desired spatial and temporal resolution (e.g., Arnold et al., 2010). Hence, this dissertation aims at improving the spatial representation of basin hydrology and flow processes in the SWAT model.

1.2 Materials and Methods

1.2.1 The SWAT model

The eco-hydrological model SWAT has proven to be a useful modeling tool for a wide range of scales and environmental conditions. Over the past decade SWAT has been used worldwide to estimate anthropogenic, climate and other impacts on water resources. Besides numerous applications in the U.S., SWAT has also been used extensively in Europe. In the literature many specific SWAT applications have been reported. Arnold and Fohrer (2005) and Gassman et al. (2007) summarized many of these. Numerous applications exist using the outlet gauge discharge data for calibration and validation purposes. They range from hydrologic and water resource assessments (water discharge, groundwater dynamics, soil water, snow dynamics, and water management) through water quality (land-use and land-management change in agriculture), climate change impacts, and pollutant assessments (Gassman et al., 2007; Krysanova and Arnold, 2008). Furthermore, SWAT can account for the effects of best management practices (Arabi et al., 2006), identify critical source areas (e.g., White et al., 2009) and has shown its capability to adequately represent general trends of water quality changes resulting from various measures based on land use and management change (e.g., Fohrer et al., 2005).

SWAT is a physically based watershed-scale model, developed to simulate the impact of land management practices on the water cycle, the flow of sediment, the nutrient cycle and the behavior of pesticides and bacteria in complex watersheds. All model calculations are carried out in daily time steps, whereas the model output can be obtained at a daily to annual time scale (Arnold et al., 2013). Recent versions of the model also provide for simulations on an hourly time step, if hourly precipitation data is available.

The model divides the hydrology of a watershed into two major phases. (1) The land phase of the hydrologic cycle controls the quantitative flow of water, sediment, nutrients and pesticides entering the reach allocated to the sub-watershed. (2) The routing phase determines the movement of water through the channel network of the watershed to its outlet using either a variable storage coefficient method (Williams, 1969) or the Muskingum routing method (e.g., Linsley et al., 1982).

Simulated hydrologic processes in the land phase include surface and subsurface flow mechanisms. Calculation of surface runoff is performed using either the SCS (Soil Conservation Services) curve number (Soil Conservation Service Engineering Division, 1972) or Green and Ampt (Green and Ampt, 1911) infiltration equation. Lateral subsurface flow in the soil profile is calculated with a kinematic storage model estimated simultaneously with percolation. Groundwater flow from shallow aquifers to streams is simulated by creating a shallow aquifer storage using the classic linear tank storage model (Brutsaert, 2005). SWAT offers using either the Hargreaves (Hargreaves and Samani, 1985), the Priestley-Taylor (Priestley and Taylor, 1972), or the Penman-Monteith (Monteith, 1965) method for estimating evapotranspiration. Further model components include snow melt, transmission losses from streams, and water storage and losses from ponds. A detailed description of all components can be found in Arnold et al. (1998) and Neitsch et al. (2011b).

Setting up a watershed simulation requires definition of the spatial arrangements of the watershed's elements (e.g., sub-watersheds, reach segments, or point sources). SWAT is a semi-distributed model and the primary discretization technique used within SWAT is the sub-watershed configuration. Based on the surface topography defined by a digital elevation model (DEM), the model divides the watershed into sub-watersheds. The sub-watersheds are further subdivided into hydrological response units (HRUs) to account for heterogeneity in slope, soil type and land use. HRUs are lumped areas within a sub-watershed with a unique combination of slope class, soil type and land use (Neitsch et al., 2011b). They represent percentages of the sub-watershed area and are not spatially related to one another. This aggregation of land use or soil type maps implies a loss of spatial information during modeling, which might be important when studying diffuse matter transport in agricultural areas. SWAT is not able to model flow and transport from one landscape position to another prior to entry into the stream. Therefore, the classic HRU concept fails to simulate interactions between HRUs and is not able to represent spatial distributions of hydrologic processes that typically occur in landscapes. Efficient river basin models should, however, link upstream and downstream parts of a river basin. Hence, the non-spatial character of the HRUs and the inability to model transport processes in the land-phase of the hydrologic cycle have been identified as key

weaknesses of the model (e.g., Gassman et al., 2007; Arnold et al., 2010; Bosch et al., 2010).

To overcome these shortcomings and to fulfill the requirements for river basin management, SWAT has recently been enhanced by developing routing capabilities between landscape units (Volk et al., 2007; Arnold et al., 2010). The new SWAT landscape version simulates flow and transport processes between three landscape units (divide, hillslope, and floodplain) within a sub-watershed; surface runoff, lateral subsurface flow, and shallow groundwater flow is routed between these landscape units in the land phase of the hydrologic cycle. The landscape model significantly improves spatial representation of basin hydrology (Arnold et al., 2010; Bosch et al., 2010) and is able to capture channel and landscape flow processes related to specific landscape positions. The model was evaluated by Bosch et al. (2007a), Volk et al. (2007), Arnold et al. (2010), and Bosch et al. (2010). They concluded that simulated daily stream flow at the watershed outlet after routing across the landscape units compared well to measured flow. However, they also stated that additional development and testing of the landscape flow module is necessary to realistically represent spatial distributions of flow and transport processes within a watershed.

Using the SWAT landscape model together with a grid-based approach instead of the sub-watershed discretization would incorporate even more spatial detail into the SWAT model. A grid-based discretization avoids the aggregation of geographical datasets and preserves spatial information. There are, however, advantages and disadvantages for both the grid and the commonly used HRU method. The HRU approach used in the current landscape model provides a fast and numerically efficient model, but leads to a loss of flow paths and spatial information during modeling. The combination of the grid configuration and the new landscape model results in a fully distributed SWAT model that preserves spatial information and enables the model to simulate the impact of management practices (e.g., conservation measures) implemented in specific landscape positions on plant growth, crop yields, and runoff in full spatial detail.

1.2.2   Land use data

The anthropogenic factor land use affects the interactions between water, soil, geomorphology, and vegetation on several spatial and temporal scales in different manners and intensities. Land use acts as an interface between natural and socio-economic systems and is one parameter that controls the landscape water balance (Steinhardt and Volk, 2001). Information about the impact of land use changes on the functions of watersheds provides knowledge for the development of sustainable land use concepts (Volk, 2010).

Therefore, the effect of land use patterns on hydrologic processes should be evaluated (Lorz et al., 2007).

The quality, spatial resolution and temporal availability of model input data can compromise the use of spatially distributed models for river basin management (Beven and Freer, 2001). There are, however, numerous studies where hydrological models are applied successfully for simulating the influence of land use on catchment hydrology. Hörmann et al. (2005) give an overview of the prospects and limitations of eco-hydrological models for the evaluation of land use options in mesoscale catchments. Mostly, scenarios based on assumptions of climatic change or the influence of political decisions are investigated (Volk, 2010). Land use can have a considerable impact on the water cycle (e.g., Franklin, 1992; Miller et al., 2002), on sediment transport (e.g., Bakker et al., 2008; Ouyang et al., 2010a) and on nutrient leaching caused by agrochemical losses (e.g., Allan et al., 1997; Turner and Rabalais, 2003). Chiang et al. (2010) even stated that land use changes can mask the water quality improvements from conservation practices implemented in the watershed. However, when simulating water balances for larger catchments, only massive land use changes result in noteworthy shifts of the simulated total runoff (Volk, 2010).

Pai and Saraswat (2011) stated that accurate model prediction depends on how well land use in a watershed is represented in the model. Thus, spatially and temporally accurate land use data is crucial input data for hydrologic models. Due to the rapid development of GIS (Geographic Information System) and remote sensing systems, an increasing amount of land use data becomes available. However, land use maps based on remote sensing data are known to contain data gaps. These gaps are caused by clouds or classification thresholds (spatial data gaps) or by missing land use layers in a time series (temporal data gaps). Both kinds of gaps hamper temporal availability and spatial accuracy of land use data in a model. Existing interpolation methods of spatial data gaps (e.g., nearest-neighbor method), produce poor results for large data gaps and there are no methods available for interpolating temporal data gaps. This means that land use data based on classification of remote sensing data seldom provides the required accuracy, spatial availability and temporal observational frequency for river basin management. Hence, the simulation of land use changes on water yield in river basins has been carried out in a great number of research projects, but mostly without considering the spatial distribution of land use (Lorz et al., 2007). Recent and future river basin management, however, requires a spatially distributed description of basin hydrology and land use to enable management practices as a factor in river basin management (Volk et al., 2007). Thus, there is a high demand for accurate and spatio-temporal complete time series of land use data. Currently both, quality and spatial distribution of land use data within

hydrologic simulations hamper the applicability of models like SWAT for river basin management.

1.3   Research topics and outline of the dissertation

This dissertation aims at improving the watershed-based eco-hydrologic model SWAT to enhance its suitability for integrated river basin management. The improvements have been investigated with the focus on (1) enhancing the spatial representation of flow processes within the SWAT model and (2) developing a space-time interpolation and revision approach for remotely sensed land use data to provide more accurate model input data. The central research tasks are:

Research Task 1: Incorporating more spatial detail into SWAT by developing a model interface that setups SWAT in a grid-based discretization scheme.

Research Task 2: Developing routing capabilities between grid cells and adapting the SWAT hydrologic algorithms from the sub-watershed to the hillslope scale.

Research Task 3: Improving SWAT input parameters by deriving input data from remotely sensed data.

All tasks are addressed to the **central research question**: Does the incorporation of more spatial detail into a SWAT model help to fulfill the requirements of integrated water basin management?

Chapter 2 presents an interface that was developed to set up SWAT in a grid-based discretization scheme: SWATgrid. A grid-based setup turns SWAT from a spatially semi-distributed to a fully-distributed model. The gridded approach incorporates more spatial detail into the model and avoids a loss of spatial information that is inherent to the primarily used sub-watershed approach. An application study of a grid-based SWAT setup was performed in the Lake Fork watershed (556 km^2, Texas, USA). Chapter 2 addresses research task 1 by comparing the sub-watershed and grid approach and analyzing the input effects of the two discretization techniques on model output.

In Chapter 3, a SWATgrid application study is presented to prove the general functioning of the grid-based approach. Hydrologic studies that use the SWAT model require

calibration to fit the model to the environmental and hydrologic conditions of the catchment. Compared to the sub-watershed approach, the grid-based setup significantly increases model computation time and hence hampers calibration according to established calibration guidelines. Chapter 3 describes how a set of calibrated parameters obtained from a computationally efficient sub-watershed based setup can be used to calibrate the corresponding grid-based model by down-scaling the parameter values to the grid scale. In addition, this chapter analyzes input effects of the grid-based discretization technique on SWAT model output. A sub-catchment of the River Elbe, the Bünzau catchment (210 km^2, Schleswig-Holstein, Germany), served as test site to present and validate the proposed methodology.

To capture the channel and landscape flow and transport processes related to specific landscape positions, the landscape routing model developed by Volk et al. (2007) and Arnold et al. (2010) was modified to link these processes to the grid scale. Therefore, Chapter 4 presents the development and evaluation of a grid-based version of the SWAT landscape model. The new model is fully distributed and able to capture the channel and landscape flow processes and distribute surface runoff, lateral subsurface flow and shallow groundwater flow between grid cells. Model testing includes evaluation of model output at discrete locations (i.e. stream gages), and a qualitative analysis of spatially distributed hydrologic model output at the grid scale. The study area is the 334 km^2 Little River experimental watershed in Georgia (USA).

Spatially detailed distributed models require high resolution input data to accurately represent the spatial and temporal status of the watershed. Despite the rapid development of geographic information systems and remote sensing techniques for data acquisition, the temporal availability, spatial resolution and accuracy of input data (e.g., climate, topography, land use, soil) is often too coarse for detailed modeling. Chapter 5 presents a space-time Interpolation and revision approach for Remotely Sensed Land use data (IRSeL) developed to improve model input data. IRSeL improves the data set by filling data gaps in the temporal and spatial dimension of a land use data set and minimizing classification errors based on statistical analysis. An area around the city of Neumünster (Schleswig-Holstein, Germany) that is part of the Bünzau catchment (see Chapter 3) served as a test site to demonstrate IRSeL's functioning, effectiveness, limitations, and challenges.

The aim of Chapter 6 is to assess the impact of the accuracy and temporal representation of land use data on hydrologic SWAT model output, which includes a sensitivity analysis of the grid-based SWAT model to variations of input land use data. The Bünzau catchment is taken to simulate hydrology using conventional and IRSeL revised land

use input data. The impacts of the different land use data sets on water balance, flow components, and streamflow are analyzed.

Finally, Chapter 7 summarizes the main findings of this dissertation and presents an answer to the central research questions. It also discusses hydrologic processes and their representation in the SWAT model across spatial scales, summarizes the implications of the results for river basin management. Advantages, shortcomings, boundaries and limitations of distributed grid-based SWAT modeling and the proposed methodologies are presented. An outlook is given, which lists further research needs that were identified in this study.

Chapter 2

SWATgrid: An interface for setting up SWAT in a grid-based discretization scheme

H. Rathjens and N. Oppelt

Abstract

This paper presents a model interface that enables the user to incorporate spatial detail into a SWAT (Soil and Water Assessment Tool) model run.

For modeling purposes a watershed has to be spatially discretized. All currently developed interfaces preparing SWAT input data use the sub-watershed discretization scheme. The application of this concept results in a loss of spatial information in the input data such as land-use or soil type maps. Setting up SWAT in a grid-based scheme would avoid this loss of information. Therefore an interface preparing the input data for setting up SWAT based on grid cells was developed: "SWATgrid". SWATgrid allows the user to incorporate spatial detail into a SWAT model run and enables the coupling of spatial information such as remote sensing data with SWAT.

In this article the functionality of SWATgrid will be demonstrated by comparing results of SWATgrid with conventional SWAT model results. The development of the grid-based discretization scheme will be presented using a SWAT test data set. Current

developments as well as problems that occured will be discussed and future steps will be pointed out.

2.1   Introduction

The eco-hydrological model SWAT (Soil and Water Assessment Tool (Arnold et al., 1998)) has proven to be a very useful modeling tool for a wide range of scales and environmental conditions. Over the past decade SWAT has been used worldwide to estimate anthropogenic, climate and other influences on a wide range of water resources. Besides numerous applications in the U.S. driven by the needs of government agencies, SWAT has also been used extensively in Europe. In the literature many specific SWAT applications have been reported. Gassman et al. (2007) summarized many of these. Numerous applications exist using the outlet gauge discharge data for calibration and validation purposes. They range from hydrological and water resource assessments (water discharge, groundwater dynamics, soil water, snow dynamics, water management) through water quality assessments (land-use and land-management change in agriculture) and climate change impacts and pollutant assessments (Gassman et al., 2007; Krysanova and Arnold, 2008).

Simulation of the hydrological balance is essential for watershed applications. The first step in setting up a watershed simulation is to define the spatial arrangement of the elements of the watershed, such as sub-watersheds, reach segments and point sources (Neitsch et al., 2010). For reasons of computational efficiency and availability of interfaces to prepare the input data, the primary technique used within SWAT is the sub-watershed configuration. The watershed is divided into sub-watersheds which are further subdivided into hydrologic response units (HRUs). The HRUs represent percentages of the sub-watershed area and are not spatially related within a SWAT simulation (Gassman et al., 2007). Individual areas of similar soil, topography and land-use are lumped together within a sub-watershed to form a HRU. This approach fails to show the interaction between the HRUs as they are not directly linked but are all routed individually to the sub-watershed outlet (Arnold et al., 2010). Depending on the scale of the sub-watershed, high resolution spatial data such as land-use or soil maps can be lost. Many studies have examined SWAT hydrology and water quality response to changes in the sub-watershed scale (FitzHugh and Mackay, 2000; Chen and Mackay, 2004; Jha et al., 2004; Haverkamp et al., 2005; Arabi et al., 2006; Cho et al., 2010). These studies have emphasized that total streamflow is affected very little by watershed subdivision level, whereas predicted sediment yield and many parameters of water quality are directly related to sub-watershed size. Jha et al. (2004) observed hat organic nitrogen (N)

and phosphorus (P) in streamflow decrease as the area of the sub-watersheds decreases, while opposite trends were found for nitrate and mineral P.

Due to the rapid development of remote sensing systems, more and more spatial information becomes available as raster data. Currently remote sensing data used in SWAT applications include the generation of land-use maps (Ouyang et al., 2010b; Pandey et al., 2005; Xue et al., 2008) or the derivation of management practices (Quansah et al., 2008; White et al., 2010). Due to limited availability of climate data in developing countries Yan et al. (2010) derived spatial climate data from remote sensing systems as SWAT input data. Evapotranspiration data obtained from remote sensing systems are used for calibration (Immerzeel and Droogers, 2008) or sensitivity and uncertainty analysis (Xie and Zhang, 2010). Therefore, a high potential for deriving spatially detailed model parameters already exists. A high resolution grid-based approach avoids potential loss of information and thus may improve model results. The use of smaller sub-watersheds instead of grid cells would yield similar results, but incorporating raster data into the sub-watershed approach would also require data transformation from a simple grid geometry to a patchy geometry of irregular polygons. Therefore, a grid-based approach makes it easier to integrate grid input or validation data in SWAT simulations.

In theory it is possible to take a grid based approach with the SWAT model since its inception (Arnold et al., 1994; Neitsch et al., 2010). Nevertheless, SWAT uses the sub-watershed configuration as the primary discretization scheme (Arnold et al., 2010; Neitsch et al., 2010); all GIS input interfaces use the sub-watershed discretization. These interfaces are currently not able to delineate a watershed using a grid cell discretization (Neitsch et al., 2010). Thus, there are only few applications and studies which actually have used the grid approach.

White et al. (2009) used a grid-based approach to identify small areas with disproportionately high pollutant losses (i.e. critical source areas). Every possible combination of soils, slope, and land-cover was simulated as an individual HRU in SWAT using custom software. While many studies have assessed the impacts of spatial detail on the sub-watershed configuration, few have assessed the output of different discretization schemes for the same watershed. Manguerra and Engel (1998) illustrated the sensitivity of SWAT runoff prediction to different schemes (HRU or sub-watershed and grid configuration). They figured out that the discretization scheme did not result in any significant discrepancies for the predicted stream runoff hydrograph. Four subdivision methods were compared by using a modified SWAT version with a landscape routing method in Arnold et al. (2010): lumped (dominant soil and land-use for the whole watershed), HRUs, catena and grid. Their results suggest that lumped models can be calibrated as well as the grid and catena configuration at the basin outlet, but cannot represent the

impact of upslope management on downslope positions, which causes unrealistic spatial model output. A high resolution grid approach would include the impact of an upslope grid cell on a downslope grid cell and provide accurate spatial detailed output data. Furthermore, lumped models are often less responsive to changes in land use, soil and weather conditions and need to be recalibrated with each changing scenario.

To overcome the difficulties of the sub-watershed scheme (spatial generalization, no interaction between the HRUs within a sub-watershed, missing impacts of upslope areas on downslope positions, no geographic position of HRUs within each sub-watershed, patchy subwatershed geometry) and to fill the gap for an interface that incorporates grid-based cell data into SWAT, a model input interface for setting up SWAT based on grid cells was developed: "SWATgrid". The Lake Fork SWAT example dataset (Winchell et al., 2010) was used to present and validate the program methods and algorithms. The functionality will be demonstrated by comparing conventional SWAT (version 2009) model results with the results of the grid based approach.

2.2   The SWAT model

SWAT is a physically-based watershed-scale model, developed to simulate the impact of land management practices on the water cycle, the flow of sediment, the nutrient cycle and the behavior of pesticides and bacteria in complex watersheds. The hydrology of a watershed is divided into two major phases: (1) The land phase of the hydrologic cycle controls the quantitative flow of water, sediment, nutrients and pesticides entering the reach allocated to the sub-watershed. The substances SWAT passes from the sub-watershed to the reach at a given time step are termed as loadings of the particular sub-watershed. (2) The routing phase, determining the movement of loadings through the channel network of the watershed to its outlet. All model calculations are carried out in daily time steps, whereas the model output can be obtained at a daily to annual time scale (Neitsch et al., 2005).

According to Neitsch et al. (2010) the three most common techniques to discretize a watershed are

- grid cell,

- representative hillslope and

- sub-watershed discretization.

All of these techniques have strengths and applications for which they are most appropriate. Due to the routing command language utilized in SWAT, it is theoretically possible to use any of these schemes to model a watershed (Neitsch et al., 2010).

However, there are basically two separate parts to the software: the model executable and the interface. Interfaces are necessary to define and discretize a watershed and to prepare the input data to match the required SWAT format. The SWAT model executable uses simple text files for both input and output. These files are created, modified and displayed in the interface.

The first level of subdivision is the sub-watershed. The sub-watersheds are spatially related and have a geographic position in the watershed. Fig. 2.1 illustrates a typical sub-watershed discretization and a grid-based configuration for the Lake Fork watershed. Each of the sub-watersheds contain at least one HRU, a tributary channel and a main channel or reach (Neitsch et al., 2010). Using the sub-watershed discretization scheme, the land area in a sub-watershed may be divided into several HRUs, which represent a part of a sub-watershed with relative uniform land-use, management and soil attributes. These areas are combined to form one HRU, while in reality they may be scattered throughout a sub-watershed. So this concept may describe the heterogeneity of a sub-watershed well, but information about the spatial distribution is lost and no interaction exists between HRUs in one sub-watershed. Loadings of each HRU are calculated separately and then summed to determine the total loadings of the sub-watershed. This implies a loss of spatial information during modeling, which might be important for existing applications, for example when studying diffuse substance discharges in agricultural areas or changing discharge patterns due to land use changes within a sub-watershed. For these applications it may be useful to run the model grid cell discretized. In SWATgrid, the sub-watersheds are divided into a large number of grid cells, which are characterized by both a defined cell size and their geographic position. Similar to a sub-watershed, each grid cell contains one HRU, a tributary and a main channel. SWAT processes are calculated for every grid cell individually; therefore SWAT output can be directly linked to individual grid cells (and thus to specific locations in a watershed).

2.3   SWATgrid

SWATgrid is a command line based program suite written in the programming language Fortran 90. SWATgrid contains tools to generate SWAT input ("SWATgrid_fig", "SWATgrid_inp") as well as output ("SWATgrid_out") data. SWATgrid_fig and SWATgrid_inp preprocess input data to set up SWAT in a grid cell discretization scheme (see Fig. 2.2) and SWATgrid_out generates maps from SWAT output files (see Fig. 2.3).
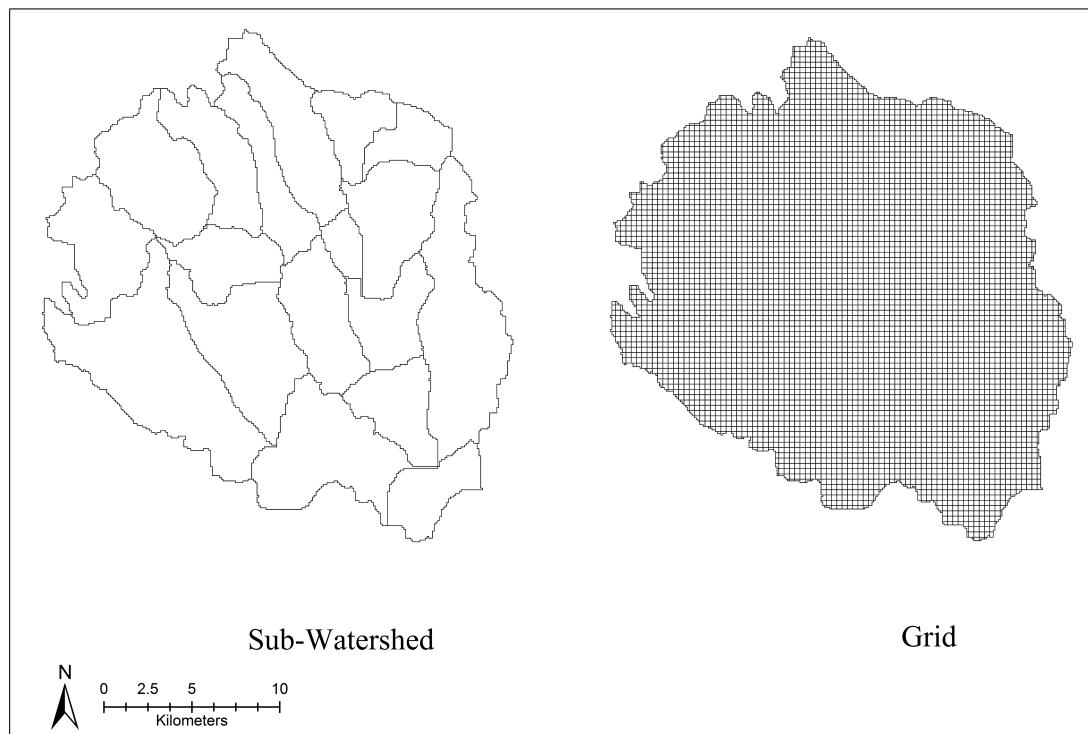
Sub-Watershed   Grid

FIGURE 2.1: Sub-watershed and grid-based configuration for the Lake Fork watershed

2.3.1   Preprocessing SWAT input data

The process of preparing the input data can be distinguished into two consecutive steps:

- Step 1: Defining the elements (sub-watersheds and reach segments) of the watershed and their spatial arrangement. This is done using a watershed configuration file (.fig) (Neitsch et al., 2010), which specifies the spatial relationship of objects within the watershed and instructs SWAT how to route the loadings through the channel network of the watershed. The generation of this file is performed by SWATgrid_fig, using the digital landscape analysis tool TOPAZ (TOPographic PArametriZation, version 3.1 (Garbrecht and Martz, 2000)).

- Step 2: Preprocessing remaining input files of given data using SWATgrid_inp. The required input data and output files is explained below.

2.3.1.1   Step 1: Generation of the watershed configuration file

The first step is the processing of a raster digital elevation model (DEM) using TOPAZ, a software package for automated analysis of digital landscape topography. The overall objective of TOPAZ is to provide drainage characteristics based on the application of the deterministic eight-neighbour (D8) method (Douglas, 1986; Fairfield and Leymarie,
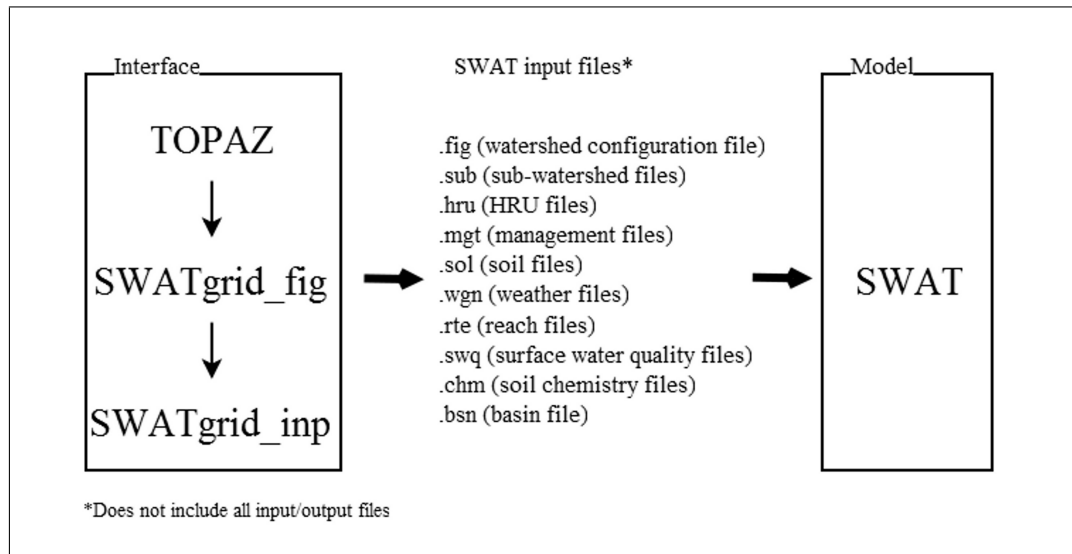
FIGURE 2.2: SWATgrid_fig, SWATgrid_out and SWAT interdependence and application order

1991). The processing of the digital elevation model using TOPAZ provides the following data as a raster output:

- watershed boundary,

- local flow vector or drainage direction for every grid cell in one of eight directions,

- number of upstream cells draining into each cell,

- start and end points of flow paths and

- a map of the channel network including the stream order.

These TOPAZ output files are used by SWATgrid_fig to generate a watershed configuration file for SWAT. The general functioning of the SWATgrid_fig algorithms is explained below.

The TOPAZ output files contain their respective information for a rectangular grid. Because SWAT is a watershed-based model the information is only needed for the part of the grid inside the watershed. The watershed boundary file is used to delimit information to the watershed area.

After modifying and loading the TOPAZ output files, SWATgrid_fig writes the configuration file. Neitsch et al. (2010, see chapter 2 and appendix B) provide a detailed description of the watershed configuration file and the routing command language used. The set-up of the watershed configuration file for different discretization techniques is also explained.

Due to the HRU concept implemented in SWAT, spatial variability during simulation can only be enhanced by increasing the number of sub-watersheds. Thus to incorporate the spatial information given by raster data, each grid within the watershed has to be defined as a sub-watershed. The horizontal resolution of the DEM therefore corresponds to the maximum possible spatial variability. Dixon and Earls (2009) described the effects of several resolutions of DEMs in SWAT watershed modeling and Chaubey et al. (2005) refer to the effects of DEM data resolution on SWAT output uncertainty. They deduced that every effort must be made to integrate DEM data at a high resolution to minimize uncertainties in the model predictions.

Due to the large number of sub-watersheds being defined, small changes in the SWAT 2009 code have to be made. In *modparm.f* the dimension of *hydgrp*, *kirr* and *snam* has to be set to the number of sub-watersheds needed. This does not affect the simulation and produces only optical artefacts in some output files (sub-watershed numbers greater than 9999 are displayed as ****).

SWATgrid_fig starts with defining every grid cell within the watershed as a sub-watershed by writing the sub-watershed command, the hydrograph storage location number where SWAT stores the data of the loadings from the sub-watershed (Neitsch et al., 2010) and the sub-watershed number for each cell in the watershed configuration file. Information of the watershed boundary given by the modified TOPAZ output data is necessary during this step. This command simulates the land phase of the hydrologic cycle.

Then the stream loadings are routed step-by-step through the flow path network, beginning by routing the loadings of the headwater grid cells (grid cells with no upstream) through the watershed. SWATgrid_fig writes the following terms into the watershed configuration file:

- the route command,

- the hydrograph storage location number containing the input data to be routed through the reach,

- the storage location number where SWAT saves the results from the route simulation and

- the number of the reach segment (corresponds to the number of the sub-watershed) the inputs are routed through.

In this way the route command simulates the routing phase of the hydrological cycle using TOPAZ data concerning the number of upstream cells draining into each cell.

Finally, SWATgrid_fig continues to route the loadings through the reach network by writing the "route" and "add" (Neitsch et al., 2010) commands. The number of upstream cells draining into each cell and the local flow vectors provided by TOPAZ are used to identify the routing sequence. The start and end points of flow paths are used as termination conditions.

2.3.1.2 Step 2: Preparing the remaining input files

SWATgrid_inp is a tool for generating input data for SWAT by retaining the spatial variability of the available grid files that should run on a grid based discretization scheme. The required input and the functioning of SWATgrid_inp are explained in the following.

The input data can be divided into three groups, which are required by SWATgrid_inp.

- Files containing general input data, such as information about the location and resolution of the grid data, the management practices, and databases of soil types and groundwater parameters.

- Files containing information about modeling options, climate inputs, databases, and the location of weather stations.

- Grid files containing spatial information such as a soil and land cover map, a map of the channel network, a digital elevation model, a map containing the local flow vectors, and the watershed boundary.

SWATgrid_inp allows the user to vary SWAT input parameters. Parameters affecting the land phase can be defined in dependence of soil type and land cover for each grid cell. The DEM is used to derive topographic features as well as the local flow vectors. This can be implemented by running for-loops on the raster data enabling the generation of SWAT files that include detailed spatial information.

Parameters concerning the routing phase (e.g. trapezoidal channel dimensions or hydraulic conductivity) determine the movement of water and its loadings (sediments, nutrients, pesticides, ...) through the channel network of the watershed to the outlet. SWATgrid_inp enables the user to set these parameters for each grid cell depending on the stream order (Horton-Strahler number (Horton, 1945; Strahler, 1952)) and the number of upstream cells.

The implementation of water bodies into a SWAT simulation is managed via land-use maps. SWATgrid_inp allows the user to set parameter information regarding water
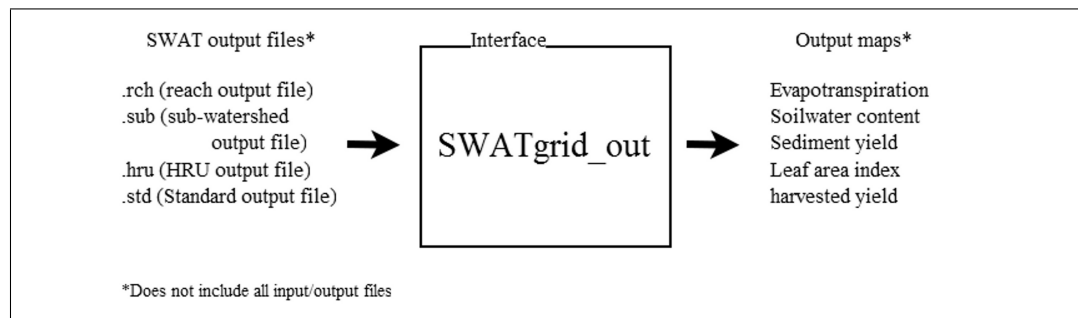
FIGURE 2.3: General organization of SWATgrid_out

levels, sediment and nutrient concentrations for each grid cell or water body individually. Administration parameters such as definition of flood seasons or the hydraulic conductivity may be set according to the conventional SWAT.

After generating the input files, the SWAT modeling takes place, where the SWATgrid input files can be used in the same way as the standard input data.

2.3.2   Displaying SWAT output files

The availability of spatially distributed model output is a major advantage of SWATgrid. SWATgrid_out is an automatic and effective tool to generate grids of SWAT output files (see Fig. 2.3). Every parameter calculated at sub-watersjed, reach or HRU level could be spatially illustrated and processed for further applications using GIS software.

2.4   Results and discussion

2.4.1   SWAT model set-up

To test SWATgrid the SWAT example data set (Lake Fork Watershed in northeast Texas) was used (see Fig. 2.4). This data set can be downloaded at the SWAT-website (Winchell et al., 2010). The functionality of SWATgrid will be demonstrated by comparing conventional SWAT model results derived by ArcSWAT with the results of the grid-based approach. In both model runs all parameters have been set without any calibration as described in Winchell et al. (2010, Section 16: The Example Data Set).

The sub-watershed discretization scheme divides the watershed into 18 sub-watersheds (see Fig. 2.1 and 2.4) and 128 HRUs. When using the input data prepared by SWATgrid the basin is discretized to 55561 grid cells (100×100 m), each containing a single HRU. This demonstrates not only an advanced spatial representation of existing heterogeneities but also a mapping of spatial relationships between the grid cells (see Fig. 2.1).
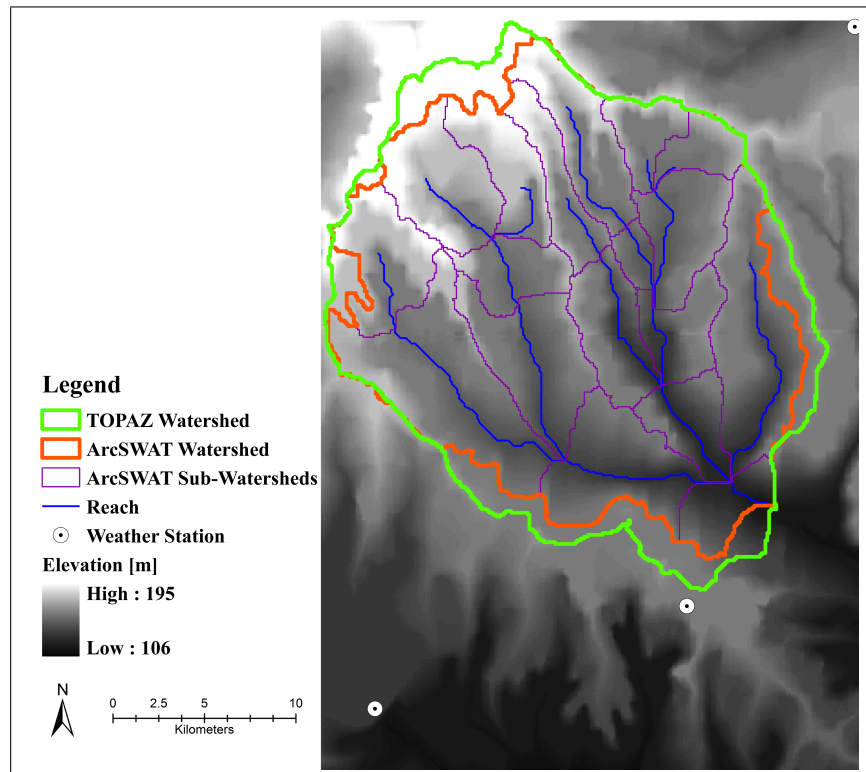
FIGURE 2.4: River basin overview

As input data, the SWAT example data set provides raster datasets for the Lake Fork Watershed in the Albers Equal Area projection with a resolution of 100×100 m: a digital elevation model, a soil map (U.S. general soil map STATSGO) and a land-use grid differing between six classes. Databases containing management practices and groundwater and soil parameters are included. Precipitation and temperature data of three weather stations are used as climate input data as well as climate data for the SWAT weather generator (Neitsch et al., 2005). The input data enable a model run for a time period between January 1st 1977 and December 31st 1978 (Winchell et al., 2010).

2.4.2 Watershed delineation

Looking at the ArcSWAT basin it becomes obvious that the watershed boundary does not run along the ridges (see Fig. 2.4 and Winchell et al. (2010)). The watershed boundary derived with TOPAZ seems to be more realistic and is defined by the DEM grid cells with the highest elevation. This results in a different size of the catchment area: The watershed derived by ArcSWAT has a size of 48683 ha whereas TOPAZ determines an area of 55561 ha, resulting in a difference of 6878 ha or 14.13 %.

The watershed delineation between the two schemes needs to match in order to make a comparison. Thus, the watershed delineation derived by TOPAZ was imported to the

TABLE 2.1: Mean annual watershed parameters of the water balance equation of model runs

Parameter	sub-watershed discretization [mm]	grid cell discretization [mm]	relative difference [%]
Precipitation	1241.90	1241.20	-0.06
Snow fall	76.30	70.61	-7.46
Snow Melt	76.25	70.54	-7.49
Sublimation	0.05	0.07	40.00
Surface runoff	431.07	425.22	-1.36
Lateral soil runoff	1.82	1.92	5.49
tile runoff	0.00	0.00	0.00
Groundwater runoff	135.11	152.98	13.23
Revap*	8.84	9.44	6.79
Deep aquifer recharge	7.76	8.75	12.76
Total aquifer recharge	155.16	174.90	12.72
Total water yield	566.58	555.44	-1.97
Percolation out of soil	164.18	161.52	-1.62
Evapotranspiration	601.20	610.40	1.53
Potential evapotranspiration	1105.10	1112.90	0.71
Transmission losses	1.41	24.68	1650.35

* water in the shallow aquifer returning to the root zone

ArcSWAT interface. As a result the watershed size is equal in both schemes, but the kind of discretization differs.

2.4.3 Mean annual water balance

The SWAT output file (*output.std*) provides mean annual parameters of the water balance of the catchment. Table 2.1 demonstrates, that most output parameters of the water balance equation are in the same range. Large relative differences of approximately 10 % are found at parameters concerning the snow cover, groundwater and transmission losses.

The values of snow fall and snow melt between the two model runs differ by 7.5 %. The spatial allocation of climate data occurs in SWAT at sub-watershed level, dependent on the center coordinate. This means that each sub-watershed receives the data of the weather station closest to the sub-watershed. Due to the number of sub-watersheds the allocation of the grid-based approach is more realistic. The weather stations provide measured precipitation and temperature, other climate parameters are simulated using the SWAT weather generator. Differences between the three weather stations can be

observed only with regard to temperature. Thus, the more accurate allocation of the weather stations to every sub-watershed explains varying model outputs.

The differences of the aquifer recharge terms are all about 13 %. The spatial arrangement and the new composition of the different soil types seem to be an important cause for these differences. The aquifer recharge depends on the hydrological characteristics of soil type, land-cover and slope. The allocation of these parameters is more detailed when using the grid-based approach. Furthermore, rarely occuring soil types are not taken into account by the sub-watershed scheme, but this cannot explain the differences observed.

Transmission losses seem to have the greatest impact. Transmission losses are losses of surface flow caused by leaching through the streambed into the aquifer. They are a function of hydraulic conductivity, channel width, length and flow duration (Neitsch et al., 2005). The average channel length and width are set dependent on upstream area and stream order. Every grid cell has an associated reach or main channel, where the stream loadings are routed through, so the overall length of the fluvial network is larger when using the grid cell discretization scheme. All these facts result in an overestimation of transmission losses. The absolute difference of total aquifer recharge is 19.74 mm and the difference in transmission losses is 23.27 mm. Some difference may also be caused by the spatial arrangement and the new composition of the different soil types.

However, the grid-based approach seems to work at an annual time scale. The spatial distribution of modeled discharge for the year 1978 (see Fig. 2.5), which indicates a stream network, confirms this statement. The ArcSWAT reach network (see Fig. 2.4) and the grid based discharge results behave concordantly.

2.4.4   Outflow at the watershed outlet

When considering the monthly runoff at the catchment outlet it is obvious that the model results match very well (see Fig. 2.6). Let $X_m = (x_1, \ldots, x_{24})$ be the monthly runoff results of the two year model run using the sub-watershed discretization scheme and let $Y_m = (y_1, \ldots, y_{24})$ be the results by using the grid cell discretization scheme and let $\bar{x}$ and $\bar{y}$ be the arithmetic mean respectively. The correlation coefficient between the two data sets is defined as

$$R_{X_m, Y_m} = \frac{\sum_{i=1}^{24} (x_i - \bar{x})(y_i - \bar{y})}{\sqrt{\sum_{i=1}^{24} (x_i - \bar{x})^2 \sum_{i=1}^{24} (y_i - \bar{y})^2}} \approx 0.9977, \tag{2.1}$$

which demonstrates that the results of the two model runs agree well.
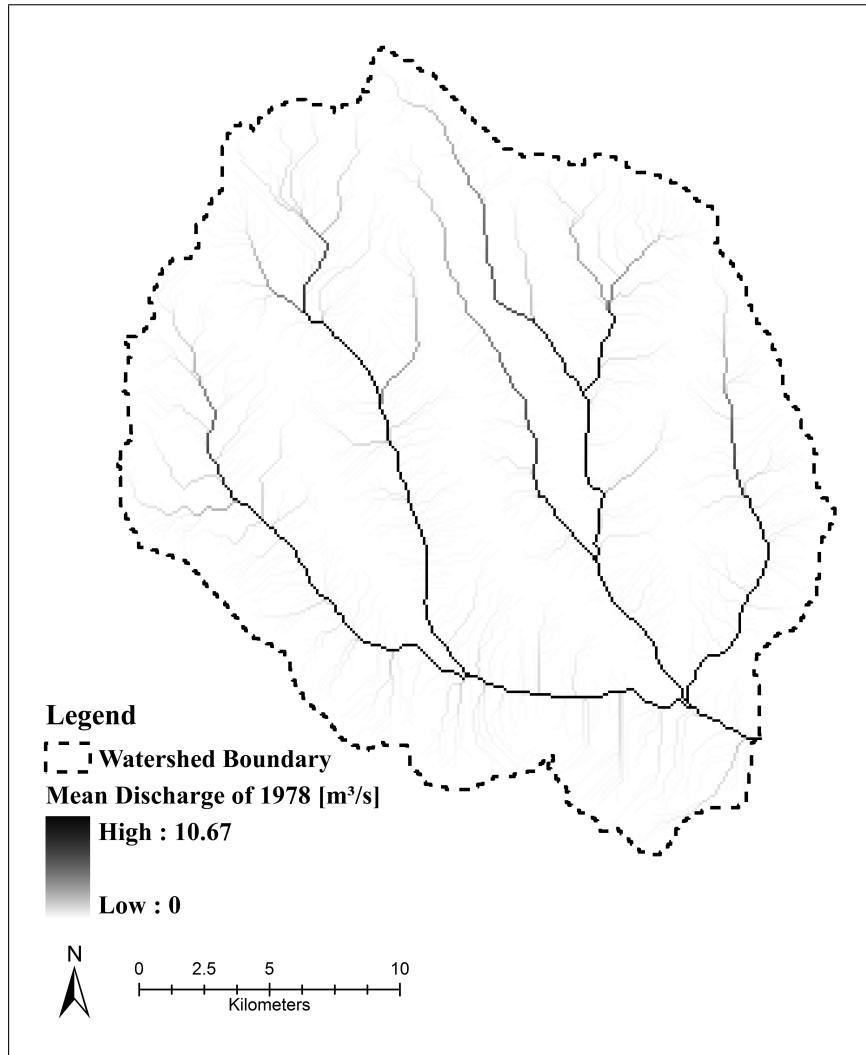
FIGURE 2.5: Spatial distribution of mean yearly discharge in 1978
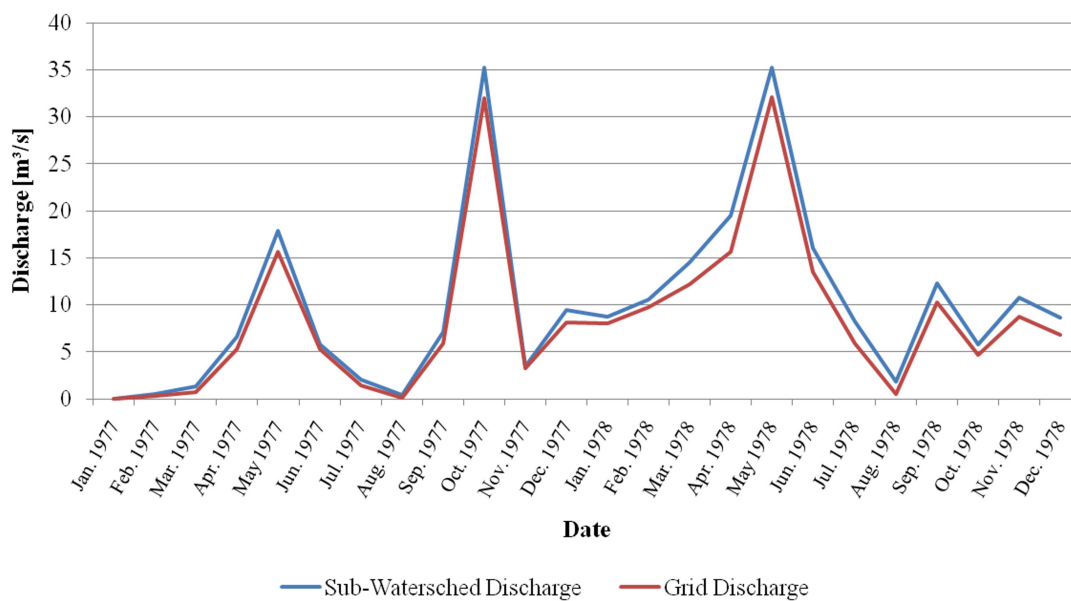
FIGURE 2.6: Monthly outflow at the outlet of both model runs
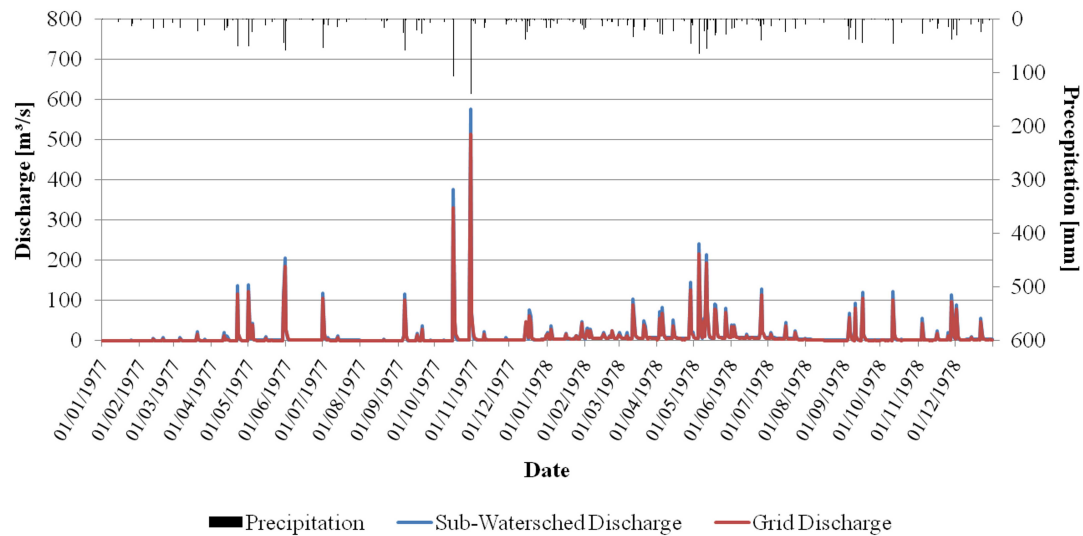
FIGURE 2.7: Daily outflow of both model runs at the outlet

The monthly runoff values of the sub-watershed scheme are little higher than the values of the grid cell discretization scheme (see Fig. 2.6). This is most probably due to the fact that the drainage density (total channel length divided by drainage area) increases as the number of sub-watersheds or grid cells increases. As a result transmission and deep aquifer losses increase and reduce discharge (see Table 2.1).

The same phenomenon is found when examining the differences of daily outflow at the watershed outlet (see Fig. 2.7), where the grid-based approach generally underestimates daily discharge.

However, model results match well. The observed underestimation of discharge caused by a high drainage density could be fixed in the model set-up by decreasing the effective hydraulic conductivity of the tributary channel alluvium from 0.5 to 0.15 mm/h. This lowers groundwater runoff (to 133.37 mm), aquifer recharge (deep to 7.66 mm, total to 153.11 mm) and transmission losses (to 1.74 mm). All other values of the water balance equation do virtually not change. Thus, the results match better (see Table 2.1).

2.5 Future steps

The model results demonstrate the general functioning of the grid-based approach. The parameters of the water balance equation temporally match very well, proving the potential to run SWAT in a grid-based discretization scheme in a complex watershed. For future investigations the following aspects should be considered:

Besides the improvement of SWATgrid to a user-friendly program, testing the approach in a well-documented catchment will be the next step. Model improvement is achieved

by analyzing the sub-watershed discretization scheme. When the outputs of each HRU are summed up to determine the total loadings of the sub-watershed (Neitsch et al., 2005), information about the flow paths is lost.

A more difficult task is the determination of the channel dimension. This problem is currently solved by setting the dimension in functional dependencies to the stream order and the number of upstream cells draining into the grid cell. However, every SWAT grid cell has at least one main and one tributary channel (Neitsch et al., 2005) and the edges of every cell might be shorter than the distance to the nearest channel. Therefore, this approach results in an overestimation of the overall length of the reach network and thus of the drainage density. The current version of SWAT does not allow sediment and runoff to distribute between cells or sub-watersheds in the land phase of the hydrologic cycle. Therefore, interaction between grid cells is part of the routing phase and channel routing processes are hold where no channel exists. This limitation hardly effects model results of the water balance equation, while inaccurate results of sediment transport and nutrient cycling parameters are to be expected. Modifying the SWAT code to enable this distributional flow should be the second step.

However, to enable interaction between the grid cells by using the land-phase, modifications of the SWAT code and the routing command language are necessary. Arnold et al. (2010) developed a command routing structure similar to the sub-watershed routing (Neitsch et al., 2010), which enables an overland routing fraction. Currently, the new developed routing method is used in a modified version of SWAT, but might be implemented in one of the next SWAT versions. This would simplify the solution of flux interaction concerning transmission losses, sediment transport and nutrient cycling.

The primary goal of the grid-based approach is to incorporate spatially distributed data and information into a simulation. DEMs and soil type maps are often available and remote sensing products might be used for classifying the land cover. Moreover, remote sensing data provides the potential to integrate the monitoring of vegetation growth and condition or water quality. Thus, the development of methods determining SWAT input parameters using remote sensing products will be the third topic to be addressed.

2.6 Conclusion

The grid-based discretization scheme allows the user to incorporate spatially distributed information into a SWAT model run and future model runs may use spatial data for improving model results.

The command line based model interface SWATgrid enables the user to set up SWAT based on grid cells. It is an automatic tool to process all files required by SWAT. SWATgrid_fig generates the watershed configuration file, while the remaining input files are generated by SWATgrid_inp. Finally SWAT model results can be used by SWATgrid_out to generate maps. The general functioning of SWATgrid has been proven by comparing conventional model results with the grid based approach, which correspond well: The overall coefficient of determination of daily and monthly mean of the water equation are about 0.99. The overestimation of the reach network can explain individual high differences between the conventional and the grid-based model run. To address these issues, modifications of the SWAT code are necessary. In some topics such as nutrient cycle or reach dimensions, future research is needed.

Due to the rapid development of GIS and remote sensing an increasing amount data with high spatial and temporal resolution becomes available. The integration of these data in well-established eco-hydrological models seems to be very promising for an enhanced spatial analysis of environmental issues in a watershed. Therefore, the challenges and problems inherent to the grid based approach can be justified.

Taking spatially variable input data into account is one advantage, obtaining spatial output data in the resolution of the provided DEM is another. Output data can be processed by several applications, an advantage which enables detailed analysis of every output grid cell with known geographical position.

Chapter 3

SWAT model calibration of a grid-based setup

H. Rathjens and N. Oppelt

Abstract

The eco-hydrological model SWAT (Soil and Water Assessment Tool) is a useful tool to simulate the effects of catchment processes and water management practices on the water cycle. For each catchment some model parameters (e.g. ground water delay time, ground water level) remain constant and therefore are used as constant values; other parameters such as soil types or land use are spatially variable and thus have to be spatially discretized. SWAT setup interfaces process input data to fit the data format requirements and to discretize the spatial characteristics of the catchment area. The primarily used configuration is the sub-watershed discretization scheme. This spatial setup method, however, results in a loss of spatial information which can be problematic for SWAT applications that require a spatially detailed description of the catchment area. At present no SWAT interface is available which provides the management of input and output data based on grid cells. To fill this gap, the authors developed a grid-based model interface.

To perform hydrological studies, the SWAT user first calibrates the model to fit to the environmental and hydrological conditions of the catchment. Compared to the sub-watershed approach, the grid-based setup significantly increases model computation time and hence aggravates calibration according to established calibration guidelines.

This paper describes how a conventional set of sub-watershed SWAT parameters can be used to calibrate the corresponding grid-based model. The procedure was evaluated in a sub-catchment of the River Elbe (Northern Germany). The simulation of daily discharge resulted in Nash-Sutcliffe efficiencies ranging from 0.76 to 0.78 and from 0.61 to 0.65 for the calibration and validation period respectively; thus model performance is satisfactory. The sub-watershed and grid configuration simulate comparable discharges at the catchment outlet ($R^2 = 0.99$). Nevertheless, the major advantage of the grid-based set-up is an enhanced spatial description of landscape units inducing a more realistic spatial distribution of model output parameters.

3.1   Introduction

The eco-hydrological model SWAT (Soil and Water Assessment Tool (Arnold et al., 1998)) is a useful tool for a wide range of scales and environmental conditions. In literature manifold SWAT applications have been reported; the topics cover hydrological and water resource assessments (water discharge, groundwater dynamics, soil water, snow dynamics, water management), water quality assessments (land-use and land-management change in agriculture), climate change impacts, and pollutant assessments (Gassman et al., 2007); a detailed review can be found in Gassman et al. (2007) and Krysanova and Arnold (2008).

To set up a SWAT model run, the watershed has to be delineated and the spatial arrangement of catchment elements (e.g. sub-catchments, reach segments and point sources) has to be defined (Neitsch et al., 2011a). The most popular setup is the sub-watershed configuration, where the catchment is divided into sub-catchments and further sub-divided into hydrologic response units (HRUs). The HRUs represent percentages of the sub-catchment area (Gassman et al., 2007). Individual areas of similar soil, topography and land-use are lumped together within a sub-catchment to form an HRU while in reality they are scattered throughout the sub-catchment. Thus this approach fails to show the interaction between the HRUs as they are spatially unlinked but routed to the outlet of the sub-catchment separately (Arnold et al., 2010).

The grid-based setup within SWAT overcomes the difficulties of the sub-watershed configuration (Rathjens and Oppelt, 2012b). The user is able both to refine the spatial resolution of a SWAT model and to obtain spatially distributed model output data. Various GIS (Geographic Information System) applications can process the grid-based output; now the model output of every grid cell with its defined geographical position can be analysed. Due to the open-source status of the SWAT code the grid-based approach will continue to evolve as users determine needed improvements, which is an

advantage in comparison to other catchment scale raster-based models such as MIKE-SHE (Refsgaard and Storm, 1995), TOPMODEL (Beven and Kirkby, 1979) or WASIM (Schulla, 1997). The grid based approach, however, significantly increases computation time. Arnold et al. (2010) stated that, applying a one-hectare grid cell size (approx. 50,000,000 grid cells) to the the Upper Mississippi River basin, the simulation of a single year would require about 13 computation days on a 2.6 GHz processor.

After processing of the input data, model calibration is performed, i.e. model output and in-situ data are compared to improve model input parameters iteratively. According to Neitsch et al. (2011a) the calibration of stream flow is performed in two consecutive steps. The model is calibrated for average annual conditions first; then the user shifts to monthly or daily records to fine-tune the calibration. To obtain sufficient calibration results several model runs might be performed. Model validation follows calibration; the input parameters, which were derived during calibration, now are used to test the resulting model performance for a series of subsequent years (Moriasi et al., 2007). Most applications use the discharge at the catchment outlet to calibrate and validate model performance.

For the grid-based model setup, however, this time-consuming procedure is impractical. Therefore, this paper provides a method for grid-based SWAT setups to calibrate daily discharge at the catchment outlet. To perform this analysis, calibration parameters are derived with a sub-watershed configuration and then transferred to a grid-based model. The GIS interface ArcSWAT (Winchell et al., 2010) is used to generate the input files for the conventional sub-watershed setup; SWATgrid (Rathjens and Oppelt, 2012b) is used to setup the grid cell model. A sub-catchment of the River Elbe, the Bünzau catchment, serves as test site to present and validate the proposed methodology.

3.2 Materials and methods

3.2.1 Study area

The Bünzau catchment is located in the Northern German lowlands (see Fig. 3.1); it covers an area of 210 km^2 and is characterized by flat topography and shallow groundwater levels. The mean annual precipitation is 857 mm and the mean annual temperature is 9.51 °C (stations Neumünster and Padenstedt (2000-2009)) (DWD, 2011). The Rivers Buckener Au and Fuhlenau merge north of Aukrug-Innien and form the origin of the River Bünzau; the Rivers Höllenau and Bredenbek form two downstream tributaries. Several drainage pipes and ditches also flow into the Bünzau, which flows in southern direction for 16 km before it flows into the Stör River. The gauge Sarlhusen is located
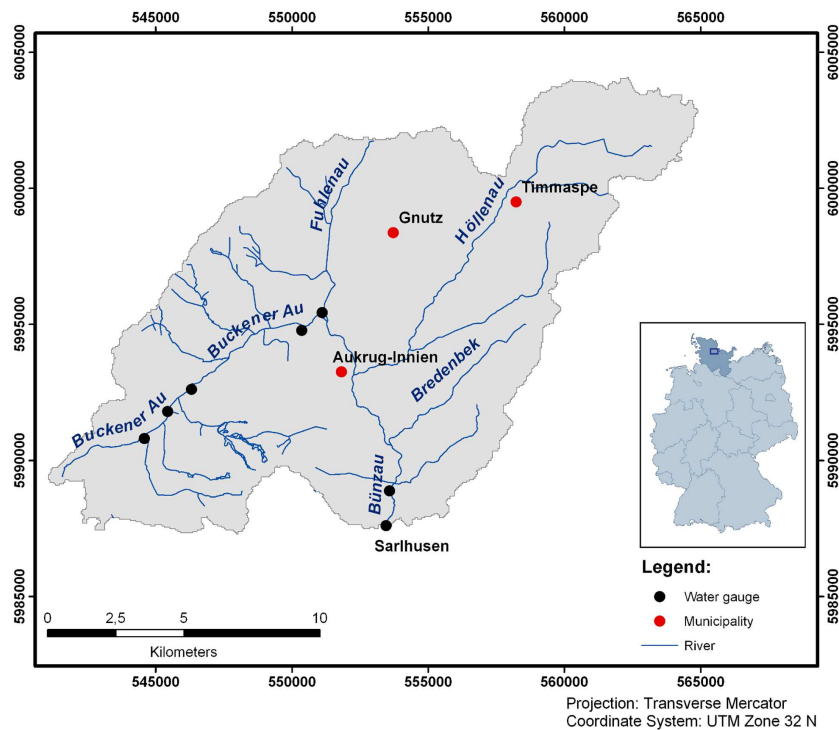
FIGURE 3.1: The Bünzau catchment and its location in Germany.

close to the catchment outlet, where an average discharge of 2.51 m^3/s was measured between 2000 and 2009.

In the Bünzau catchment dominant soils types are podzols and planosols; histosols are found in river valleys and depressions. High proportions of arable land (43 %) and pasture (30 %) indicate an intense agricultural use; Fig. 3.2 shows the land use in 2009 as well as the distribution of soil types.

3.2.2 The SWAT model

SWAT (Arnold et al., 1998) is a physically based catchment-scale model; it was developed to simulate the water cycle, the corresponding fluxes of energy and matter (e.g. sediment, nutrients, pesticides and bacteria) as well as the impact of management practices on these fluxes. The design of the model is modular and includes components for hydrology, weather, sedimentation, crop growth, nutrients and agricultural management. A detailed description of all components can be found in Arnold et al. (1998) and Neitsch et al. (2011b).

The simulated hydrological processes include surface runoff (SCS (Soil Conservation Services) curve number or Green and Ampt infiltration equation), percolation, lateral
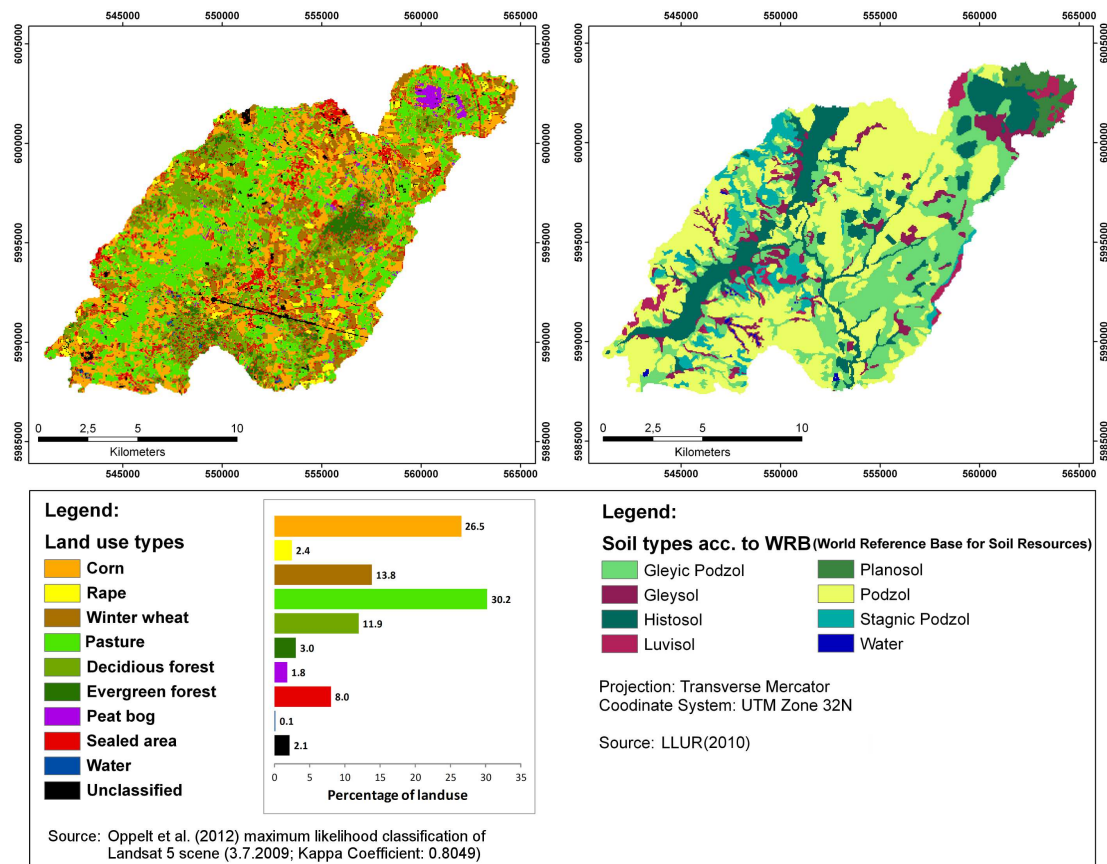
FIGURE 3.2: Land use and soil types in the Bünzau catchment.
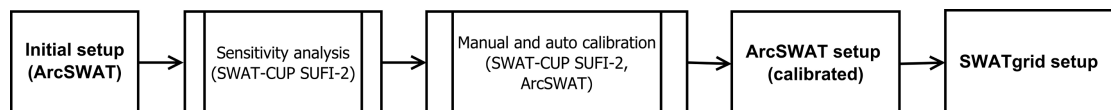
FIGURE 3.3: Grid-based model calibration in chronological order.

flow, groundwater flow from shallow aquifers to streams, evapotranspiration (Hargreaves, Priestley-Taylor or Penman-Monteith method), snowmelt, transmission losses from streams and water storage and losses from ponds (Arnold et al., 1998).

In this study the SCS curve number method (Soil Conservation Service Engineering Division, 1972) was used to calculate surface runoff; Penman-Monteith method was applied to estimate potential evapotranspiration.

3.2.3 Model evaluation

To evaluate model performance four quantitative statistics were applied, i.e. the root mean square error observations standard deviation ratio (RSR; Moriasi et al., 2007),

TABLE 3.1: Model input data sources.

Data type	Source	Data description and properties
Topography (DEM)	LVA (2008)	Digital elevation model, 5 m × 5 m resolution
Soil map	Finnern (1997)	Physical properties of the soil (e.g. available water capacity), scale 1:100 000
	LLUR (2010)	Physical properties of the soil (e.g. available water capacity), scale 1:25 000
Land use map 2009	Oppelt et al. (2012)	Classifications based on Landsat 5 imagery, 30 m × 30 m resolution (03.07.2009)
Climate data	DWD (2011)	Daily measured values of temperature, precipitation, wind speed, relative humidity (Neumünster station 2000-2007, Padenstedt station 2007-2009) and daily measured values of precipitation (Gnutz station 2000-2006)
Discharge	LKN (2011)	Daily discharge data of the Bünzau river at gauge Sarlhusen (2000-2009)

coefficient of determination (R^2), Nash-Sutcliffe efficiency (NSE; Nash and Sutcliffe, 1970) and percent bias (PBIAS; Gupta et al., 1999).

Most simulation studies use different model evaluation techniques to compare simulated output and in-situ measurements (Moriasi et al., 2007). Thus, no comprehensive standardization is available for model evaluation. Moriasi et al. (2007) presented several model evaluation statistics and a step-by-step guideline for model calibration and evaluation. They also reviewed value ranges of evaluation statistics and corresponding performance ratings. They concluded that model simulation for discharge is satisfactory if NSE > 0.50 (see also Santhi et al., 2001) and RSR < 0.70 (see also Singh et al., 2004) and -25 % < PBIAS < 25 %.

The RSR standardizes root mean square error (RMSE) values using the standard deviation of in-situ data and thus enables a comparison of error values of different studies. RSR values can range from 0 to $+\infty$; RSR = 0 indicates that RMSE = 0 or that the model simulation fits perfectly to the measured data. Large positive RSR values indicate a poor model performance (Moriasi et al., 2007).

The coefficient of determination determines which proportion of in-situ variance can be explained by the model. The values range from $0 < R^2 < 1$ where higher values indicate less error variance.

The NSE is a normalized statistical index, which is often used to assess the quality of hydrological models. It determines the relative magnitude of the residual variance between simulated and measured data compared to the in-situ data variance. NSE ranges from $-\infty$ to 1. An NSE of 1.0 corresponds to a perfect match of modeled and observed data (Moriasi et al., 2007).

PBIAS indicates whether the modelled data tend to be larger or smaller than the corresponding in-situ values. The optimum value is PBIAS = 0.0 %; positive PBIAS values indicate a model bias underestimation, whereas negative values indicate a bias overestimation (Gupta et al., 1999).

3.2.4   Model input data

To setup a SWAT model, the essential input data are a digital elevation model (DEM), soil types, land use and climate (see also Table 3.1). For this study all data were transformed from Universal Transverse Mercator (UTM) to the Albers Equal Area projection.

The DEM is provided by the Land Survey Office Schleswig-Holstein with a vertical resolution of 0.5 m and a horizontal resolution of 5 m (LVA, 2008).

The land use map (see Fig. 3.2) is based on a classification of Landsat 5 imagery from July 3rd, 2009 (overall-accuracy: 83 %, Cohen's kappa coefficient (Cohen, 1960): 0.80). Land use classifications for the years 2009, 2010 and 2011 are used to derive crop rotations planted by the local farmers. Based on these results, SWAT management practices were set as three-year crop rotation (wheat - wheat - rapeseed), mono-cultural corn and pasture. Winter wheat and rape were planted at the end of September and harvested at the beginning of August; corn is planted at the end of April and harvested at the end of September.

Daily climate values from January 1st, 2000 to December 31st, 2009 on temperature, precipitation, wind speed and humidity are integrated in the simulation as a composition of three German Weather Service stations (see Table 3.1).

3.2.5   Model setup

This section demonstrates both how different discretization schemes affect the simulated water balance and whether sub-watershed setups may be used to calibrate grid-based model approaches. Fig. 3.3 shows the methodology, which is explained in the following sub-sections.

TABLE 3.2: Mean annual values of water balance components calculated by the two model setups.

Parameter [mm]	ArcSWAT Setup	SWATgrid Setup	Difference
Precipitation	853.80	853.80	0.00
Surface runoff	10.35	12.54	2.19
Lateral runoff	60.402	43.81	-16.59
Tile runoff	1.95	3.25	1.30
Groundwater runoff	290.47	303.48	13.01
Total water yield	362.95	362.88	-0.07
Percolation out of soil	297.40	310.69	13.29
Evapotranspiration (ET)	483.40	482.20	-1.20
Potential (ET)	628.60	627.80	-1.20

3.2.5.1   Initial setup (ArcSWAT)

The ArcSWAT interface was used to carry out the basic model setup: catchment and sub-catchment areas were delineated using the DEM (LVA, 2008); then the catchment was divided into sub-catchments. ArcSWAT calculated nine sub-catchments for the Bünzau catchment. Based on the formation of unique combinations of slope, land use and soil types, the sub-catchments were further divided into 480 HRUs. Finally, daily climate values (see Table 3.1) from 2000 to 2009 (DWD, 2011) were included into the setup.

3.2.5.2   ArcSWAT setup (calibrated)

After the initial setup, SWAT-CUP (Abbaspour, 2007) was applied to identify the most sensitive model parameters. Sensitivity analysis was carried out using the optimization algorithm SUFI-2 (Sequential Uncertainty Fitting; Abbaspour (2007)). The results showed a strong influence of groundwater parameters (GWQMN, ALPHA_BF, GW_REVAP, REVAPMN), which confirms observations by Dobslaff (2005) and Schmalz and Fohrer (2009). To perform a manual calibration of the most sensitive parameters established guidelines for SWAT model calibration (Santhi et al., 2001; Moriasi et al., 2007; Neitsch et al., 2011a) were applied. Afterwards a second SWAT-CUP calibration was carried out; calibration parameters include the runoff curve number (CNOP), soil available water capacity (SOL_AWC), soil evaporation compensation factor (ESCO), groundwater parameters (GWQMN, ALPHA_BF, GW_REVAP, REVAPMN) and hydraulic conductivity (CH_K, SOL_K). A detailed description of each parameter is provided by Neitsch et al. (2011a).

TABLE 3.3: Model performance (RSR, R^2, NSE and PBIAS) during calibration (Cal) and validation (Val) period for the different setups.

Setup	RSR		R^2		NSE		PBIAS [%]	
	Cal	Val	Cal	Val	Cal	Val	Cal	Val
ArcSWAT	0.47	0.60	0.78	0.67	0.78	0.65	-2.97	11.16
SWATgrid	0.49	0.62	0.77	0.64	0.76	0.61	-2.94	11.29

3.2.5.3 SWATgrid setup

The calibrated input parameter set was transferred to the grid based setup using the SWATgrid interface (Rathjens and Oppelt, 2012b); no further calibration was carried out. Therefore, the model parameter set remained equal except for the discretization scheme.

Using SWATgrid the catchment was discretized into 84,273 grid cells with a grid resolution of 50 m by 50 m. To enable a comparison of setups the SWATgrid setup was applied for the same time period.

The grid-based setup significantly increases the model computation time. While the ArcSWAT setup (480 HRUs) takes 30 seconds on a single 2.67 GHz processor, the SWATgrid setup lasts about 12 hours per year of simulation.

3.3 Results and discussion

3.3.1 Mean annual water balance

SWAT calculates annual means for the water balance components (see Table 3.2); for both setups the resulting values are realistic. Dobslaff (2005) and Schmalz and Fohrer (2009) reported similar values for the study area. The results of both model setups demonstrate that groundwater runoff dominates the water balance, a fact that is caused by the low gradients in the catchment. Table 3.2 also shows that the results of both setups are comparable.

Regarding total water yield and evapotranspiration the model setups fit very well. Lateral runoff calculated by SWATgrid, however, is 16.59 mm lower than indicated by ArcSWAT. SWATgrid compensates this effect by higher amounts of groundwater runoff (13.01 mm), surface runoff (2.19 mm) and tile runoff (1.30 mm). The runoff components strongly depend on the hydrological characteristics of soil type, land use and slope for which SWATgrid provides a more detailed distribution. Despite these differences, the
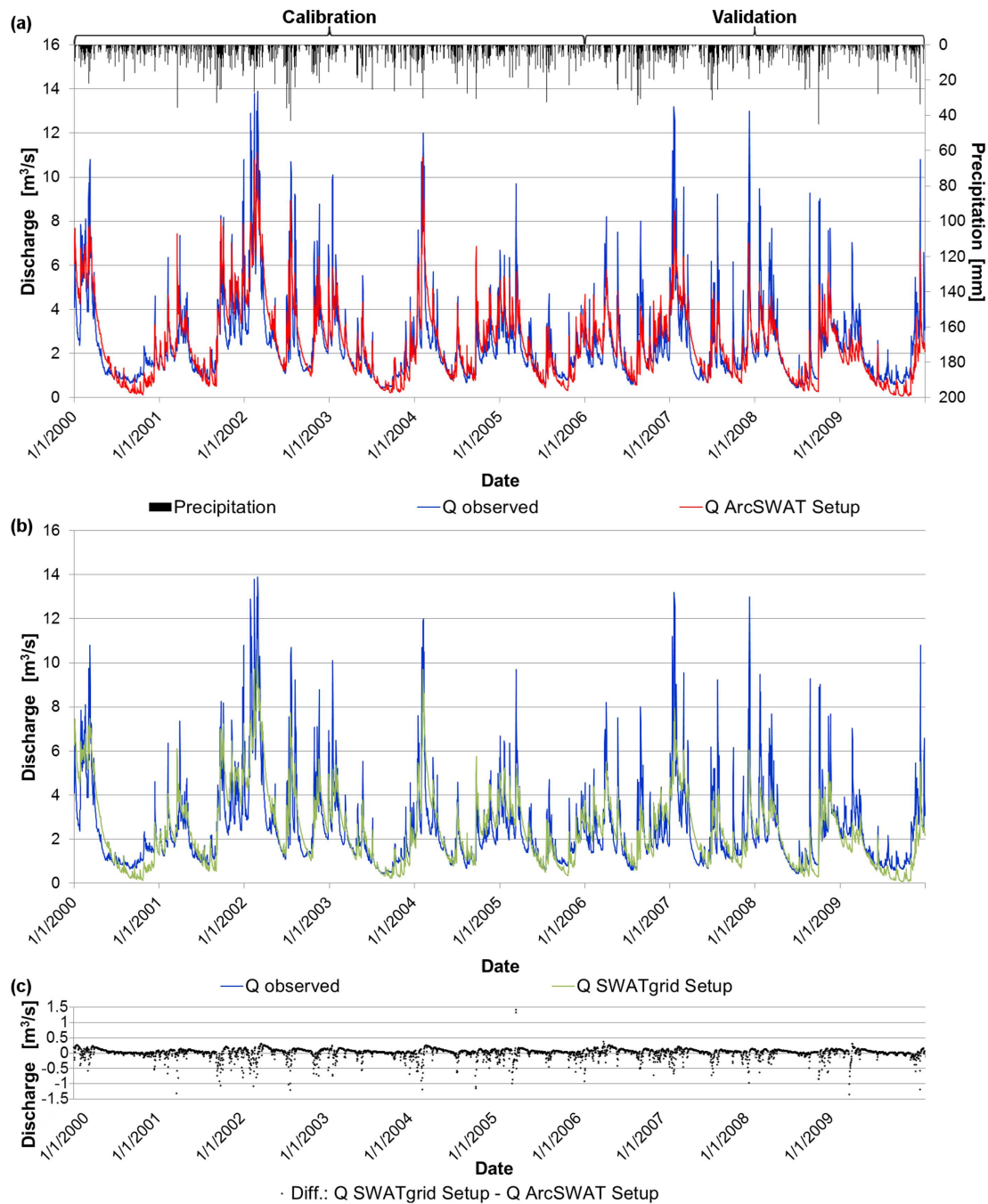
FIGURE 3.4: Measured and simulated daily discharge (calibration period 2000-2005, validation period 2006-2009) at the gauge Sarlhusen (a) ArcSWAT setup, (b) SWATgrid setup, (c) differences of simulated daily discharge (SWATgrid setup - ArcSWAT setup).

two model setups are consistent and confirm previous studies (Dobslaff, 2005; Schmalz and Fohrer, 2009). To summarize both model setups result in a sufficient representation of hydrological processes in the Bünzau catchment.

3.3.2 Simulation of daily discharge

Measures of model performance including RSR, R^2, NSE and PBIAS values are listed in Table 3.3. Figure 3.4 presents daily discharge values that resulted from the ArcSWAT and SWATgrid setups in comparison to values measured at the gauge Sarlhusen. Overall comparison of daily discharge simulation values (2000 - 2009) resulted in a high coefficient of determination ($R^2 = 0.99$).

The model evaluation indices RSR, R^2 and NSE demonstrate that simulated and measured daily discharge agree well for both the calibration and the validation period. The indices also indicate that the ArcSWAT setup performs slightly better that the SWATgrid setup. This might be explained by two facts: (1) values of summer and winter peak flows are higher in ArcSWAT; (2) ArcSWAT shows a faster and more realistic recession of discharge (see also Fig. 3.4). The different proportions of fast and slow runoff components (see also section 3.3.1), i.e. surface, lateral and groundwater runoff are generated at HRU or grid-cell level. Thus, modifications that affect the distribution and composition of land use, soil types and slope do have an impact on modelled streamflow components.

Values of PBIAS of the different model setups range from -3 to 11 %. The PBIAS differences between the setups are less than 0.2 percentage points; the low number indicates that the modelled discharge is insensitive to changing discretization schemes. Drainage density (total channel length divided by drainage area) increases as the number of grid cells or sub-catchments increases. As a result transmission and deep aquifer losses increase and reduce discharge. Thus, these losses cause the lower runoff calculated by the SWATgrid setup compared to the ArcSWAT setup (see Table 3.3). Nevertheless, the differences are relatively small compared to the differences of discharge components caused by the kind of discretization. Similar observations were made by Bingner et al. (1997), FitzHugh and Mackay (2000), Chen and Mackay (2004), Jha et al. (2004), Haverkamp et al. (2005), Arabi et al. (2006) and Cho et al. (2010).

In summary, model performance statistics shows that simulated and observed daily discharge is similar for both the calibration and the validation period. The grid-based model calculates daily discharge at the catchment outlet according to the sub-watershed model. The calibration of the grid-based model using the sub-watershed parameter set

resulted in a satisfactory model performance. Statistical indices (RSR, R^2, NSE and PBIAS) confirm this finding.

3.4   Conclusion

The grid-based discretization scheme (SWATgrid) integrates spatially distributed data into a SWAT model run and enables detailed analysis of every output grid cell at its geographical position. The grid-based setup significantly increases the model computation time. While the conventional ArcSWAT model run takes 30 seconds on a single 2.67 GHz processor, the SWATgrid setup lasts about 12 hours per year of simulation; therefore calibration using existing guidelines is impractical.

A time efficient procedure to calibrate grid-based setups was evaluated in a lowland catchment in Northern Germany. An ArcSWAT interface was applied to provide an initial, un-calibrated sub-watershed setup. Afterwards, the most sensitive parameters to water balance were obtained using SWAT-CUP. The sub-watershed setup then was calibrated with established manual and automatic calibration techniques. The resulting parameter set was transferred to a grid-based setup using the SWATgrid interface.

The Bünzau catchment, a sub-watershed of the River Elbe, served as a test site to evaluate the proposed methodology. Model performance according to (Moriasi et al., 2007) was derived using statistical indices (RSR, R^2, NSE and PBIAS). All indices showed a satisfactory model performance.

Daily discharge derived from the grid configuration matched well with the sub-watershed discharge (ArcSWAT setup) at the catchment outlet ($R^2 = 0.99$). Thus, established sub-watershed calibration techniques (Santhi et al., 2001; Moriasi et al., 2007; Neitsch et al., 2011b) can be used to obtain a parameter set for a grid-based SWAT setup. The results presented, however, are limited to the study area; further studies could compare this calibration method with a "real" grid-based model calibration to confirm these findings.

Chapter 4

Development of a grid-based version of the SWAT landscape model

H. Rathjens, N. Oppelt, D. D. Bosch, J. G. Arnold, and M. Volk

Abstract

Integrated river basin models should provide a spatially distributed representation of basin hydrology and transport processes to allow for spatially implementing specific management and conservation measures. To accomplish this, the Soil and Water Assessment Tool (SWAT) was modified by integrating a landscape routing model to simulate water flow across discretized routing units. This paper presents a grid-based version of the SWAT landscape model that has been developed to enhance the spatial representation of hydrology and transport processes. The modified model uses a new flow separation index that considers topographic features and soil properties to capture channel and landscape flow processes related to specific landscape positions. The resulting model is spatially fully distributed and includes surface, lateral, and groundwater fluxes in each grid cell of the watershed. Furthermore it more closely represents the spatially heterogeneous distributed flow and transport processes in a watershed. The model was calibrated and validated for the Little River Watershed (LRW) near Tifton, Georgia (USA). Water balance simulations as well as the spatial distribution of surface runoff, subsurface flow and evapotranspiration are examined. Model results indicate that groundwater flow is

the dominant landscape process in the LRW. Results are promising and satisfactory output was obtained with the presented grid-based SWAT landscape model. Nash-Sutcliffe model efficiencies for daily stream flow were 0.59 and 0.63 for calibration and validation periods and the model reasonably simulates the impact of the landscape position on surface runoff, subsurface flow and evapotranspiration. Additional revision of the model will likely be necessary to adequately represent temporal variations of transport and flow processes in a watershed.

4.1   Introduction

River basin models are valuable tools for examining the impact of land use and management on landscape hydrology, sediment transport and water quality. The Soil and Water Assessment Tool (SWAT) has proven to be a suitable tool under many landscape conditions and in most applications the prediction accuracy was satisfactory for obtaining knowledge of the hydrologic system and the watershed processes (Arnold and Fohrer, 2005; Gassman et al., 2007). However, previous studies showed that the assessment of the effects of conservation practices on watershed-scale water quality relies strongly on the flow and transport models used (e.g., Mausbach and Dedrick, 2004). The SWAT model typically utilizes a hydrologic response unit (HRU) approach. The watershed is divided into sub-watersheds which are further subdivided into HRUs. However, the SWAT routing command language enables the model to use an HRU, a representative hillslope or a grid cell configuration, alone or in combination, to model a watershed (Arnold et al., 1994, 2013). Nevertheless, SWAT uses the HRU configuration as the primary discretization scheme (Gassman et al., 2007; Arnold et al., 2013) and all GIS (Geographic Information System) input interfaces use the computationally efficient HRU discretization. Thus, there are only few SWAT applications and studies which actually have used a different discretization approach (e.g., Manguerra and Engel, 1998; White et al., 2009; Arnold et al., 2010; Rathjens and Oppelt, 2012a,b).

Within the HRU approach all areas in a sub-watershed with the same combination of soil, topography and land use are lumped to form an HRU. The HRUs represent percentages of the sub-watershed area and are not spatially related. Water, sediment and agricultural chemical yields generated in the HRUs are currently routed directly into the stream channel and SWAT is not able to model flow and transport from one landscape position to another prior to entry into the stream. The non-spatial character of the HRUs and the inability to model transport processes in the land-phase of the hydrologic cycle (Neitsch et al., 2011b) have been identified as key weaknesses of the model (e.g., Gassman et al., 2007; Arnold et al., 2010; Bosch et al., 2010). To fulfill the

requirements of river basin management, integrated models should provide a spatially distributed representation of basin hydrology and transport processes (Arnold et al., 2010; Bosch et al., 2010). The incorporation of greater spatial detail into SWAT has therefore been investigated with the focus on (1) developing routing capabilities between landscape units (Volk et al., 2007; Arnold et al., 2010) and (2) developing a grid-based SWAT model setup (Rathjens and Oppelt, 2012b).

The newly developed SWAT landscape model is able to capture the hydrologically different channel and landscape flow and transport processes related to specific landscape positions (Arnold et al., 2010). The model links watershed processes from the hillslope to the watershed scale using the concept of hydrologic landscape units (divides, hillslopes, floodplains; see Volk et al., 2007) and routes surface runoff, lateral subsurface flow, and shallow groundwater flow between these landscape routing units. The model was tested by Arnold et al. (2010) and Bosch et al. (2010); both studies concluded that additional development and testing of the SWAT landscape model is necessary to confirm model operation. In particular, the landscape model may require additional detail to properly describe interactions between soil surface, vadose zone, and groundwater to accurately represent the hydrology in landscapes where subsurface processes dominate (Bosch et al., 2010). The results are, however, "encouraging" (Bosch et al., 2010) and show a realistic representation of landscape flow and transport processes in a watershed. A detailed description of the landscape routing model is given by Arnold et al. (2010).

Understanding the two mechanisms of landscape and channel network transport is crucial for obtaining knowledge of the hydrologic system of a watershed (e.g., Robinson et al., 1995; D'Odorico and Rigon, 2003; Drewry et al., 2006). Many studies have focused on analyzing the effects of landscape processes on the hydrologic response in a watershed by examining differences between landscape and channel flow travel times (e.g., van der Tak and Bras, 1990; Rinaldo et al., 1995; D'Odorico and Rigon, 2003). They concluded that in small to medium size watersheds the share of landscape and channel processes is essential to estimate streamflow at the outlet, whereas in larger river basins landscape processes are less significant than channel and floodplain processes. Studies examining the spatial variability of landscape and channel processes within watersheds (e.g., Rinaldo et al., 1991; Saco and Kumar, 2002) suggest that it is more realistic to use spatially varying parameters to represent the different flow processes. Therefore, hydrologic models require a spatially detailed description of landscape and channel flow processes controlling runoff generation and routing that can be provided by a grid-based approach.

There are, however, advantages and disadvantages for both, the grid and the commonly used HRU method. The HRU approach inherent in the current landscape model provides

a fast and numerically efficient model, but leads to a loss of spatial information during modeling and does not account for landscape position. This might be important for existing applications, for example when studying diffuse matter transport in agricultural areas. The grid configuration enables the model to simulate the impact of landscape position on management, such as conservation measures, plant growth, crop yields and runoff in spatial detail (Arnold et al., 2010). The appropriate spatial resolution and discretization method depends on the purpose of modeling and the availability of data sources. If the model's aim is the replication of aggregated events (e.g., monthly values at the watershed outlet) in a data scarce area the HRU approach may be adequate. But if the modeler's scope is a spatial description of a hydrologic system (e.g., detection of critical source areas) a spatially distributed model is recommended, because spatial patterns of topography and subsurface characteristics often exert significant control over hydrological processes within a watershed (Schulz et al., 2006).

Furthermore, the process of calibrating a model at stream gages does not necessarily improve the spatial accuracy of the model (e.g., Arabi et al., 2006; White et al., 2009). Data collected at discrete locations contain no information concerning the source, only that it must have originated somewhere upstream. Therefore, spatial model results can be used to refine the model and help to detect disregarded processes, when spatial patterns of model output indicate that the model is not representing the system's behaviour adequately (Bennett et al., 2013).

The purpose of this study was to develop a grid-based, spatially distributed hydrologic model that represents channel and landscape transport mechanisms and includes surface, lateral, and groundwater fluxes in each grid cell of the watershed. Prior grid applications (e.g., White et al., 2009; Rathjens and Oppelt, 2012b) are characterized by the lack of landscape flow routing between grid cells (i.e., interaction between grid cells was part of in-stream processes in the routing phase) or used a constant coefficient for each landscape unit for partitioning landscape and channel flow (Arnold et al., 2010). Therefore, an index of hydrologic similarity used by TOPMODEL (Beven and Freer, 2001) was modified to differentiate channel and landscape processes. Stepwise testing in experimental watersheds at various scales and under different hydrologic, climatic and topographic conditions will be developed to evaluate the model. The testing will include (1) evaluation of model output at discrete locations (i.e., stream gages), (2) qualitative, and (3) quantitative analysis of hydrologic model output at the grid scale, (4) examination of water quality at stream gages, and (5) at the grid scale, and (6) testing of in-stream processes.

Here we cover the first two points; in particular, it is the aim of this paper (1) to present a grid-based version of the SWAT landscape model, (2) to test the hydrologic components

of the SWAT landscape model at a stream gage and at the grid-scale, and in addition (3) to analyze the impact of a new parameter that controls the proportions of channel and landscape flow in the watershed. The model is evaluated by comparing observed and simulated daily discharge at the catchment outlet and analyzing the spatial distribution of simulated surface runoff, subsurface flow and evapotranspiration. The study area is the Little River Watershed (LRW), a coastal plain watershed near Tifton (Georgia, USA).

4.2 Materials and methods

4.2.1 Study area

The Little River Watershed (LRW) is located near Tifton in Central South Georgia (see Figure 4.1). It covers an area of 334 km^2 and is characterized by a relatively flat topography and a dense stream network (1.54 km·km^{-2}). The streams are surrounded by broad, flat alluvial floodplains, river terraces and gently sloping uplands with gradients of less than 5 % and channel slopes ranging between 0.1 and 0.5 % (Sheridan, 1997).

Figure 4.1 gives an overview of the LRW stream network, topography, land use and soil type distributions. Land use types occurring in the LRW are row crop agriculture, pasture and forage, upland forest, riparian forest, urban land and water areas. Riparian forest wetlands dominate the landscape close to the stream channels, while upland areas are mostly characterized by agricultural use (Bosch et al., 2004). The most common soil types are sands and sandy loams with high infiltration rates, which are underlain by the shallow, relatively impermeable Hawthorne formation. This formation restricts downward movement of water and promotes lateral movement of shallow groundwater from uplands to the stream channels (Sheridan, 1997; Cho et al., 2013).

The climate is classified as humid subtropical with mean annual precipitation of 1208 mm (1922-1988) and a mean annual temperature of 19.1 °C (Sheridan, 1997). Rainfall often occurs as short-duration, high-intensity convective thunderstorms during midsummer and winter months (Bosch et al., 1999).

Hydrology and water quality of the LRW have been monitored since 1967 (Sheridan, 1997). Additionally, many research projects including several SWAT related studies (e.g., Bosch et al., 2004; Feyereisen et al., 2007; Cho et al., 2009, 2013) have investigated water quantity and quality aspects during the past decades (see Bosch et al., 2010). Bosch et al. (2010) tested the SWAT landscape model in a sub-basin of the LRW. A frequently reported difficulty when modeling the LRW is the saturation condition
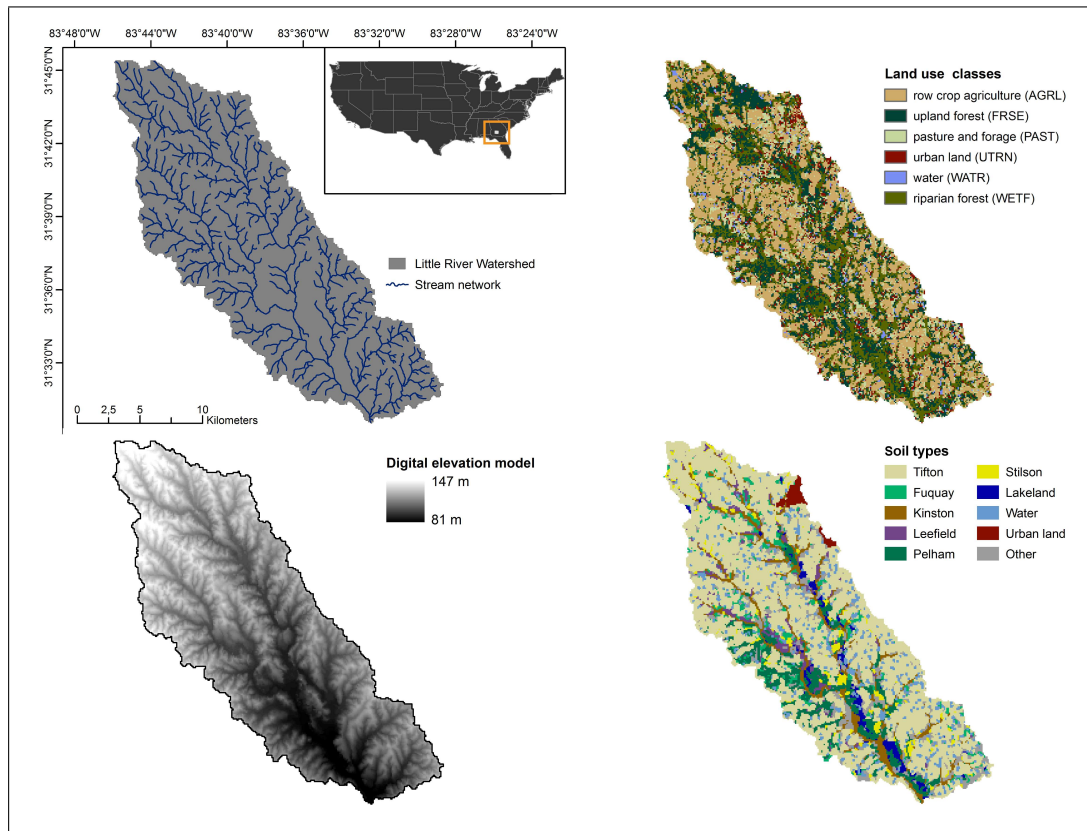
FIGURE 4.1: Overview of the Little River watershed near Tifton in Georgia (USA), its stream network, digital elevation model, and land use and soil maps.

of the alluvial aquifer (e.g., Shirmohammadi et al., 1986; Bosch et al., 2004). Runoff processes in the LRW are mainly characterized by infiltration excess overland flow, but saturation excess flow dominates when the shallow aquifer and the vadose zone are near saturation, which is a normal condition from December to April. SWAT considers primarily infiltration excess runoff mechanisms (White et al., 2009) and thus previous studies underpredicted the observed data during saturated conditions and overpredicted discharge during dry conditions, while further calibration of the models would likely yield mixed results (Bosch et al., 2004).

4.2.2 SWAT and the SWAT landscape model

SWAT (Arnold et al., 1998) is a catchment-scale model developed to simulate hydrology and water quality under varying land use and management conditions. The simulated hydrologic processes include surface runoff, percolation, lateral and shallow groundwater flow, evapotranspiration, snow melt, transmission losses from streams, channel routing and water storage in and losses from ponds. A detailed description of all components can be found in Arnold et al. (1998) and Neitsch et al. (2011b).

SWAT divides the hydrology of a watershed into two major phases: (1) the land phase of the hydrologic cycle controls the amount of water entering the channel. (2) The routing phase determines the movement of water through the channel network to the watershed outlet (Neitsch et al., 2011b). The current SWAT version does not distinguish individual routing units in the land phase of the hydrologic cycle. Accordingly, the model is not able to simulate runoff and infiltration processes that typically occur in a landscape. Volk et al. (2007) and Arnold et al. (2010) developed a landscape routing method that enables surface, lateral and groundwater flow interaction across the landscape between divides, hillslopes and floodplains. The model uses a coefficient for each landscape unit to partition the amount of flow into landscape and channel flow.

The grid-based version of the SWAT landscape model refines the concept of the three discrete landscape units and uses a modified version of a topographic index that ranges between 0 and 1 to spatially describe the landscape position of each grid cell. Valley and floodplain grid cells have values close to 1, while grid cells near the divide have values close to 0. The grid landscape routing model computes surface runoff, lateral and shallow groundwater flow for each grid cell individually. While Arnold et al. (2010) used a constant flow separation ratio, the new grid-based model estimates spatially distributed proportions of channel and landscape flow with the modified topographic index.

4.2.2.1   Surface runoff

The model simulates surface runoff using the curve number method. To determine velocity (V_s) and ultimately travel time (trt), Manning's equation is used assuming a one-meter overland flow strip (see also Volk et al., 2007; Arnold et al., 2010):

$$V_{s,i} = q_{s,i}^{0.4} \cdot \tan(\beta_i)^{0.3} \cdot \eta_i^{-0.6}, \quad i = 1, \ldots, n,$$

where n is the number of grids in the watershed and i is the number of a particular grid cell. $q_{s,i}$ is the flow rate, β_i is the slope angle, and η_i is Manning's n. Travel time [h] is

$$trt_i = sl_i \cdot (3600 \cdot V_{s,i})^{-1},$$

where sl_i is the slope length. Infiltration is calculated by multiplying the travel time by the saturated hydraulic conductivity:

$$I_i = trt_i \cdot K_i + R_{c,i}, \quad i = 1, \ldots, n,$$

where I_i is infiltration, K_i is saturated hydraulic conductivity, and $R_{c,i}$ is roughness storage.

4.2.2.2 Lateral flow

The model calculates lateral flow volumes with a kinematic storage model (Arnold et al., 1998) as a function of saturated hydrologic conductivity, slope, slope length, and porosity (see also Volk et al., 2007; Arnold et al., 2010):

$$Q_{lat,i} = 0.048 \cdot SW_i \cdot K_i \cdot \tan(\beta_i) \cdot (\phi_{d,i} \cdot sl_i)^{-1}, \quad i = 1, \dots, n,$$

where SW_i is soil water, and $\phi_{d,i}$ is porosity. The model also estimates surface seeps during saturated conditions, which is considered as surface run-on to the next landscape unit. Lateral flow (summed from each soi layer) flows to the adjacent downslope grid cell and is distributed to each soil layer. When water enters the adjacent downslope grid cell, it is subject to soil evaporation, plant water uptake, lateral soil flow, percolation and groundwater recharge (Arnold et al., 1998).

4.2.2.3 Shallow groundwater

Groundwater flow is simulated as routing through a series of linear storage elements (i.e., grid cells) using the classic linear tank storage model (e.g., Brutsaert, 2005). In addition to routing flow to the next grid cell, water may also be lost to groundwater evaporation or to seepage to the deep aquifer.

4.2.2.4 Landscape routing and channel interaction

Surface runoff and subsurface flow from each grid cell is routed through the landscape or contributes to streamflow. The share of landscape and channel flow is estimated for each grid cell individually with the modified topographic index (see next section).

4.2.3 Spatial distribution of landscape and channel flow

The SWAT landscape model enables the distribution of runoff between grid cells in the land-phase of the hydrologic cycle. This raises the question which part of the flow is routed as channelized flow and which part is routed through the landscape. The concepts of hydrologically sensitive areas (HSAs, e.g., Walter et al., 2000; Agnew et al., 2006), morphological types of channel heads (e.g., Montgomery and Dietrich, 1994) and

channel head detection by average source areas (Jaeger et al., 2007) were selected as useful methods to develop an index for partitioning landscape and channel flow.

HSAs are areas within a watershed where the probability that runoff will occur is high. The importance of runoff generating areas for watershed management is well documented in the literature. These areas have commonly been identified using topographic indices (e.g., Beven and Kirkby, 1979; O'Loughlin, 1986; Beven and Freer, 2001; Lyon et al., 2004). Agnew et al. (2006) used a topographic index (λ) that considers variations in slope and soil properties to detect HSAs. They found that the general patterns of high hydrologic sensitivity are similar to those of high λ values. The topographic index they used takes the form

$$\lambda_i = \ln \left(\frac{A_i}{\tan\left(\beta_i\right) \cdot K_i \cdot Z_i} \right) \in \mathbb{R}_{>0}, \qquad i = 1, \ldots, n, \tag{4.1}$$

where n is the number of grids in the watershed and i is the number of a particular grid cell. λ_i is the topographic index [$\ln(\mathrm{d}\ \mathrm{m}^{-1})$], A_i is the upslope contributing area per unit contour length [m], β_i is the local surface topographic slope angle, K_i is the mean saturated hydraulic conductivity of the soil [$\mathrm{m}\ \mathrm{d}^{-1}$] and Z_i is the soil depth [m]. λ can be easily calculated for each grid cell in a watershed and solely requires a DEM and soil data that are necessary for SWAT modeling (see also Agnew et al., 2006). Grid cells with high λ_i values are expected to have a high probability to generate runoff and to be dominated by channel flow.

Channel heads represent a boundary between hillslope and channels and can be defined as the initiation of a channel (Montgomery and Dietrich, 1989). They tend to have characteristic morphologic forms and have been classified as either gradual (a swale that gradually changes into a channel) or abrupt (channel initiation caused by seepage water and erosion). Both abrupt and gradual channel heads are likely to occur in a watershed. However, Montgomery and Dietrich (1989) stated that depending on climate, topography and soil properties, one of the channel head types is likely to be dominant in a watershed. To reasonably represent the dominant channel head type two modifications of λ were developed in this study. First, λ is transformed into two normalized indexes:

$$\lambda_{\mathrm{norm},i}^{a} = \frac{\lambda_i}{\max_{i=1,\ldots,n}\{\lambda_i\}} \in (0,1] \quad \text{and} \tag{4.2a}$$

$$\lambda_{\mathrm{norm},i}^{g} = \frac{\lambda_i - \min_{i=1,\ldots,n}\{\lambda_i\}}{\max_{i=1,\ldots,n}\{\lambda_i\} - \min_{i=1,\ldots,n}\{\lambda_i\}} \in [0,1], \qquad i = 1,\ldots,n. \tag{4.2b}$$

where $\lambda_{\mathrm{norm}}^{a}$ is used for watersheds where abrupt channel heads dominate and $\lambda_{\mathrm{norm}}^{g}$ is used for watersheds dominated by gradual channel heads.

Second, λ_{norm}^a and λ_{norm}^g are adjusted to realistically represent the position of channel head locations in the watershed. Channel heads represent the major boundary between landscape and channel flow processes. Thus, the channel head location is a crucial parameter to realistically represent flow and transport processes in a watershed. Jaeger et al. (2007) stated that an average source area size based on field surveys may provide the most practical method for identifying channel head locations. Therefore, the drainage density (DD [km^{-1}]) of the watershed is used to adjust λ_{norm}^a and λ_{norm}^g values. The drainage density is defined by the length [km] of all channels in the watershed divided by its total drainage area (DA [km^2]). Therefore, the smallest λ_{norm}^a and λ_{norm}^g values are set to zero (i.e., no channel flow) until the sum of all $\lambda_{\text{norm},i}^a$ and $\lambda_{\text{norm},i}^g$ values multiplied with the unit contour length of the current grid cell divided by the total drainage area matches the drainage density of the watershed. The resulting normalized indexes can be stated as $\lambda_{DD,i}^a, \lambda_{DD,i}^g \in [0,1]$, $i = 1, \ldots, n$ satisfying

$$DD \approx \frac{\sum_{i=1}^n \lambda_{DD,i}^a l_i}{DA} \approx \frac{\sum_{i=1}^n \lambda_{DD,i}^g l_i}{DA}, \tag{4.3}$$

where l_i [km] is the unit contour length of the current grid cell.

The indexes solely differ in the method selected for normalization (see Eq. 4.2a and 4.2b). Equation (4.2a) leads to discontinuous distribution of channelized flow fractions, whereas equation (4.2b) results in a continuous distribution. Hence, $\lambda_{DD,i}^a$ represents the fraction of channelized flow for grid cell i in a watershed dominated by abrupt channel heads and $1 - \lambda_{DD,i}^a$ represents the fraction of landscape flow. The same applies for $\lambda_{DD,i}^g$ in watersheds dominated by gradual channel heads.

4.2.4   Modelling framework

The interface SWATgrid (Rathjens and Oppelt, 2012b) was used for developing grid-based SWAT model input using weather data and spatially distributed geographic datasets (digital elevation model (DEM), soil and land use data). An overview of the essential input data sources is given in Table 4.1. Differences between the weather stations can dominate the spatial model output. To spatially analyze the output of the SWAT landscape model, values of all weather stations were aggregated to one data set and integrated in the simulation.

SWATgrid divides the watershed into linked grid cells. Flow paths are determined from the DEM using the digital landscape analysis tool TOPAZ (Garbrecht and Martz, 2000), and runoff from a grid flows to one of the eight adjacent grid cells. A small grid size is necessary to ensure an accurate representation of the flat topography in the

LRW. A small grid size, however, leads to an increase of computation time and memory requirements of the model. As a compromise between an accurate spatial representation of landscape patterns and a manageable model, DEM, soil and land use data were resampled to a resolution of 100 m (1 ha).

Grid-based simulations with the SWAT landscape model were conducted for a five-year period from 2004 to 2008, plus a two year warm-up period from 2002 to 2003. The accuracy of simulated streamflow, water budgets and spatial patterns of model output were examined for this period. Three model setups were developed to evaluate the grid-based landscape model and to analyse the sensitivity of the flow separation ratio. The primary setup (*Model 1.0DD*) is used for the evaluation of the grid-based landscape model and the additional setups (*Model 1.5DD* and *Model 0.5DD*) are used for analyzing the impact, sensitivity and uncertainty of the flow separation ratio on model output.

Model 1.0DD uses the original drainage density DD and λ_{DD}^{a} to represent the share of channelized and landscape flow in the watershed as realistic as possible. *Model 1.0DD* was calibrated manually to fit simulated to observed daily discharge. The grid discretization requires more computation time than the commonly used HRU approach; the LRW model takes approximately one hour per simulated year on a single 2.67 GHz processor. As a consequence, manual calibration was performed by comparing simulated and observed discharge at the watershed outlet for the year 2004 only. The calibrated parameter set was validated using the time period from 2005 to 2008. A sensitivity analysis for SWAT LRW simulations was previously conducted by Bosch et al. (2004) and Cho et al. (2013). Their results showed a strong influence of groundwater parameters. Based on these studies and a manual sensitivity analysis five parameters were

TABLE 4.1: Data sources for the LRW (downloadable at ftp://www.tiftonars.org/).

Data type	Scale / Resolution	Source	Data description and usage
Topography	30 m	Georgia GIS Data Clearinghouse	Digital Elevation Model (DEM), model input
Land use	30 m	Sullivan et al. (2007)	Land use classification based on Landsat 7 imagery (20 Jul 2003), model input
Soils	1 : 12 000	Soil Survey Geographic Database (SSURGO)	Soil physical properties, model input
Weather	25 stations (rainfall), 2 stations (temperature, wind speed, relative humidity, solar radiation)	Bosch et al. (2007b)	Daily weather data (1 Jan 2004 to 31 Dec 2008), model input
Streams	7.5 minute quadrangle	Sullivan et al. (2007)	Mapped stream network, model validation
Discharge	1 Station	Bosch and Sheridan (2007)	Daily discharge data, model calibration and validation

TABLE 4.2: SWAT input parameters chosen for hydrologic calibration and final calibrated values.

Parameters	Default	Lower limit	Upper limit	Value
ESCO.bsn	0.95	0.0	1.0	1.00
SURLAG.bsn	4.0	0.05	24	0.15
GW_DELAY.gw	31.0	0.0	500	0.75
ALPHA_BF.gw	0.048	0.0	1.0	0.96
GWQMN.gw	0.0	0.0	5 000	50.0

chosen for model calibration: soil evaporation compensation factor (ESCO), groundwater parameters (groundwater delay time (GW_DELAY), baseflow alpha factor (ALPHA_BF), threshold depth of water in the shallow aquifer required for return flow to occur (GWQMN)), and surface runoff lag coefficient (SURLAG). Table 4.2 shows the parameters selected for calibration, their ranges and their calibrated values. A detailed description of each parameter is provided by Arnold et al. (2013). Standard test statistics recommended by Moriasi et al. (2007) (i.e., the coefficient of determination (R^2), Nash-Sutcliffe efficiency (NSE, see Nash and Sutcliffe, 1970) and percent bias (PBIAS, see Gupta et al., 1999)) as well as visual comparisons of observed and simulated data were used to evaluate daily, monthly and yearly streamflow simulations. At this stage, it was not possible to perform a spatially distributed calibration of the model. Thus, spatial distributions of model output were evaluated qualitatively. It was examined whether spatial patterns of model output reasonably reflect hydrologic processes that are expected to occur in the landscape.

In *Model 1.5DD* and *Model 0.5DD* the drainage density of the watershed, which determines the proportions of channel and landscape flow, was modified to analyze the sensitivity and uncertainty of the flow separation ratio. The drainage density in *Model 1.5DD* is 1.5 times larger than in *Model 1.0DD*, whereas in *Model 0.5DD* it is half as large; all remaining parameters were set to the same values as in *Model 1.0DD*. The factors 0.5 and 1.5 correspond to previously observed variations in drainage density (e.g., Gregory and Walling, 1968; Moglen et al., 1998). Thus, *Model 0.5DD* and *Model 1.5DD* results indicate the range of uncertainty of the proposed approach. A comparison was made between simulated results obtained using *Model 1.0DD*, *Model 1.5DD* and *Model 0.5DD*. Time series of daily simulated streamflow at the watershed outlet as well as spatial patterns of model output were compared.

4.3   Results and discussion

4.3.1   Spatial analysis and differences of the partitioning ratios

The development of a grid-based SWAT landscape model requires the spatial partitioning of landscape and channel flow to realistically represent flow and transport processes in a watershed. In this paper the topographic index λ (Eq. 4.1) that has been commonly used to identify runoff generating areas was modified to obtain estimates of partitioning ratios (see Eq. 4.2a and 4.2b). Figure 4.2 shows the spatial and frequency distributions of λ, λ_{DD}^a and λ_{DD}^g values in the LRW. The histograms (Figure 4.2d-f) visualize the effects of normalization and adjustment to the drainage density. The overall share of channel and landscape flow is determined by the drainage density of the watershed and is the same for λ_{DD}^a and λ_{DD}^g, but the ratios differ in their frequency distributions. While calculations using the index λ_{DD}^g result in few cells with no channel flow λ_{DD}^a calculations results in a large proportion of grid cells with no channel flow (i.e., $\lambda_{DD,i}^a = 0$) and in compensation a small number of grid cells with a high share of channel flow (≥ 0.3). Both indexes realistically represent the share of channel and landscape flow determined by the drainage density of the watershed. Their spatial patterns suggest a stream network (Figure 4.2a-c) similar to the mapped network (see Figure 4.1).

Channel heads represent the boundary between landscape and channel flow and are thus considered as a crucial parameter to realistically represent flow and transport processes in a watershed. The methods selected for normalization result in a continuous (λ_{DD}^g) and discontinuous distribution (λ_{DD}^a) of channelized flow fractions (see Figure 4.2e and f), causing abrupt and gradual channel heads in the corresponding maps (see Figure 4.2b and c). Previous channel initiation studies by Montgomery and Dietrich (1988, 1989) found that in basins with gentle slopes and infiltration excess overland flow, which applies for the LRW, channel heads caused be seepage erosion occur more frequently than gradual channel heads. Therefore, the λ_{DD}^a map is used to evaluate the grid-based SWAT landscape model.

Both landscape and channel processes are related to heterogeneously distributed parameters within the watershed (such as soil properties, land use, topography, stream roughness, and other physical properties). The newly developed separation index considers this spatial variability within watersheds and shows the capability to realistically represent spatial distributions of flow and transport processes in the LRW. There is, however, a remaining uncertainty inherent to the analysis of flow and transport processes in watersheds. The results should be considered as a rough estimate of landscape and channel flow separation; future studies should focus on the identification of channel
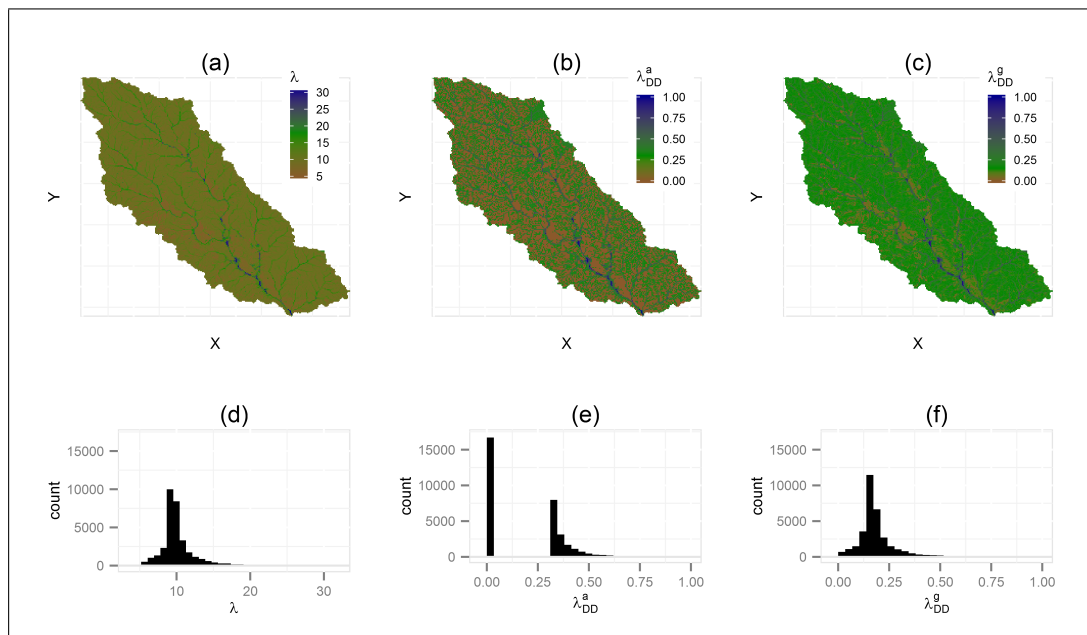
FIGURE 4.2: Spatial and frequency distributions of the topographic indexes λ, λ_{DD}^a and λ_{DD}^g used for channel and landscape flow separation in the LRW.

head locations in different landscapes and the validation of the proposed flow separation methodology.

4.3.2   Model evaluation at the watershed outlet

4.3.2.1   Calibration and validation results

One aim of this research was to assess how well the new grid-based landscape configuration performs. For this purpose simulations were conducted for the period from 2004 to 2008 using λ_{DD}^a for estimating the share of landscape and channelized flow (*Model 1.0DD*). Precipitation in the LRW is variable from year to year with a long term (1922-1988) annual mean of 1208 mm. During the simulation period precipitation varies between 884 and 1204 mm (2004: 1204 mm, 2005: 1197 mm, 2006: 884 mm, 2007: 896 mm, 2008: 1116 mm). Distribution within the year is also highly variable, although the fall months are typically dry (Sheridan, 1997).

Measures of model performance including PBIAS, R^2 and NSE values are listed in Table 4.3. They indicate satisfactory to good model performance during both calibration and validation periods. Monthly NSE and R^2 values are better than daily values, a result that is often observed in model applications (Moriasi et al., 2007).

The hydrograph of daily streamflow for the 5-year period (see Figure 4.3a) indicates that the grid-based SWAT model simulated daily streamflow satisfactorily in both low and

TABLE 4.3: Summary of performance measures of grid-based *Model 1.0DD* SWAT simulations for the LRW for 2004 (calibration period) and from 2005 to 2008 (validation period).

Periods	Streamflow [mm/a]		PBIAS [%]	NSE		R^2	
	Observed	Simulated		Daily	Monthly	Daily	Monthly
Calibration	297	275	7.18	0.60	0.92	0.59	0.92
Validation	212	193	8.96	0.63	0.79	0.65	0.82
Entire Period	229	210	8.50	0.62	0.81	0.63	0.83

high flow conditions. The model, however, tends to underpredict discharge peaks during the entire period. Confirming the high variability of precipitation from year to year, streamflow also varies significantly between the individual years of the simulation period. In 2004 and 2005, observed streamflow is comparatively high (297 and 433 mm) while from 2006 to 2008 values are lower (139 mm on average). During the drier years zero-flow conditions were observed repeatedly. The model generally predicts the trends in observed data well and a tendency of over-predicting streamflow during zero-flow conditions that was reported by Bosch et al. (2004) and Feyereisen et al. (2007) does not occur. There are, however, differences in magnitude and duration of observed and simulated daily streamflow. In dry years the model generally overpredicts streamflow during wetting-up periods and simulates flow events in periods where none were observed. The observed baseflow component increases slowly, while the simulated baseflow rises too rapidly. The opposite is happening during drying periods, where observed streamflow decreases slowly while the simulated streamflow falls too rapidly. The simulated hydrograph during wetting-up and drying periods indicates an underestimation of the available groundwater storage. Greater groundwater storage would lead to slower filling in the wetting-up period and a longer hydrograph on the falling side. The underestimation of available groundwater storage could be related to the comparatively high precipitation in the calibration year (2004). Saturation occurred throughout this year and groundwater storage capacity is insignificant for model performance. Another factor contributing to the error in simulated daily streamflow was the hydrograph timing, which was observed by Bosch et al. (2004). The simulated hydrograph peaks occur approximately one day prior to the observed peaks; shifting the simulated daily streamflow values one day forward during the entire simulation period increases NSE values from 0.62 to 0.71 and R^2 values from 0.63 to 0.73.

Figure 4.3b displays monthly observed and simulated discharge values. The graphs confirm the differences between simulated and observed streamflow volume during wetting-up and drying periods. The underestimation of streamflow peaks leads to an underestimation of flow volumes in wet months; the model, however, performs well in average conditions, which is confirmed by monthly NSE and R^2 values (see Table 4.3).
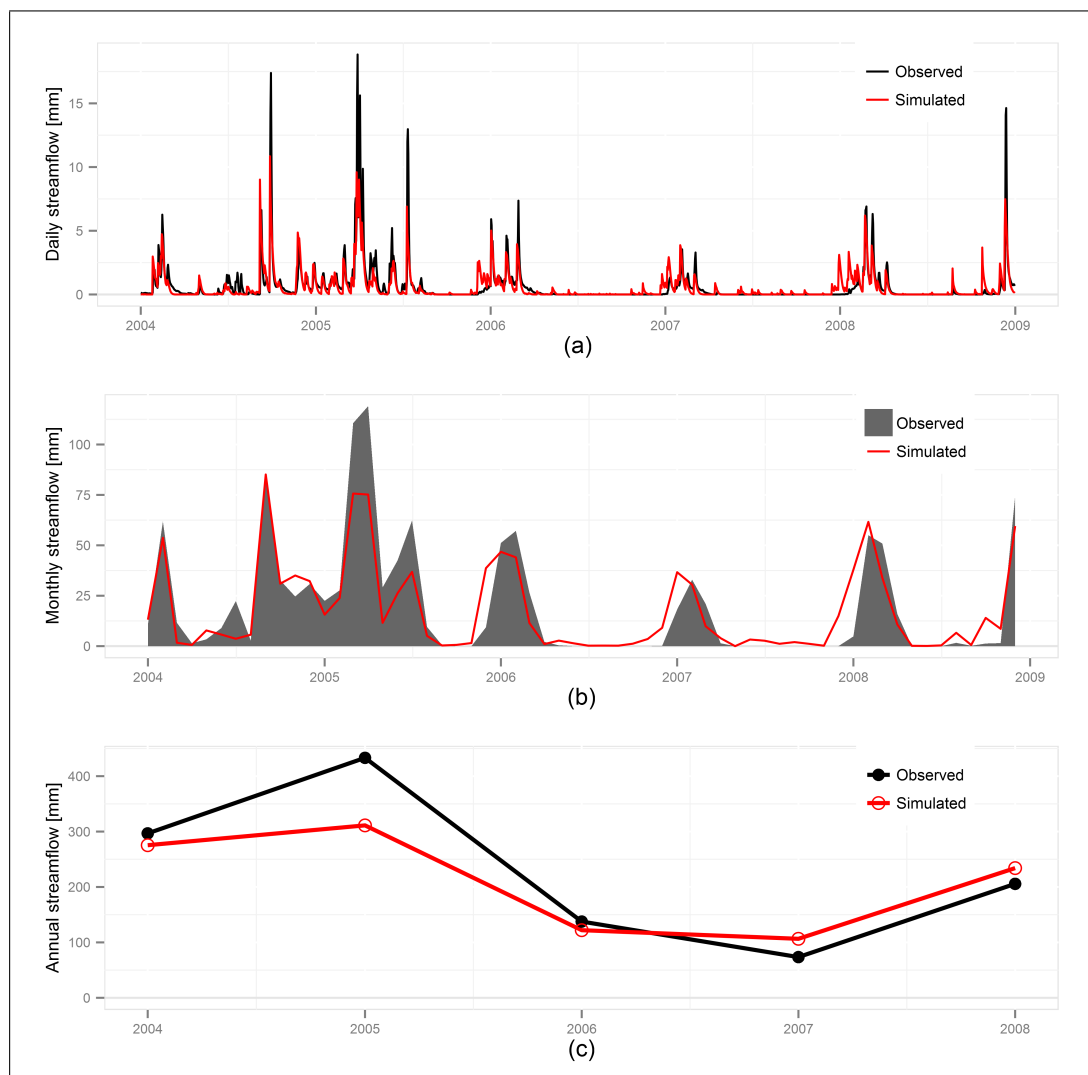
FIGURE 4.3: Observed and simulated (*Model 1.0DD*)(a) daily, (b) monthly and (c) annual total streamflow for the LRW from 2004 to 2008.

The annual time series of observed and simulated streamflow for the simulation period is shown in Figure 4.3c. Visual comparison confirms the calculated PBIAS values. In general, the model tends to underpredict annual discharge, which is mainly caused by the underestimation of discharge peaks during wet periods.

4.3.2.2   Sensitivity of the partitioning ratio

The separation ratio of landscape and channel flow turned out to be a crucial parameter to realistically represent flow and transport processes in a watershed. The impact of the partitioning ratio on streamflow at the watershed outlet is analyzed by comparing the results of *Model 1.0DD*, *Model 1.5DD* and *Model 0.5DD*. Figure 4.4 shows observed and daily streamflow of the three models from 1 Nov 2005 to 30 Apr 2006, a time period including wetting-up, drying, average and peak flow conditions (see also Figure 4.3).
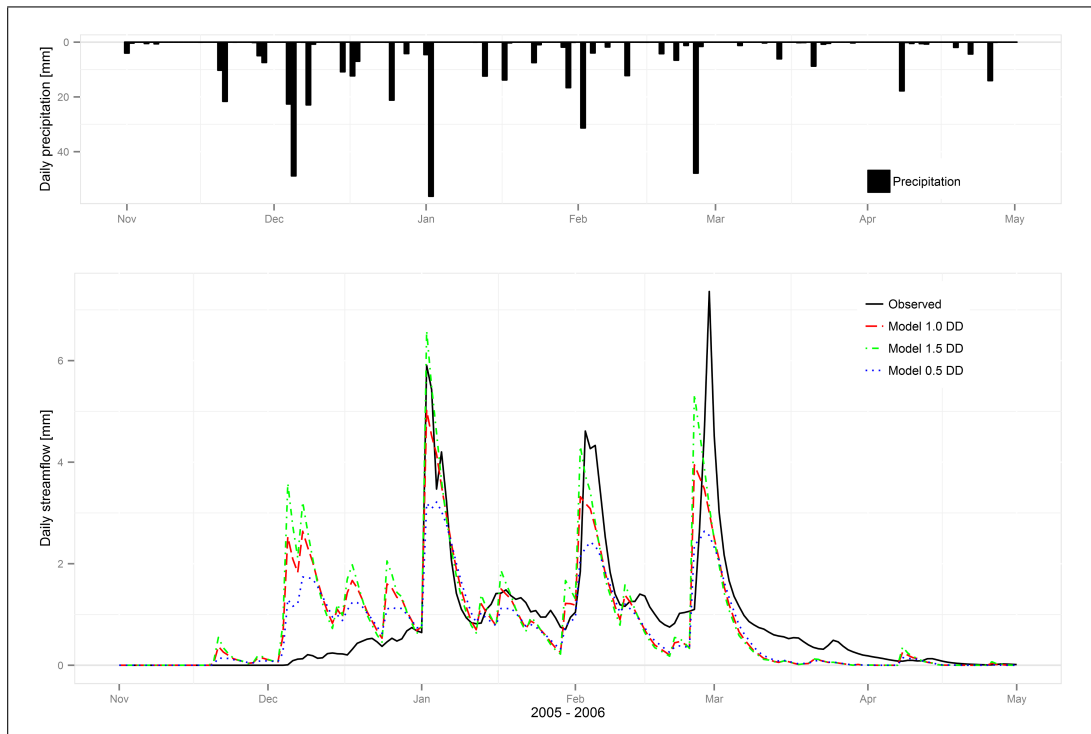
FIGURE 4.4: Precipitation and observed and simulated daily stream flows of *Model 1.0DD*, *Model 1.5DD* and *Model 0.5DD* in the LRW from 1 Nov 2005 to 30 Apr 2006.

Model 1.5DD has a higher share of channel flow than *Model 1.0DD* and the hydrograph responds quickly to precipitation events. As a consequence, *Model 1.5DD* performs worse during wetting-up and drying periods, but simulates streamflow peaks more accurately than *Model 1.0DD*. However, the simulated hydrograph timing is too early. *Model 0.5DD* has the lowest share of channel flow. As a consequence, water remains longer in the watershed and streamflow rises and falls more slowly than *Model 1.0DD*. Accordingly, *Model 0.5DD* simulates discharge during wetting-up and drying periods more accurately than *Model 1.0DD*, but clearly underestimates peak events.

In summary, the simulated hydrographs displayed in Figure 4.4 indicate that the models perform differently depending on the saturation of the watershed. *Model 0.5DD* predicts streamflow most realisticly during wetting-up and drying periods; *Model 1.5DD* realistically simulates discharge peaks when the watershed is saturated; and *Model 1.0DD* shows good performance during average streamflow. These results suggest that landscape and channel flow processes in a watershed vary depending on watershed saturation on temporal scales ranging from a single storm to seasonal fluctuations. Therefore, the prediction of discharge during wetting-up periods still remains a challenge in hydrologic modeling (e.g., Pinol et al., 1997; Beven and Freer, 2001).

The grid-based SWAT landscape model uses an index for flow separation that is based on the topographic index λ (Eq. 4.1) and the drainage density (DD) of the watershed.

TABLE 4.4: Precipitation (P [mm]) events $\geq$ 5 mm, accumulated runoff (Q [mm]) in the five days following the end of the precipitation event, and the ratio of Q to P for the first ten precipitation events between Nov 2005 and Mar 2006.

Event no.	Date	P [mm]	Q [mm]	Q / P
1	20 Nov 2005 – 26 Nov 2005	31.86	0.00	0.00
2	28 Nov 2005 – 3 Dec 2005	12.35	0.00	0.00
3	4 Dec 2005 – 13 Dec 2005	95.07	1.25	0.01
4	15 Dec 2005 – 23 Dec 2005	30.01	3.35	0.11
5	25 Dec 2005 – 7 Jan 2006	86.14	28.37	0.33
6	13 Jan 2006 – 22 Jan 2006	26.43	12.55	0.47
7	23 Jan 2006 – 28 Jan 2006	8.37	5.97	0.71
8	29 Jan 2006 – 6 Feb 2006	53.76	21.71	0.40
9	11 Feb 2006 – 15 Feb 2006	12.23	6.38	0.52
10	18 Feb 2006 – 3 Mar 2006	61.37	31.32	0.51

Implicit in this index is the assumption of a constant upslope area (A_i) at every location in the watershed. This means the model expects downslope flow in the entire landscape, which is clearly not the case when the landscape is dry. During such periods large amounts of rainfall may produce little or no streamflow response at the gauging stations.

Table 4.4 shows the LRW streamflow-precipitation ratio for the first ten precipitation events after a dry period; there is almost no response to the first three events. As the wetting-up progresses the streamflow-precipitation ratio increases before it levels off at a ratio of 0.5. The wetting-up of the watershed leads to saturation and downslope flow of water in the shallow aquifer. Further wetting will start to link unsaturated areas within the watershed. As the wetting-up period continues, the landscape becomes more saturated, the upslope areas that contribute surface and subsurface flow increase and the water yield per unit of rainfall increases in a non-linear way (see Table 4.4). Therefore, it is expected that the effective contributing area varies over time (see also Barling et al., 1994; Pinol et al., 1997; Beven and Freer, 2001) and is not ideally represented by a constant upslope area derived from the DEM. Studies from Dunne and Black (1970), Hewlett and Nutter (1970) and Dunne et al. (1975) confirm these results. They stated that the size of runoff generating areas varies over time with watershed saturation on temporal scales ranging from a single storm to seasonal fluctuations.

In this context, the assumption of a steady drainage density can also be questioned. Moglen et al. (1998) reported that the drainage density is a seasonally variable parameter influenced by the climate, mainly precipitation, in the watershed. They illustrated seasonal changes in drainage density that result from sinusoidal variability in precipitation. The occurrence of zero-flow conditions confirms a seasonal variance of drainage density in the LRW. During dry periods, parts of the watershed do not produce significant downslope flow and channel head locations are expected to move downslope.

Hence, the assumptions of a steady effective upslope area and a steady drainage density limit the model's capability to accurately simulate runoff peaks and discharge during wetting-up periods. A dynamic flow separation ratio could be based on the index used in this study and additionally include a space-time representation of soil or shallow aquifer saturation, the interaction between precipitation and streamflow, and dynamics of the effective upslope areas contributing to runoff generation.

4.3.3   Spatial analysis

A major advantage of the grid-based model is the availability of spatially distributed model output. This section evaluates spatial model output at the grid scale and analyzes the impact of the flow separation ratio on the spatial distribution of model output.

4.3.3.1   Spatial model evaluation

The spatial distribution of *Model 1.0DD* output parameters shows the impact of topography, landscape position, land use classes and soil types on model output. To evaluate the grid-based SWAT landscape model, spatial distributions of surface runoff (SURQ, see Figure 4.5a), lateral flow (LATQ, see Figure 4.5b), groundwater runoff (GWQ, see Figure 4.5c) and evapotranspiration (ET, see Figure 4.5d) were analyzed. At this stage, the model is not spatially calibrated, so the spatial output can not be evaluated quantitatively and was analyzed qualitatively instead.

As expected, the highest SURQ values occur on urban areas. The model simulates more surface runoff in the upland areas than in the floodplain areas adjacent to the channel network. This can be explained by the comparatively steep, mostly agricultural upland areas. However, sands and sandy loams with high infiltration rates dominate in these parts of the watershed and thus, most of the water infiltrates and is not routed through the landscape as surface runoff.

The spatial patterns of LATQ and slope values are similar and the spatial distribution of LATQ values is reasonable. The highest LATQ values occur on the steepest slopes, while almost no lateral flow occurs in the valley bottoms. In the steeper areas the model routes the lateral flow through the landscape, whereas in the flat parts the water percolates to the shallow groundwater aquifer.

In contrast to SURQ and LATQ, GWQ patterns indicate a routing scheme. This means the main portion of flow routed through the landscape is groundwater flow, which increases as the water moves across the watershed from the upland areas to the valleys. Groundwater flow of several upslope grid cells concentrates in grid cells located directly
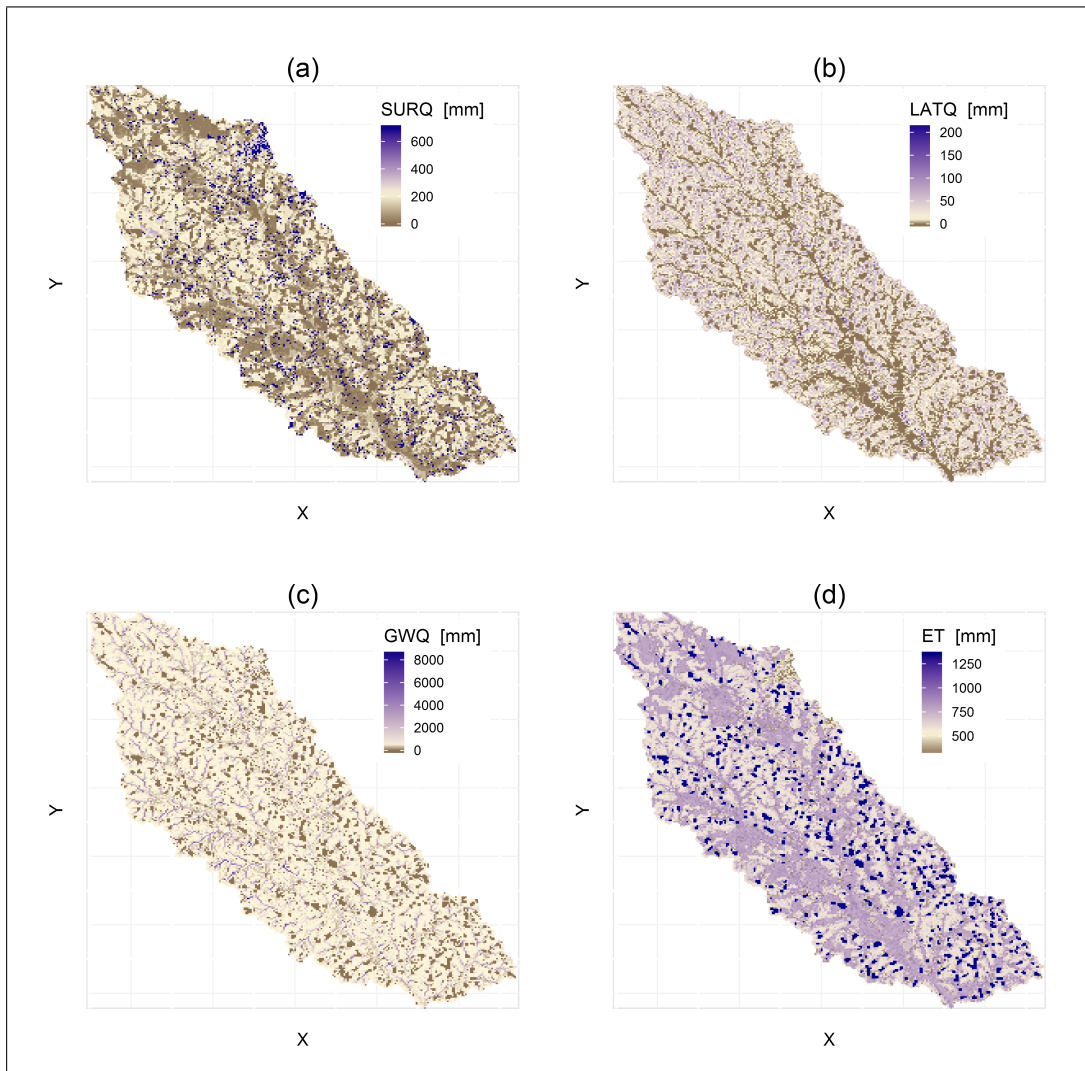
FIGURE 4.5: *Model 1.0DD* simulated average annual (a) surface runoff [mm], (b) lateral runoff [mm], (c) groundwater runoff [mm] and (d) evapotranspiration [mm] in the LRW from 2004 to 2008.

upslope of channel heads, before it enters the stream channel. In these grid cells GWQ values can be extraordinarily high ($\geq$ 5000 mm), although this only affects 55 of 330055 grid cells in the LRW. The amount of groundwater decreases considerably as soon as the water enters a stream channel. As the topographic index λ_{DD}^a determines the position in the landscape where the water is passed from the land-phase to the routing phase, GWQ and λ_{DD}^a (see Figure 4.5c and 4.2d) patterns look similar.

Considering inflow from higher landscape positions, the model produces more ET in the valley bottoms than in the upland areas. Highest ET values occur in the water and forested wetland areas around the channel network, while the urban land and agricultural areas on higher landscape positions produce less ET (see Figure 4.5d).
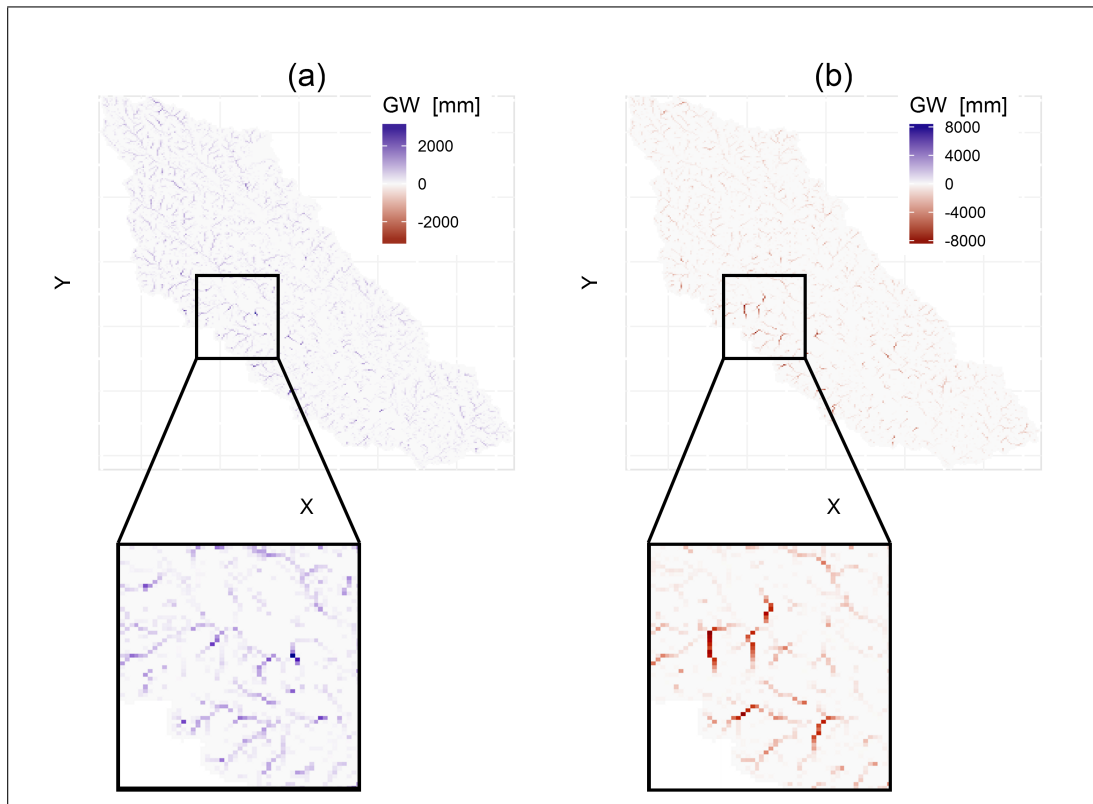
FIGURE 4.6: Differences ((a) *Model 1.0DD − Model 1.5DD* and (b) *Model 1.0DD − Model 0.5DD*) of simulated average annual groundwater runoff [mm] in the LRW from 2004 to 2008.

4.3.3.2   Spatial sensitivity of the partitioning ratio

To spatially analyze the impact of drainage density, channel head location and flow separation ratio on model output, differences in SURQ, LATQ, GWQ and ET between the three models (*Model 1.0DD - Model 1.5DD* and *Model 1.0DD - Model 0.5DD*) were analyzed. Differences in SURQ, LATQ and ET are relatively small and occur in small areas. Therefore, spatial differences of SURQ, LATQ and ET are described in the text and Figure 4.6 solely shows the GWQ difference maps.

In general, the *Model 1.0DD − Model 1.5DD* distributions are dominated by positive values, while the *Model 1.0DD − Model 0.5DD* patterns mainly contain negative values. The higher drainage density in *Model 1.5DD* compared to *Model 1.0DD* results in a lower share of landscape flow and larger amounts of channel flow. The higher drainage density reduces the impact of landscape processes in the watershed and SURQ, LATQ, GWQ and ET values in *Model 1.5DD* are generally smaller than in *Model 1.0DD*. For the same reason the *Model 1.0DD − Model 0.5DD* distributions mainly contain negative values.

The highest differences in SURQ values occur on urban and agricultural land and on steep slopes and high LATQ differences occur at steep slopes in the upland areas. As surface and lateral flow are relatively low in the LRW, SURQ and LATQ differences are small ($\leq$ 10 and 4 mm, respectively). ET differences are in the 40 mm range and mainly occur in the upland areas, where the impact of the flow separation ratio is particularly large. In contrast to the SURQ, LATQ and ET results, GWQ differences are very high (up to 8000 mm). When the drainage density decreases, channel heads move downslope and the share of landscape groundwater flow increases (see Figure 4.6). Thus, differences in GWQ are strongly impacted by differences in channel head locations and indicate a routing scheme that depicts the upslope (*Model 1.0DD − Model 1.5DD*) and downslope (*Model 1.0DD − Model 0.5DD*) movement of channel head locations.

In general, the differences between the model output maps are reasonable and the results show that the flow separation ratio is a crucial parameter for simulating the spatial distributions of surface runoff, subsurface flow processes, and evapotranspiration in a watershed.

4.4   Conclusion

In this study, a grid-based version of the SWAT landscape model was developed to simulate processes across grid cells in the land-phase of the hydrologic cycle. The fully distributed model includes surface, lateral, and groundwater fluxes in each grid cell of the watershed. The model was calibrated and validated for the Little River Watershed (LRW, 334 km^2) near Tifton, Georgia. The results suggest that the grid-based landscape model simulated the streamflow hydrograph at the outlet of the LRW satisfactorily which is confirmed by the performance measures. The new model predicts trends in observed data well and previously reported discrepancies between observed and simulated streamflow e.g., during zero-flow conditions (Bosch et al., 2004; Feyereisen et al., 2007), does not occur. However, model calibration can still be improved. Errors in the simulated streamflow can be attributed to an underestimation of streamflow peaks and an overestimation of streamflow during wetting-up periods. An additional challenge is the extensive computation time associated with the grid based approach, which impedes model calibration.

The new model requires a spatial description of landscape and channel flow processes. For this purpose a flow separation ratio was selected that proved to be a crucial parameter for a plausible representation of flow and transport processes in a watershed. The estimation of the partitioning ratio is based on a topographic index and considers soil properties, topography, the drainage density of the watershed, and the morphology of

the channel heads. The resulting index has shown the capability to plausibly represent the spatial distribution of flow and transport processes in a watershed. The proposed separation index assumes a steady drainage density and a steady size of the upslope area contributing to runoff. However, the results of this study suggest that both assumptions can be questioned. Drainage density and effective upslope contributing areas seem to vary over time with landscape saturation on temporal scales ranging from a single storm event to seasonal fluctuations. The selected separation index is able to reasonably depict spatial variations of flow and transport processes in a watershed, but fails to represent their temporal variations. Comparisons between the measured and simulated hydrographs confirm that a dynamic partitioning ratio would significantly improve the model.

As the availability of spatially distributed model output is a major advantage of the grid-based model, the spatial distribution of the hydrologic components was analyzed qualitatively. The spatial LRW model results indicate that the grid-based landscape model is able to reasonably simulate the impact of the landscape position on surface runoff, subsurface flow and evapotranspiration. To assess the impact of drainage density on model output a total of three models with different drainage densities that were obtained from literature were constructed. Considerable differences in the resulting spatial distributions of flow components and evapotranspiration suggest a strong influence of drainage density and flow partitioning ratio and indicate the range of uncertainty of the proposed approach. Thus, the results presented should be considered as a rough estimate of the spatial distribution of hydrologic components and the presented methodology should be considered as a first step in the development of the grid-based SWAT model. In general, the grid-based SWAT landscape model is able to provide a plausible basis for water quantity and quality simulations when a detailed spatial analysis is required.

However, results presented in this paper are only valid for the LRW. To reduce the range of model uncertainty additional development, calibration and testing of the grid-based SWAT landscape model at various scales with different hydrologic and landscape characteristics is necessary. Future studies will follow the stepwise testing of the model and focus on the quantitative evaluation of hydrologic components, and on the validation of the proposed flow separation methodology in small scale basins. In addition, future research will include the development of a dynamic flow separation ratio and spatial model validation using remote sensing data (e.g., evapotranspiration (see Glenn et al., 2010; Vinukollu et al., 2011) or soil moisture (e.g., Cashion et al., 2005; Pierdicca et al., 2010)). As testing and development of the model is expanded, the full utility of the model will be realized.

Due to the large number of spatial units in large watersheds, computation time of the grid-based model is very long and thus grid-based model development and application seems to be most efficient for small-scale watersheds. Furthermore, the spatial resolution of input data (climate, topography, land use, soil) is often too coarse for detailed grid-based modeling. However, geographic information systems and remote sensing techniques develop rapidly and an increasing amount of spatially and temporally detailed data becomes available. The integration of these data into the SWAT landscape model seems to be very promising for enhanced spatial analysis of environmental issues within a watershed.

4.5   Acknowledgments

Chapter 5

An interpolation and improvement approach for remotely sensed land cover data

H. Rathjens, K. Dörnhöfer, and N. Oppelt

Abstract

Land cover data gives the opportunity to study interactions between land cover status and environmental issues such as hydrologic processes, soil properties, or biodiversity. Land cover data often bases on classification of remote sensing data that seldom provides the requisite accuracy, spatial availability and temporal observational frequency for environmental studies. Thus, there is a high demand for accurate and spatio-temporal complete time series of land cover. In the past considerable research was undertaken to increase land cover classification accuracy, while less effort was spent on interpolation techniques. The purpose of this article is to present a space-time interpolation and revision approach for remotely sensed land cover data. The approach leverages special properties known for agricultural areas such as crop rotations or temporally static land cover classes. The newly developed IRSeL-tool (Interpolation and improvement of Remotely Sensed Land cover) corrects classification errors and interpolates missing land cover pixels in the temporal or spatial dimension. The easy-to-use tool solely requires an initial land cover data set. The IRSeL specific interpolation and revision technique, the data input requirements and data output structure are described in detail. A case

study in an area around the city of Neumünster in Northern Germany from 2006 to 2012 was performed for IRSeL validation with initial land cover data sets (Landsat TM image classifications) for the years 2006, 2007, 2009, 2010 and 2011. The results of the case study showed that IRSeL performs well; including years with no classification data Cohen's kappa values for IRSeL interpolated pixels range from 0.53 to 0.77. IRSeL application significantly increases the accuracy of the land cover data; kappa values rise about 0.08 in average resulting in kappa values of at least 0.84. Considering estimated reliabilities, the IRSeL tool provides a temporally and spatially completed and revised land cover data set that allows drawing conclusions for land cover related studies.

5.1   Introduction

Land cover is a fundamental variable that impacts on and links many parts of the environment (Foody, 2002). Furthermore, it is well established that land cover significantly effects processes related to biogeochemical cycling (Turner and Rabalais, 2003), soil erosion (Ouyang et al., 2010b), water quality (Allan et al., 1997), water quantity (Miller et al., 2002), sustainable land use and biodiversity (Burkhard et al., 2012). DeFries and Eshleman (2004) identified interactions between land cover change and hydrologic processes as a major future research issue. Thus, there is a high demand for continuously available land cover maps. During the past decades, researchers used time series of land cover data for characterising, understanding and evaluating patterns of land cover change. Kroll et al. (2012), for example, used time series of land cover data to detect changes in ecosystem services, Guo and Gifford (2002) estimated the effects of land cover change on soil carbon stocks, Jenerette and Wu (2001) developed an urban land cover change model based on time series of remote sensing land cover data, and Pai and Saraswat (2011) evaluated the impact of land cover change on the hydrologic cycle.

In this context, the terms "land cover" and "land use" are often used synonymously. Land cover is defined as "the observed physical cover of the Earth's surface". In contrast, land use is "characterised by the arrangements, activities and inputs people undertake in a certain land cover type" (FAO, 1997; FAO/UNEP, 1999). Remote sensing has shown the ability to provide a map-like representation of the Earth's land cover status using satellite imagery and image-processing software (e.g., Foody, 2002). The process of land cover mapping is typically based on image classification techniques that convert the spectral response of the Earth's surface into a thematic map depicting land cover classes. Over the last decade remote sensing and GIS (Geographic Information System) developed rapidly and increased the availability of land cover data. Thus, remote sensing became a commonly used source for land cover mapping.

Understanding the significance of land cover as an environmental variable and predicting the effects of land cover change is, however, limited by the availability of accurate land cover data (Foody, 2002). For many applications the accuracy of image classifications is often judged insufficient (Townshend, 1992; Gallego, 2004; Foody, 2008). A commonly stated accuracy measure is 85 % correct allocation (Foody, 2008). Reviewing 15 years of classification studies, Wilkinson (2005) stated that, despite all effort, no upward trend in classification accuracy could be observed. In addition, remotely sensed land cover data sets are often characterised by missing data in either the spatial or temporal dimension. In general, an area remains unclassified if (1) no image data is available for a required point in time, e.g., one year in a time series (temporal gap) or (2) no defined spectral class is adequate for the pixel or clouds mask parts of the image (spatial gaps). Despite an increasing availability, the acquisition of land cover data with sufficiently high temporal availability and accuracy remained challenging; statistical analysis and interpolation techniques are able to improve both.

There have been numerous attempts to advance spatio-temporal analysis including the development of new data models and the extension of statistical techniques to the space-time domain. Wentz et al. (2010) provided a review and references for various space-time interpolation methods with details on how existing spatial interpolation methods (e.g., inverse distance weighting, splining, kriging or spatial regression) may be extended to the temporal dimension. They stated that most efforts, however, have focused on interpolation in either the spatial or the temporal dimension. Thus, they developed an ensemble approach which integrates multiple techniques and uses ancillary data to create a complete data set in the temporal and spatial dimension for any Earth-related data. They used point data sets which tend to have a high observational density in the temporal dimension (e.g., climate data) and spatially highly dense raster data (e.g., Landsat data). Other land cover related space-time interpolation approaches (e.g., Clarke and Hoppen, 1997; Clarke and Gaydos, 1998; Jenerette and Wu, 2001; Goldstein et al., 2004) focus on the re-creation and prediction of urban sprawl.

Any interpolation technique has, however, advantages and limitations which depend on both the spatial and temporal variation in the data. In the past, considerable research was undertaken to increase land cover classification accuracy (Foody, 2008), while less effort was spent on agricultural land cover interpolation techniques. Currently, no interpolation technique exists for time series of remotely sensed land cover data which addresses spatial and temporal gaps.

Most environmental studies demand accurate and spatio-temporal complete time series of land cover data; the authors therefore developed a tool to improve existing land cover series. The IRSeL (**I**mprovement of **R**emotely **Se**nsed **L**and cover) approach interpolates

remotely sensed land cover data, considering characteristics of agriculturally used areas such as land cover changes or crop rotations. IRSeL improves the data set by (1) removing unclassified pixels using an individual function for each no-data pixel and (2) minimising classification errors based on statistical analysis. Since the approach bases on the statistics of the initial land cover data set, it can be applied in data scarce areas where no further spatial data is available; it solely requires an appropriate initial land cover data set of the area of interest.

This study has two major objectives: (1) to introduce an efficient and easy-to-use approach to improve remotely sensed land cover series and (2) to demonstrate its effectiveness, limitations and challenges. An area around the city of Neumünster (Schleswig-Holstein, Germany) served as a test site, where an initial land cover series from 2006 to 2012 was available. Based on this data, the paper describes the IRSeL framework and explains its components and processors; overall management structure and data flow handling is outlined afterwards. Using the Neumünster data series IRSeL turned out as an efficient and easy-to-use post-classification tool.

5.2   Materials and methods

5.2.1   Study area

The study area (Figure 5.1) is located near the city of Neumünster in the federal state of Schleswig-Holstein (Germany) and covers an area of approximately 1237 km^2. The flat landscape is interspersed with lakes and wetlands; urban areas cover the central part while arable land, pasture and forests characterise the surroundings indicating an intense agricultural use. The areas west of Neumünster are sandur outwash plains predominated by corn and pasture on sandy and peaty, less fertile soils. Moraines of the Weichselian glaciation form the eastern part of the study area; where winter wheat and rape occur on the more fertile, loamy soils. Farmers plant corn mono-culturally or apply a three-year crop rotation of winter wheat – winter wheat – rape (Oppelt et al., 2012).

5.2.2   Landsat data, image classification, reference data and classification accuracy

Five almost cloud-free Landsat-5 TM (level 1T, see Geological Survey (U.S.), 1998) images were available to classify the study area in a time period between 2006 and 2012 (see Table 5.1). The Landsat path 196, row 22 data entirely covered the study area; subsets (1511 × 910 pixels) were used for the classification (see Figure 5.1). The map
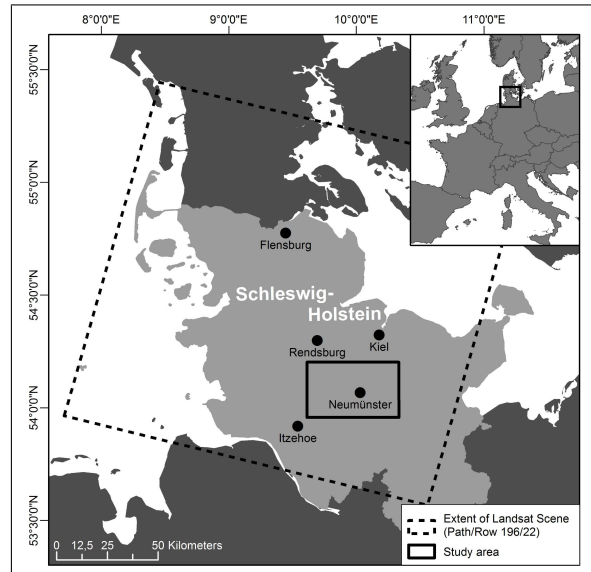
FIGURE 5.1: The study area and its location in Germany.

projection of the entire data set was Transverse Mercator UTM zone 32N, WGS84; in addition, the images were co-registered with high accuracy.

For each classification, the input consisted of the green and red wavelengths of the visible spectral region as well as the near and mid infrared (bands 2, 3, 4, 5 and 7). Due to atmospheric influences the blue wavelengths (band 1) were excluded. Radiances [W/(m^2 μm ster)] were retrieved from the original grey values [Digital Number] of the Landsat TM level L1T products by means of the equations supplied by the Science Data Users Handbook (Geological Survey (U.S.), 1998). Clouded parts were masked prior to the classification. All datasets were classified using a pixel-based, supervised maximum likelihood approach included in the image analysis software ENVI 4.2 (ITTVIS, 2006).

Supervised classification approaches require reference data, which was collected during field mappings for the years 2009 to 2012; each of the field mappings covered about 5 % of the study area. Prior to 2009, no detailed survey was available. Therefore, a

TABLE 5.1: Landsat-5 TM data used for classification, co-registration accuracies (root mean square error (RMSE) in Y and X direction),

Year	Acquisition date	co-registration accuracy RMSE–Y / RMSE–X	Cloud coverage	Unclassified area	OA
2006	2006-06-09	0.64 m / 0.61 m	4.36 %	10.74 %	84 %
2007	2007-04-25	0.69 m / 0.66 m	0.66 %	5.56 %	86 %
2008	-	-	-	100.00 %	87 %
2009	2009-07-03	0.70 m / 0.63 m	0.32 %	2.95 %	-
2010	2010-08-07	0.62 m / 0.52 m	0.30 %	4.40 %	85 %
2011	2011-08-26	0.73 m / 0.64 m	7.26 %	11.90 %	76 %
2012	-	-	-	100.00 %	-

TABLE 5.2: Land cover classes and number of pixels (#) used for accuracy assessment.

Land cover class	#	Description
CSIL	∼ 4000	Forage and energy corn silage
RAPS	∼ 2500	Rapeseed
WWHT	∼ 4000	Crop fields, mainly winter cereals (winter wheat, winter rye, winter barley, winter triticale)
PAST	∼ 4000	Pasture, meadow
FRSD	∼ 3400	Deciduous forest land, mixed forest land, groves, orchards
FRSE	∼ 4400	Evergreen forest land
WETN	∼ 1300	Non-forested wetland
WATR	∼ 3900	Permanent water areas, lakes and streams
URBN	∼ 1100	Urban land, residential, commercial services, industrial, transportation

dataset provided by the Ministry of Energy, Agriculture, the Environment and Rural Areas Schleswig-Holstein (MLUR, 2010) complements the information. It contains annual agricultural data on field block level of the European IACS (Integrated Administration and Control System) database from 2006 onwards. ATKIS (Official Topographical Cartographic Information System LVA, 2007) data of the year 2007 served as reference for land cover classes which remain static over time (e.g., forest, water bodies, urban areas, wetlands). Reference pixels were set to cover all land cover classes and then randomly divided into two groups (for classifier training and accuracy assessment).

Since the land cover data set is mainly used as input for hydrologic models (see Rathjens and Oppelt, 2012b; Oppelt et al., 2012), distinctions were made between classes that are expected to have a different hydrological behaviour. Table 5.2 presents the nine resulting land cover classes. Class histograms were checked for normality; then a supervised maximum likelihood classification was performed. The maximum likelihood classifier calculates probability density functions for each class based on the spectral behaviour of the training pixels. During classification, the pixels are assigned to the class with the highest probability for all spectral bands. A pixel is not assigned to any class if all probabilities are below a user-defined threshold (Campbell and Wynne, 2011), which was set to 0.95. No post-classification refinements such as urban masks or filter techniques were applied.

Cross-tabulations of classified versus reference data (see Table 5.2) generate error matrices. To ensure the comparable accuracy statistics over the years, the same set of reference data was used for temporally static classes (FRSD, FRSE, WETN, WATR and URBN, see Table 5.2 for abbreviations). For arable land and pasture (CSIL, RAPS, WWHT and PAST) reference pixels were chosen separately for each classification or year. Overall accuracy (OA), kappa coefficient and per-class (user's and producer's accuracy (UA, PA))

statistics (see Congalton, 1991) were derived from the confusion matrices, which also included unclassified areas. OA measures the percentage of pixels allocated correctly. The kappa coefficient incorporates the off-diagonal elements of the confusion matrices (i.e. classification errors) and represents agreement obtained after removing the proportion of agreement that could be expected to occur by chance (Cohen, 1960). Values equal to 1 indicate a perfect agreement between observed and classified pixels, while values equal to 0 indicate that there is no agreement among classification and reference other than what would be expected by chance. UA provides the share of correctly allocated pixels compared to the total number of pixels classified into a particular class. Thus, $1-$UA identifies the error of commission. PA is the percentage of correctly classified pixels to all reference pixels a class. A value close to 1 indicates a large proportion of the pixels that were assigned correctly. Hence, $1-$PA represents the error of omission.

The accuracy target of a thematic map derived by an image classification depends on the specific application for which the land cover data should be used (e.g., hydrologic modelling or ecosystem service assessment). Although a generally applicable accuracy is not appropriate, a widely reported value is 85 % (e.g., Foody, 2008). For the present land cover classifications OAs range from 76 to 87 % (see Table 5.1). Referring to Foody (2008), the 2006 and 2011 classification accuracies might be judged insufficient. Misclassifications occurred particularly in urban and wetland areas (URBN and WETN). Furthermore, considerable parts of the land cover maps remained unclassified (up to 11.90 %); no land cover information is available for the years 2008 and 2012 (see Table 5.1).

5.3 IRSeL: An interpolation and improvement approach for remotely sensed land cover data

5.3.1 IRSeL framework

The goal of IRSeL is to refine land cover maps in both the spatial and temporal dimension (see Figure 5.2). To handle data flow, IRSeL uses two temporal analysis processors (TP1 and TP2), one spatial interpolation processor (SP) and two temporal interpolation processors (TP3 and TP4). The remotely sensed land cover maps form a gridded space-time cube L. Using L as input, TP1 provides an average (or mode) land cover grid $\overline{L}$; then TP2 is applied to calculate change statistics or crop rotations for each land cover class. A maximum likelihood processor integrates the output from TP1, TP2 and temporally static land cover classes to refine L. This maximum likelihood processor combines three interpolation processors (SP, TP3 and TP4). For each no-data pixel,
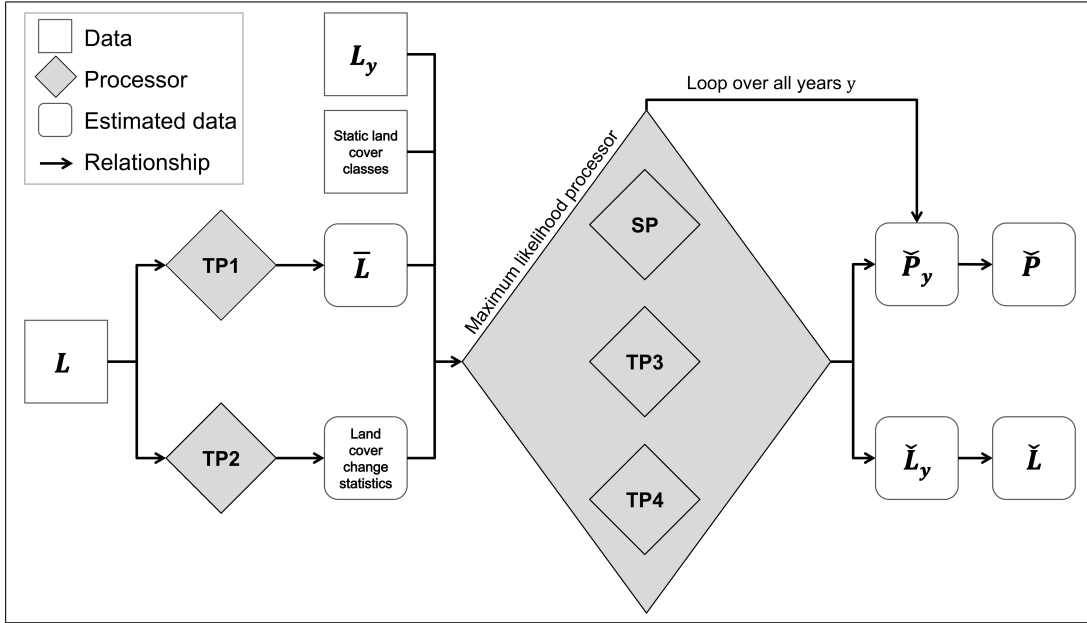
FIGURE 5.2: General organisation of IRSeL. Land cover data are input in the form of a gridded space-time cube L on a yearly time step with missing data in either the spatial or temporal dimension. A mode land cover grid ($\overline{L}$) is derived from TP1 and land cover change or crop rotation statistics are provided by TP2. The maximum likelihood processor integrates a spatial processor (SP), two temporal processors (TP3 and TP4) and the intermediate data to interpolate the land cover cube for each year y of the period of interest to complete the space-time cube. $\check{P}$ provides reliabilities for the interpolated and revised pixels; and $\check{L}$ represents the completed and revised space-time cube.

these processors calculate occurrence probabilities of all land cover classes; SP is based on the spatial neighbourhood; TP3 is based on preceding time layers while succeeding time layers set up TP4. Accordingly, the maximum likelihood processor calculates the land cover class which is most likely to occur for each no-data pixel.

Based on the initial data set L, IRSeL creates a complete space-time cube $\check{L}$. Input and output of IRSEL as well as the relationship between the processors are illustrated in Figure 5.2 and will be explained in detail below.

5.3.2   IRSeL input data

IRSeL requires an initial land cover series in the form of a gridded space-time cube and a set of temporally static land cover classes. The period of interest is represented by a set Y, in which, for the given example, each $y \in Y$ represents one year; the number of rows and columns in the land cover series defines the spatial extent in "x" and "y" direction. Ω_0 is the set of land cover classes, including the "no-data" or "unclassified" class. Denote the set of temporally static land cover classes with $\Omega_S \subseteq \Omega_0$. All land cover layers are assumed to have the same spatial resolution and to cover the same area,

i.e. the number of rows (nrow) and the number of columns (ncol) remain constant; hence the set of rows is Nrow := $\{1, \ldots, \text{nrow}\}$ and Ncol := $\{1, \ldots, \text{ncol}\}$ is the set of columns. Thus, the annual land cover is arranged in a gridded data cube including no-data pixels:

$$L := (l_{y,i,j})_{y \in Y, i \in \text{Nrow}, j \in \text{Ncol}} \in \Omega_0^{|Y| \times \text{nrow} \times \text{ncol}},$$

where $l_{y,i,j}$ is the value (i.e. the respective land cover class) of a pixel with a given coordinate (y, i, j) explaining the temporal (year $y \in Y$) and spatial (row $i \in$ Nrow and column $j \in$ Ncol) location within the data cube. Define 0 as the no-data value, i.e. $l_{y,i,j} = 0$ for each no-data pixel. Hence, $l_{y,i,j}$ is a spatial data gap if $i' \in$ Nrow and $j' \in$ Ncol exist satisfying $l_{y,i',j'} \neq 0$ and a temporal data gap if $l_{y,i',j'} = 0$ for each $i' \in$ Nrow and $j' \in$ Ncol. IRSeL therefore provides a revised land cover data cube $\check{L}$ without data gaps or unclassified pixels, i.e. all elements of $\check{L}$ are from $\Omega := \Omega_0 \backslash \{0\}$.

5.3.3   Model processor TP1

TP1 calculates an average land cover to identify temporally static land cover classes. For some pixels, classification errors may lead to inter-annual variations in class assignment, even for these static land cover classes. Class assignment based on the average land cover may therefore improve the quality of the land cover data.

$\Omega_S \subseteq \Omega$ represents the land cover classes that are expected to remain static over time. Thus, $\Omega_R := \Omega \backslash \Omega_S$ are defined as land cover classes varying in the temporal dimension. Denote $\bar{l}_{i,j} \in \Omega$ for each $i \in$ Nrow and $j \in$ Ncol as the most frequently occurring land cover class in row i and column j during the period of interest; i.e. $\bar{l}_{i,j} = \text{mode}((l_{y,i,j})_{y \in Y})$. $\overline{L}$ contains the temporal most frequently occurring land cover class for each pixel. It takes the form

$$\overline{L} := (\bar{l}_{i,j})_{i \in \text{Nrow}, j \in \text{Ncol}} \in \Omega^{\text{nrow} \times \text{ncol}} \tag{5.1}$$

and can be interpreted as the average land cover layer during the period of interest.

5.3.4   Model processor TP2

TP2 calculates land cover change statistics (or crop rotations) for the entire study area and the entire period of interest. The statistics reflect the temporal land cover change in the study area; consequently they are crucial input for the space-time interpolation. For each time step, the probability of a pixel to change its land cover ($\hat{\omega} \in \Omega$ changes to $\omega \in \Omega$) is calculated; in the forward direction the probability is calculated by dividing

the number of occurring changes ($\hat{\omega}$ to ω) by the total number of changes ($\hat{\omega}$ to any $\omega' \in \Omega$); the calculation of changes backwards in time (current land cover $\hat{\omega}$, land cover in previous time step ω) is analogous. The probabilities are specified by the stochastic vectors

$$p_{\hat{\omega}} := (p_{\hat{\omega}}(\omega))_{\omega \in \Omega}, \quad p_{\hat{\omega}}(\omega) := \frac{\#_p(\hat{\omega}, \omega)}{\sum_{\omega' \in \Omega} \#_p(\hat{\omega}, \omega')} \quad \text{and}$$

$$f_{\hat{\omega}} := (f_{\hat{\omega}}(\omega))_{\omega \in \Omega}, \quad f_{\hat{\omega}}(\omega) := \frac{\#_f(\hat{\omega}, \omega)}{\sum_{\omega' \in \Omega} \#_f(\hat{\omega}, \omega')},$$

where $p_{\hat{\omega}}(\omega)$ $[f_{\hat{\omega}}(\omega)]$ determines the probability that land cover ω is the predecessor [follower] of land cover $\hat{\omega}$ and $\#_p(\hat{\omega}, \omega)$ $[\#_f(\hat{\omega}, \omega)]$ is the number of backward [forward] land cover combinations occurring in L. It is $p_{\hat{\omega}}, f_{\hat{\omega}} \in [0, 1]^{|\Omega|}$ and $\sum_{\omega \in \Omega} p_{\hat{\omega}}(\omega) = 1 = \sum_{\omega \in \Omega} f_{\hat{\omega}}(\omega)$ for each $\hat{\omega} \in \Omega$. Corresponding to the stochastic vectors, the probability measures $p_{\hat{\omega}}$ and $f_{\hat{\omega}}$ can be expressed as

$$\begin{aligned} P_{\hat{\omega}}^p : 2^\Omega \to [0, 1], \quad E \mapsto \sum_{\omega \in E} p_{\hat{\omega}}(\omega) \quad \text{and} \\ P_{\hat{\omega}}^f : 2^\Omega \to [0, 1], \quad E \mapsto \sum_{\omega \in E} f_{\hat{\omega}}(\omega) \quad \text{for each } \hat{\omega} \in \Omega. \end{aligned} \tag{5.2}$$

Thus, $(\Omega, 2^\Omega, P_{\hat{\omega}}^p)$ and $(\Omega, 2^\Omega, P_{\hat{\omega}}^f)$ are probability spaces for each $\hat{\omega} \in \Omega$. Both probability measures provide temporal land cover statistics for the study area considering preceding $(P_{\hat{\omega}}^p)$ and succeeding $(P_{\hat{\omega}}^f)$ changes in land cover.

5.3.5   Maximum likelihood processor

The maximum likelihood processor is used to find a land cover class appropriate for a specific no-data pixel; it analyses the spatial and temporal neighbourhood of the data gaps and replaces static land cover pixels that do not match $\overline{L}$. Therefore, a spatial (SP) and two temporal (TP3 and TP4) interpolation processors are applied parallel to estimate the most likely land cover class for each pixel (also shown in Figure 5.2).

5.3.5.1   Model processors TP3 and TP4

TP3 and TP4 provide occurrence probabilities of land cover classes for each no-data pixel. These probabilities base on the relation of the no-data pixel to its temporal neighbourhood and the land cover change statistics (calculated by TP2). Both processors operate analogously; TP3 analyses the preceding and TP4 the succeeding time slices. The temporal distances of the no-data pixel $l_{y,i,j} \in L$ to the corresponding pixel assigned

to a land cover class in preceding and succeeding time slices are given by:

$$
\begin{aligned}
y^p_{y,i,j} &:= \begin{cases} \infty, & \text{if } \emptyset = \{y' \in Y : y' < y \wedge l_{y',i,j} \neq 0\} \\ y - \max\{y' \in Y : y' < y \wedge l_{y',i,j} \neq 0\}, & \text{else} \end{cases} \quad \text{and} \\
y^f_{y,i,j} &:= \begin{cases} \infty, & \text{if } \emptyset = \{y' \in Y : y' > y \wedge l_{y',i,j} \neq 0\} \\ y - \min\{y' \in Y : y' > y \wedge l_{y',i,j} \neq 0\}, & \text{else} \end{cases}
\end{aligned}
\tag{5.3}
$$

where $y^p_{y,i,j}$ is the temporal distance in years of $l_{y,i,j}$ to the nearest preceding data set which includes data at that particular pixel location, while $y^f_{y,i,j}$ is the temporal distance to the nearest succeeding data set.

For each no-data pixel, TP3 and TP4 calculate the probability of $\omega \in \Omega$ being assigned to a realistic land cover class; they evaluate the probability measures provided by TP2 (Eq. (5.2)) weighted by the temporal distances of the specific pixel (Eq. (5.3)). Formally, TP3 and TP4 can be stated as

$$
\frac{1}{y^p_{y,i,j}} P^p_{\omega^p}(\{\omega\}) \qquad \text{and} \qquad \frac{1}{y^f_{y,i,j}} P^f_{\omega^f}(\{\omega\}),
\tag{5.4}
$$

where $\omega^p = l_{y-y^p,i,j}$ and $\omega^f = l_{y+y^f,i,j}$ are the temporally nearest data pixels in row i and column j, specified by the temporal distances $y^p_{y,i,j}$ and $y^f_{y,i,j}$. Values close to 1 indicate a high reliability of ω while values close to 0 indicate a low estimation reliability. According to TP3 and TP4, the statistically best estimates for the actual no-data pixel are the arguments of the maximum of Eq. (5.4).

5.3.5.2 Model processor SP

SP provides occurrence probabilities of land cover classes for each no-data pixel $l_{y,i,j} \in L$, if $i' \in$ Nrow and $j' \in$ Ncol exist satisfying $l_{y,i',j'} \neq 0$ (i.e. a spatial neighbourhood of the no-data pixel exists). These probabilities rely on the relationship between the actual no-data pixel and its spatial neighbourhood. Within a year y, the spatial distance (in raster units $d_{y,i,j}$) from the no-data pixel to the nearest pixel assigned to a land use class can be expressed as

$$
d_{y,i,j} := \min\{(d_r, d_c) \in \text{Nrow} \times \text{Ncol} : l_{y,i\pm d_r,j\pm d_c} \neq 0\}.
$$

The corresponding neighbourhood $S_{y,i,j}$ is defined as a subset of the current land cover layer specified by a $d_{y,i,j} \times d_{y,i,j}$ matrix around the actual no-data pixel located in (y,i,j).

The probability for each land cover class $\omega \in \Omega$ to occur in $S_{y,i,j}$ is given by the stochastic vector

$$s_{y,i,j} := s_{y,i,j}\left(\omega\right)_{\omega \in \Omega}, \quad s_{y,i,j}\left(\omega\right) = \frac{\#_{y,i,j}\left(\omega\right)}{\sum_{\omega' \in \Omega} \#_{y,i,j}\left(\omega'\right)},$$

where $s_{y,i,j}(\omega)$ indicates the probability of ω to occur in $S_{y,i,j}$; $\#_{y,i,j}\left(\omega\right)$ indicates how often a specific land cover class ω appears in the neighbourhood $S_{y,i,j}$. It is $\sum_{\omega \in \Omega} s_{y,i,j}\left(\omega\right) = 1$ and $s_{y,i,j}\left(\omega\right) \geq 0$ for each $\omega \in \Omega$. The probability measures $P^s_{y,i,j} : 2^\Omega \rightarrow [0,1]$ associated to the stochastic vectors $s_{y,i,j}$ take a form analogous to Eq. (5.2) and $(\Omega, 2^\Omega, P^s_{y,i,j})$ forms a probability space for each no-data pixel.

SP estimates the reliability for each no-data pixel for being assigned to a realistic land cover class $\omega \in \Omega$. The estimation bases on the neighbourhood of the actual no-data pixel, weighted by its spatial distance. SP can be stated as

$$\frac{1}{d_{y,i,j}} P^s_{y,i,j}\left(\{\omega\}\right). \tag{5.5}$$

Values close to 1 indicate a high reliability of ω to be the missing land cover. According to SP, the statistically best estimate for the no-data pixel is the argument of the maximum of Eq. (5.5).

5.3.5.3   Assemblage of model processors

All model processors are combined to a maximum likelihood approach to complete the land cover space-time cube L.

For each no-data pixel, the processor estimates occurrence probabilities for each land cover class. TP3, TP4 (Eq. (5.4)) and SP (Eq. (5.5)) provide statistical information related to the temporal and spatial dimension. Together they form an individual probability measure $\check{P}_{y,i,j}$ which is used to find the statistically best land cover class for the no-data pixels. $\check{P}_{y,i,j}$, takes the form

$$\begin{aligned}&\check{P}_{y,i,j} : \Omega \rightarrow [0,1]\,,\\&\omega \mapsto \frac{1}{3y^p} P^p_{y,i,j}\left(\{\omega\}\right) + \frac{1}{3y^f} P^f_{y,i,j}\left(\{\omega\}\right) + \frac{1}{3d_{y,i,j}} P^s_{y,i,j}\left(\{\omega\}\right).\end{aligned} \tag{5.6}$$

The statistically best value $\check{\omega}_{y,i,j}$ for the no-data pixel located in (y,i,j), excluding the static land cover-classes, is given by the argument of the maximum of $\check{P}_{y,i,j}$:

$$\check{\omega}_{y,i,j} := \arg \max_{\omega \in \Omega_R} \check{P}_{y,i,j}(\omega). \tag{5.7}$$

Then the processor creates the revised land cover data set $\check{L}$. For each pixel, the original land use class (given by L), the most frequent value (given by $\overline{L}$) or the most likely value (given by Eq. (5.7)) is used. $\check{L}$ takes the form

$$\check{L} := \left(\check{l}_{y,i,j}\right)_{y \in Y, i \in \text{Nrow}, j \in \text{Ncol}} \in \Omega^{|Y| \times \text{nrow} \times \text{ncol}},$$

$$\check{l}_{y,i,j} := \begin{cases} \bar{l}_{i,j} & \text{if} \quad \bar{l}_{i,j} \in \Omega_s \\ \check{\omega}_{y,i,j} & \text{if} \quad l_{y,i,j} \in \Omega_s \cup \{0\} \wedge \bar{l}_{i,j} \notin \Omega_S \\ l_{y,i,j} & \text{else} \end{cases} \tag{5.8}$$

where the first line in the definition of $\check{l}_{y,i,j}$ represents the location of the static land cover classes. The second line fills data gaps and replaces static land cover classes if they do not match with the average land cover layer $\overline{L}$. The third line represents initial land cover classes without replacement or revision.

Finally, $\check{P}_{y,i,j}(\check{l}_{y,i,j})$ provides a statistical estimation of the reliability of the interpolated or revised land cover class. Values close to 1 represent very high reliabilities, whereas values close to 0 indicate a less reliable interpolation.

5.3.6 IRSeL accuracy assessment

The accuracy of IRSeL was evaluated by answering two questions using the test data series: (1) Does the approach work correctly for spatial and temporal data gaps? (2) Does the approach improve the existing land cover classifications?

To evaluate if the approach estimated land cover for spatial data gaps correctly, interpolated pixels for the six years (2006, 2007, 2009, 2010 and 2011) were compared to observed data using UA and PA derived from confusion matrices. To evaluate if the approach estimated land cover for temporal data gaps correctly, estimated pixels were compared to mapped data for the years 2008 and 2012, where reference data existed but no Landsat TM image was available.

To evaluate whether IRSeL replaces unclassified pixels correctly, the classification accuracies (OA, kappa, UA and PA) were compared to the statistics derived from the IRSeL maps. The same set of reference pixels was used for the accuracy assessment of the original and IRSeL modified classifications. The non-parametric McNemar's test (Foody, 2004; Agresti, 2007) was used to evaluate whether the differences in quality between original and IRSeL maps (here the difference in the proportion of correctly allocated pixels) are statistically significant.
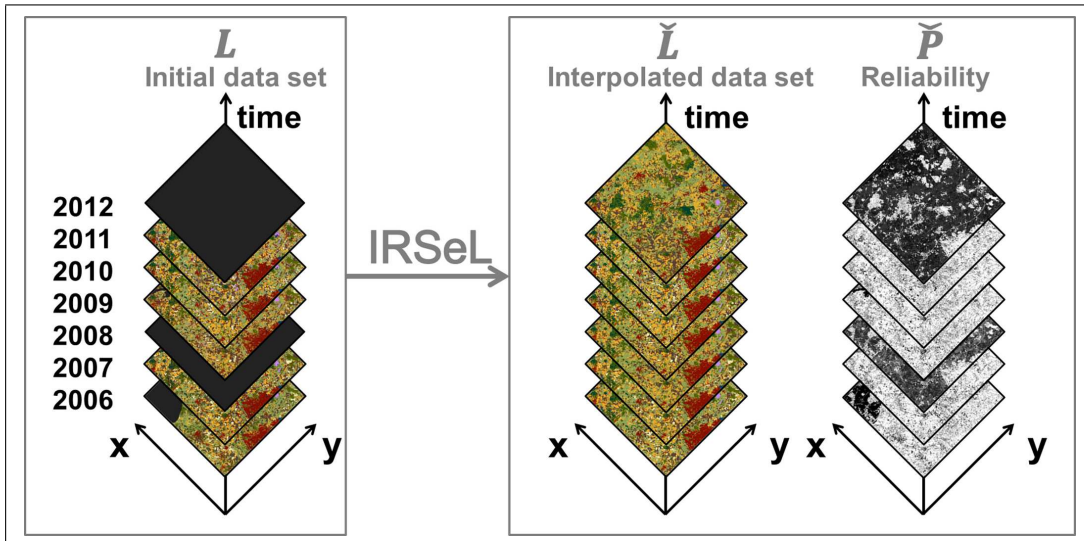
FIGURE 5.3: Scheme of the case study's land cover space-time data cube before and after IRSeL application. Black parts in the initial land cover maps (L) represent no-data areas. $\check{L}$ shows the IRSeL interpolated land cover maps. Bright (dark) areas in $\check{P}$ depict high (low) reliabilities of IRSeL adjusted areas.

5.4   Results and Discussion

Figure 5.3 illustrates the structure of the IRSeL case study. IRSeL was applied using the spatially and temporally fragmented initial land cover data set from 2006 to 2012 (see Table 5.1). In the following section results and accuracies obtained are discussed in detail.

5.4.1   Crop rotations and land cover change statistics

Figure 5.3 provides information about crop rotations calculated by TP2; moreover, it summarises the probabilities of the land cover classes to be preceded and followed by other land cover classes, which were derived from the successive $2009 - 2011$ Landsat TM classifications. The classes WATR, FRSE and FRSD showed high probabilities (> 0.60) to be the same class in the preceding and following year, while WETN and URBN exhibited lower probabilities to be static. The low probabilities of the latter are probably caused by their poor performance during the classification; knowledge about the study area, however, underpinned a static character of all these classes. Thus, these five classes were considered as static classes.

Regarding the four agricultural classes PAST, had highest probabilities (> 0.70) to be followed and preceded by the same class. The same applies for CSIL (> 0.50) whereas a RAPS pixel showed a probability > 0.50 to be WWHT in the next or previous year. WWHT appeared most likely to remain WWHT (0.27 resp. 0.36). The probabilities

TABLE 5.3: IRSeL (TP2, Eq. (5.2)) estimated probabilities of land cover change and crop rotation from the original 2006, 2007, 2009, 2010 and 2011 classifications. Bold numbers represent the highest change probabilities per class. Probabilities smaller than 0.01 are denoted as "-".

LC class	Land cover change probabilities for the next / preceding year								
current year	CSIL	RAPS	WWHT	PAST	FRSD	FRSE	WETN	URBN	WATR
CSIL	**.52** / **.53**	.04 / .04	.11 / .18	.14 / .14	.06 / .04	- / -	.01 / -	.11 / .06	- / -
RAPS	.15 / .10	.14 / .11	**.58** / **.50**	.04 / .19	.01 / .02	- / -	.01 / -	.07 / .07	- / -
WWHT	.22 / .19	.23 / .28	**.27** / **.36**	.08 / .09	.05 / .03	.04 / -	.01 / -	.11 / .05	- / -
PAST	.10 / .11	.05 / .01	.04 / .05	**.70** / **.76**	.04 / .04	- / -	.02 / .02	.06 / .02	- / -
FRSD	.06 / .09	.01 / -	.03 / .05	.08 / .08	**.67** / **.66**	.06 / .02	.01 / .01	.08 / .08	- / -
FRSE	- / .01	- / -	- / .11	- / -	.06 / .15	**.85** / **.68**	.01 / -	.07 / .06	- / -
WETN	.08 / .15	.03 / .03	.03 / .09	.49 / .38	.07 / .06	- / .02	.19 / .14	.10 / .15	- / -
URBN	.11 / .16	.05 / .03	.05 / .12	.04 / .13	.10 / .07	.03 / .02	.02 / .01	**.60** / **.46**	- / -
WATR	- / -	- / -	- / -	- / -	- / -	- / .01	- / -	- / .01	**.99** / **.97**

of WWHT rotating to CSIL or RAPS were slightly lower. These results indicate the predominance of CSIL mono-cropping and a crop rotation between WWHT and RAPS, which confirms existing studies (Oppelt et al., 2012).

5.4.2   Interpolation accuracy

5.4.2.1   Interpolation accuracy of spatial data gaps

Table 5.4 lists accuracy measures derived from spatial gaps (i.e. unclassified or masked pixels in 2007, 2009, 2010 and 2011) that were assigned to land cover classes by IRSeL. The sample size depends on the coincidental intersection of spatial data gaps and validation pixels. Accuracy measures of classes with small sample sizes were not representative, e.g., WATR in 2006 or FRSD in 2007. The use of the same validation data, however, was essential to compare accuracies of different years.

For interpolated pixels, OA and kappa values ranged from 0.63 to 0.81 and 0.53 to 0.77 respectively. The dataset of 2010 offered highest accuracies. In this year IRSeL could use land cover information from 2009 and 2011 to fill the gaps; the close temporal neighbourhood (crop rotation statistics) and the spatial neighbourhood facilitated a correct assignment.

The filling of no-data pixels with static land cover classes was based on the average land cover map $\overline{L}$ (Eq. (5.2)). Errors of commission and omission < 0.20 underpinned that IRSeL performed well for these classes. Whereas the static classes showed high accuracy measures agricultural classes exhibited high variabilities between the classes and showed inter-annual differences within a class. RAPS, for instance, tended towards low PAs but high UAs. The low crop rotation probability of this class increased the error of omission (1-PA) since actual RAPS pixels were most probably assigned to WWHT (see Figure 5.3). Gap pixels are solely assigned to RAPS if the spatial neighbourhood was

TABLE 5.4: Statistics (PA, UA, OA, kappa values and number of interpolated pixels (#)) for the 2006, 2007, 2009, 2010 and 2011 IRSeL interpolated spatial data gaps. Missing values are denoted as "-".

LC class	2006			2007			2009			2010			2011		
	PA	UA	#	PA	UA	#	PA	UA	#	PA	UA	#	PA	UA	#
CSIL	.63	.50	638	.44	.51	232	.87	.35	52	.53	.72	217	.67	.55	940
RAPS	.50	.97	133	.17	.63	168	.82	1.0	108	.26	1.0	46	.23	.51	197
WWHT	.41	.55	752	.84	.60	346	.48	.73	206	.61	.37	31	.28	.55	864
PAST	.88	.85	577	.49	.47	256	.88	.48	49	.79	.47	113	.83	.56	732
FRSD	.88	.31	17	.71	.45	7	-	-	0	.80	.92	71	.99	.94	552
FRSE	.88	.97	130	.97	.97	36	-	-	0	.91	.80	53	-	-	1
WETN	.81	1.0	58	.08	.33	12	.78	1.0	9	.97	1.0	74	.87	1.0	60
URBN	.91	.78	261	.89	.87	301	.87	.97	299	.95	.95	327	.86	.93	306
WATR	.67	.67	3	-	-	2	.93	.93	14	.99	.99	169	.81	.93	16
OA	.66			.63			.75			.81			.65		
Kappa	.57			.53			.68			.77			.57		

predominated by RAPS resulting in low errors of commission (1-UA). Between the years, the varying sample size of tested pixels hampered a direct comparison of class related accuracy measures. Summarising the filling of spatial no-data pixels, IRSeL assignment performed at least 53 % better than a random allocation (see kappa values in Table 5.4).

5.4.2.2   Interpolation accuracy of temporal data gaps

With respect to the lack of Landsat data for 2008 and 2012, kappa and OA values of interpolated pixels were ≥ 0.65 (see Table 5.5). Higher accuracies for the year 2008 (kappa 0.76) entailed from preceding and subsequent datasets whereas the IRSeL application on the year 2012 represented an extrapolation. In both cases neither remote sensing nor classification data were available; the IRSeL land cover estimation was based solely on crop rotation statistics and the average land cover map.

The average land cover map accurately represented static land cover classes and thus IRSeL maps showed high accuracies within these classes, whereas IRSeL performance for agricultural classes was on a lower level. Lower UA values for agricultural classes were related to the specific behaviour of RAPS: the low probability of RAPS in the crop rotation analysis (see Table 5.3) led to the absence of this class in IRSeL derived land cover maps; RAPS showed highest probabilities to follow or precede a WWHT pixel (0.23 resp. 0.28); at the same time, the probability for a WWHT pixel was highest to be WWHT in the next (0.27) resp. earlier year (0.36). As a result, RAPS statistically had no chance to be set in IRSeL fillings of temporal data gaps. Furthermore, RAPS was a sparsely and unevenly distributed land cover in the study area (see Figure 5.4). According to the probabilities, IRSeL falsely assigned RAPS pixels to WWHT. Considering a complete lack of data otherwise, PAs and UAs of agricultural classes were acceptable, although they miss the 0.75 accuracy target for classifications (Foody, 2008). Referring to kappa as an aggregated accuracy measure, IRSeL performed for extrapolated land

TABLE 5.5: Accuracy measures (PA, UA, OA and kappa values) for the 2008 and 2012 IRSeL interpolated temporal data gaps. Missing values are denoted as "-".

LC class	2008		2012	
	PA	UA	PA	UA
CSIL	.67	.69	.46	.48
RAPS	.00	-	.00	-
WWHT	.68	.56	.54	.36
PAST	.97	.68	.71	.73
FRSD	.96	.89	.96	.88
FRSE	.92	.98	.92	.98
WETN	.93	1.0	.93	.99
URBN	.90	.88	.90	.72
WATR	1.0	1.0	1.0	1.0
NoData	1.0		1.0	
OA	.79		.70	
Kappa	.76		.65	

cover at least 65 % better than assignment by chance (see Table 5.5). Thus, IRSeL turned out as an efficient tool for filling temporal data gaps.

5.4.3   Comparison of the original and IRSeL modified classification accuracies

Table 5.6 summarises accuracy measures for the years 2006, 2007, 2009, 2010 and 2011. The same reference pixels were used to estimate accuracies of the original classification results and the IRSeL maps; no-data pixels were included in the accuracy analysis to highlight IRSeL performance. For the entire dataset, aggregated OA and kappa values of the original classification were already on a high level ≥ 0.73; according to the McNemar's test IRSeL further improved accuracies significantly and all land cover maps clearly exceeded the accuracy target of 0.85 after IRSeL application.

IRSeL assigned land cover classes to former no-data pixels, whereas the number of reference pixels remained equal. Thus, PA increased for all classes and time steps (except for WETN in 2007 and FRSE in 2011) and erroneous omissions were reduced. Otherwise, UA values decreased, especially for some agricultural classes due to erroneous commissions (see Table 5.6). Static classes improved the most. IRSeL re-assignment for these classes was based on a comparison of the current land cover status and the average map $\overline{L}$, which reduced errors of commission and omission; therefore, PA and UA values enhanced for most static classes. The greatest improvement was achieved for URBN which performed poorly in all classifications (see Table 5.6).

2011

Original classification result for 2011

2012

IRSeL "input" 2012

Result after IRSeL application for 2011

Result from IRSeL application for 2012

Reliabilities for IRSeL adjusted pixel values (2011)

Reliabilities for IRSeL derived pixel values (2012)

Legend

no data

Land use/ land cover class and share [%] (2011 original/ 2011 IRSeL/ 2012 IRSeL)

Agricultural classes:

CSIL (14.9/21.7/22.1)

RAPS (8.7/10.1/0.0)

WWHT (11.0/14.5/23.8)

PAST (16.6/24.7/25.1)

Constant classes:

FRSD (12.3/12.5/12.5)   URBN (15.2/9.8/9.8)

FRSE (6.8/5.3/5.3)

WETN (1.8/0.4/0.4)

WATR (0.8/0.9/0.9)

Reliability

1: high reliability

0: low reliability
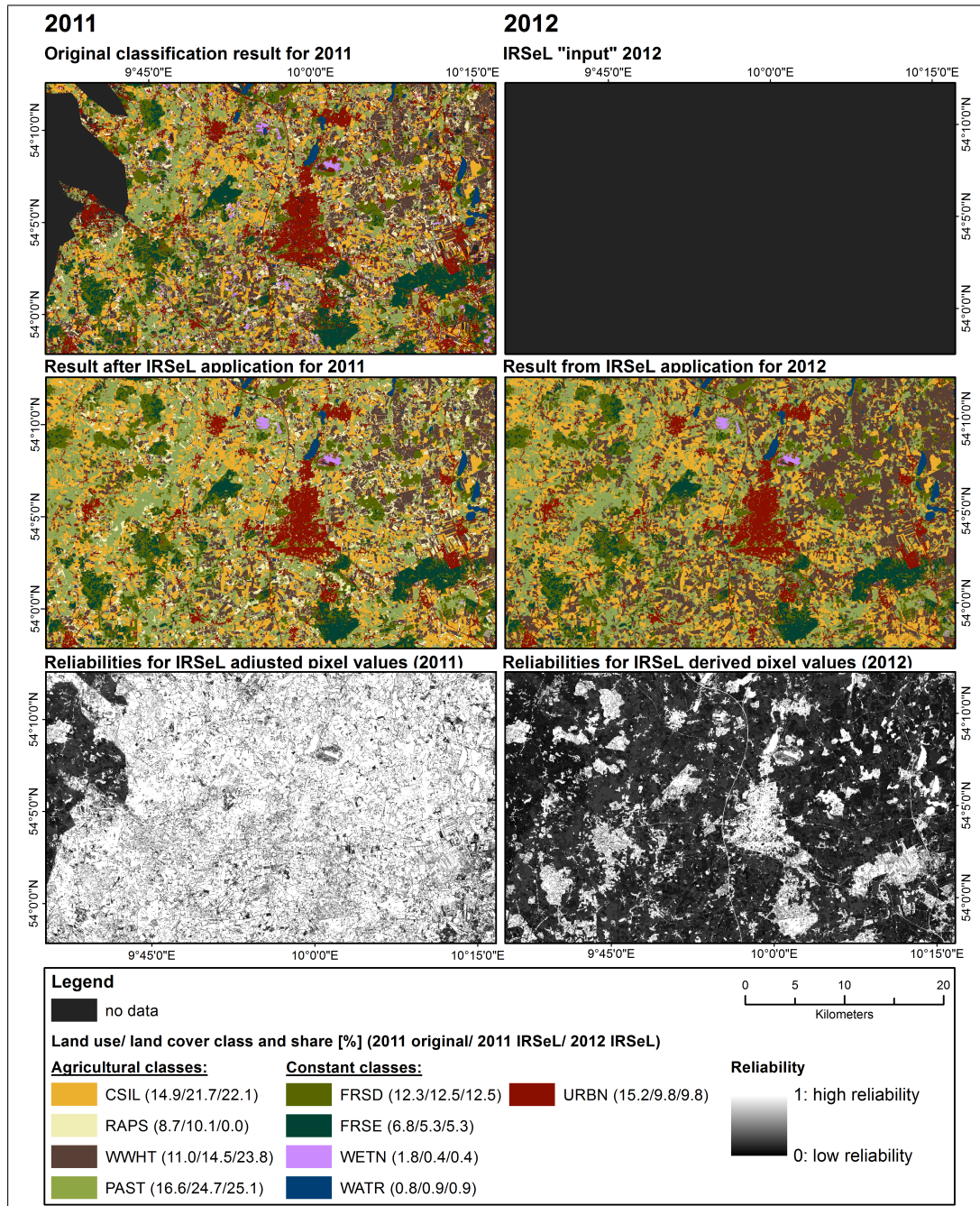
0   5   10   20

Kilometers

FIGURE 5.4: Classification results and IRSeL maps for the years 2011 (spatial data gaps) and 2012 (temporal data gap).

TABLE 5.6: Summary of original Landsat classification (before parentheses) and modified IRSeL (in parentheses) accuracies. The bottom portion lists aggregated accuracy measures (OA and kappa) and share of no-data pixels.

LC class	2006		2007		2009		2010		2011	
	PA	UA	PA	UA	PA	UA	PA	UA	PA	UA
CSIL	0.78	0.95	0.89	0.92	0.89	0.85	0.82	0.91	0.67	0.92
	(0.87)	(0.87)	(0.91)	(0.89)	(0.91)	(0.86)	(0.92)	(0.94)	(0.84)	(0.82)
RAPS	0.86	0.95	0.84	0.97	0.90	0.98	0.87	0.92	0.65	0.64
	(0.88)	(0.96)	(0.85)	(0.96)	(0.94)	(0.98)	(0.94)	(0.95)	(0.69)	(0.62)
WWHT	0.76	0.92	0.79	0.94	0.84	0.79	0.82	0.92	0.61	0.90
	(0.83)	(0.89)	(0.87)	(0.90)	(0.91)	(0.93)	(0.91)	(0.95)	(0.67)	(0.86)
PAST	0.79	0.80	0.86	0.91	0.90	0.93	0.87	0.80	0.76	0.90
	(0.92)	(0.85)	(0.90)	(0.87)	(0.92)	(0.92)	(0.95)	(0.86)	(0.92)	(0.80)
FRSD	0.90	0.88	0.87	0.83	0.92	0.93	0.94	0.83	0.75	0.84
	(0.96)	(0.87)	(0.96)	(0.87)	(0.96)	(0.89)	(0.96)	(0.89)	(0.96)	(0.86)
FRSE	0.90	0.97	0.82	0.96	0.73	0.99	0.88	0.98	0.95	0.95
	(0.92)	(0.98)	(0.92)	(0.98)	(0.92)	(0.98)	(0.92)	(0.98)	(0.92)	(0.98)
WETN	0.80	0.99	0.97	0.96	0.88	0.98	0.64	0.97	0.74	0.90
	(0.93)	(1.00)	(0.93)	(1.00)	(0.93)	(1.00)	(0.93)	(1.00)	(0.93)	(1.00)
URBN	0.63	0.74	0.66	0.46	0.59	0.41	0.57	0.45	0.68	0.44
	(0.90)	(0.75)	(0.90)	(0.78)	(0.90)	(0.82)	(0.90)	(0.84)	(0.90)	(0.76)
WATR	1.00	1.00	1.00	1.00	1.00	1.00	0.96	0.99	1.00	0.96
	(1.00)	(1.00)	(1.00)	(1.00)	(1.00)	(1.00)	(1.00)	(1.00)	(1.00)	(1.00)
NoData	0.11		0.06		0.02		0.04		0.12	
OA	0.84		0.86		0.87		0.85		0.76	
	(0.91)		(0.92)		(0.94)		(0.94)		(0.86)	
Kappa	0.82		0.85		0.85		0.83		0.73	
	(0.90)		(0.91)		(0.93)		(0.93)		(0.84)	

The confusion matrices in Table 5.7 illustrate the IRSeL performance to fill up no-data pixels and to re-arrange land cover classes exemplary for 2011. In this year the classification was based on a Landsat TM scene, which was both late in the vegetation period and partly covered by clouds (see Figure 5.4). These are typical problems when classifying optical imagery. Clouds overlay the current land cover and their shadows and feathering lead to disturbances in the spectral information of adjacent pixels. Furthermore, suboptimal image acquisition dates (early or late in the vegetation period) and lack of multi-seasonal image data hamper accurate differentiation of vegetation types (e.g., Reed et al., 1994). Owing to these difficulties the 2011 classification contained the largest number of no-data pixels within the time series and showed a comparatively poor kappa value. IRSeL, however, was able to remove all no-data pixels (pointed out by zeros in the second row of the confusion matrix in Table 5.7).

For agricultural classes the number of correctly assigned pixels (bold numbers in the table's diagonal) increased throughout. The number of erroneously assigned pixels within the agricultural classes was, however, larger after IRSeL application. The false allocation of IRSeL is evident in particular between CSIL and WWHT where the number of incorrectly allocated pixels was five times higher than in the original classification. In contrast, the number of actual agricultural pixels that were erroneously classified into a static class, particularly URBN, decreased after IRSeL application. Re-assigning these pixels reduced errors of commission for URBN. The increase in false allocation within agricultural classes generally entailed reduced UA values for CSIL, RAPS, WWHT and PAST. However, the increase in correctly assigned pixels dominated resulting in an improvement of PA values (see Table 5.6).

TABLE 5.7: 2011 Landsat classification (before parentheses) and IRSeL (in parentheses) confusion matrix. The bold elements represent the main diagonal of the matrix that contains the grid cells where the class labels depicted in the image classification and reference data set correspond. The off-diagonal elements contain pixels which showed no agreement.

Class	CSIL	RAPS	WWHT	PAST	FRSD	FRSE	WETN	URBN	WATR	Total
NoData	940	197	864	732	552	1	60	306	16	3668
	(0)	(0)	(0)	(0)	(0)	(0)	(0)	(0)	(0)	(0)
CSIL	**3242**	17	98	101	54	0	0	0	0	3512
	(4024)	(75)	(534)	(223)	(5)	(0)	(7)	(22)	(0)	(4890)
RAPS	81	**1385**	642	37	0	0	8	9	0	2162
	(106)	**(1462)**	(721)	(43)	(0)	(0)	(3)	(7)	(0)	(2342)
WWHT	26	329	**3434**	3	0	0	0	9	0	3801
	(104)	(459)	**(3768)**	(3)	(7)	(10)	(3)	(44)	(3)	(4401)
PAST	211	19	132	**3292**	7	0	4	12	0	3677
	(474)	(52)	(416)	**(3981)**	(11)	(0)	(40)	(25)	(0)	(4999)
FRSD	87	20	44	85	**2577**	181	38	20	1	3053
	(1)	(18)	(71)	(65)	**(3308)**	(332)	(16)	(11)	(1)	(3862)
FRSE	2	1	6	0	213	**4240**	6	0	0	4468
	(0)	(1)	(4)	(0)	(96)	**(4097)**	(2)	(0)	(0)	(4201)
WETN	10	18	62	17	0	0	**979**	0	0	1086
	(0)	(0)	(1)	(2)	(0)	(0)	**(1232)**	(0)	(0)	(1235)
URBN	219	130	358	82	29	35	76	**744**	1	1674
	(69)	(49)	(125)	(32)	(5)	(18)	(20)	**(990)**	(1)	(1309)
WATR	0	0	0	0	0	0	152	0	**3973**	4125
	(0)	(0)	(0)	(0)	(0)	(0)	(0)	(1)	**(3968)**	(3987)
Total	4818	2116	5640	4349	3432	4457	1323	1100	3991	31226

For static classes, the number of correctly assigned pixels generally rose for FRSD, WETN and URBN; for WATR and FRSE the number decreased. False allocations of FRSE mainly occurred with FRSD. Furthermore, IRSeL obviously removed 152 WETN pixels which were classified as WATR. According to the average map, however, these pixels represent WETN land cover. Wet weather conditions in 2011 led to temporarily appearing shallow water bodies in the wetlands. These areas may have been classified as WETN or WATR depending on the acquisition date of the satellite imagery. Since WETN was defined as a static class IRSeL adjusted these effects by using the average map.

Summarising the analysis of accuracy measures with respect to original and IRSeL-modified land cover maps showed that IRSeL filled up spatial data gaps successfully. Furthermore, IRSeL improved land cover classes whose spectral behaviour often leads to misclassified results, e.g., WETN and URBN.

5.4.4   Spatial analysis

Figure 5.4 provides a comparison between the original classification results and the IRSeL maps for 2011 (left hand side) and 2012 (right hand side). For 2011, the top image shows the original classification result. The black areas in the West represent clouded parts of the image which have been masked. URBN and no-data pixels are present at the edges of the masked area. Although a mask excluded clouds from the classification, feathering of clouds affects neighbouring pixels spectrally. Thus, pixels close to the cloud mask were susceptible to remain unclassified or to be erroneously classified as URBN, a class

that often shows a high spectral variability. In addition, URBN pixels were dispersed in the agricultural parts of the study area. WETN pixels appeared south of Neumünster and single fields and parts of the city remained unclassified.

The center image demonstrates that IRSeL reduced the scattered URBN pixels; narrow traffic routes and small villages, however, remained which might be removed by a standardly used post-classification filter. Thus, the proportion of urban areas was reduced from 15.2 % to 9.8 %. This percentage approximately meets the information of sealed area in the ATKIS data base (10.2 %, see LVA, 2007). IRSeL was also able to fill the masked areas with field structures. A simple interpolation algorithm that solely bases on spatial neighbourhoods would have been lacking to set-up realistic field patterns. IRSeL re-assigned overrepresented WETN pixels so as WETN class only appeared in the peat bog areas north of Neumünster; thus, IRSeL reduced the number of WETN pixels about 4.5 times; moreover, it was able to reduce the salt-and-pepper effects apparent in the original classification. Contrary to a standard post-classification or median filter, IRSeL did not smooth field structures but arranged angular landforms realistically.

Furthermore, IRSeL calculated reliabilities for each interpolated or revised pixel. The resulting reliability maps are illustrated at the bottom of Figure 5.4. The large no-data area in 2011 showed lowest reliabilities for the 2011 land cover map. Increasing spatial distances between no-data and land cover pixels (spatial neighbourhood) raises the importance of crop rotation statistics (temporal neighbourhood) during the allocation of land cover classes. Consequently, reliabilities were lower where the allocation of no-data pixels solely based on crop rotation statistics since the spatial neighbourhood lacked in land cover class information. Patches of higher reliabilities within the masked area occurred where IRSeL assigned static classes. Regarding the other part of the 2011 map, small patches with low reliabilities represent entire fields that remained unclassified. The south eastern part of the study area exhibited low reliabilities; here, a considerable amount of falsely classified URBN pixels had to be re-assigned. One distinct feature is the large WETN patch north east of Neumünster; reliabilities are moderate as opposed to the very high reliabilities of other static class patches. IRSeL was unable to re-assign the area surrounding the WETN patch correctly; these pixels remained URBN.

Figure 5.4 further highlights that, for 2012, IRSeL produced a realistically structured land cover map without any remote sensing data. Static pixels were adopted from the average land cover map. The crop rotation probability statistics ruled the allocation of agricultural pixels. The share of WWHT is overrepresented at the expense of RAPS. WWHT, CSIL and PAST appeared in realistically structured patterns. The spatial distribution of crop types matched previous classification results: WWHT has predominately been cultivated in the eastern part of the study area whereas CSIL and PAST

dominated the western part. Reliabilities were reasonably highest for static classes; dynamic agricultural classes showed low reliabilities. The PAST class is the agricultural class with highest reliabilities. The large no-data gap in 2011 became evident in the 2012 reliability map; the 2011 cloud mask corresponded to a low reliability area (black area in Figure 5.4). The lapse of time to an originally classified land cover pixel reduced the reliability to correctly determine a land cover class for these pixels.

The spatial analysis revealed that IRSeL interpolated spatial data gaps reasonably preserving structural landscape patterns. The tool improved existing time series, especially the assignment of static classes. IRSeL calculates probabilities based on land cover statistics, which enabled the creation of a realistic land cover map for a year with complete lack of input data.

5.5   Conclusion

Understanding the effects of land cover on the environment is a major research issue; despite an increasing availability of remote sensing data, the acquisition of land cover data with a sufficiently high temporal availability and accuracy still remains challenging. Statistical revision and interpolation techniques are able to improve both; hence, the objective of this study was to introduce and test an approach to interpolate and improve remotely sensed land cover data (IRSeL) that accounts for specific land cover characteristics such as data gaps caused by clouds, crop rotations, or temporally static land cover classes. IRSeL assigns spatial and temporal no-data pixels to land cover classes and corrects classification errors. The IRSeL re-assignment of classification errors is based on a statistically estimated average land cover map and the user's knowledge about temporally static land cover classes within the study area.

The application of IRSeL during a 7-year land cover study in a test area in Northern Germany showed that the allocation of no-data pixels as well as the re-assignment of classification errors increased the number of correct assignments and improved classification results. IRSeL assignment of no-data pixels to land cover classes led to an increasing probability of false allocation which resulted in higher commission errors but decreased erroneous omission. The accuracy of IRSeL interpolated pixels varied depending on the current land cover class and the extent of the spatial or temporal gaps. Thus, estimated reliabilities and individual accuracy statistics for each class have to be examined before drawing conclusions.

OA values of interpolated spatial gaps ranged from 0.63 to 0.81. The closer the temporal and spatial neighbourhood of the no-data pixels, the higher the accuracy values.

IRSeL corrected classification errors that typically occur when classifying optical imagery. Among these errors were false allocations caused by cloud feathering or suboptimal image acquisition dates that led to a mix-up of spectral information. Comparing original and modified classifications, the IRSeL interpolated pixels improved land cover maps by 8 percentage points in average; after IRSeL application all maps exceeded the accuracy target of 0.85. For interpolated temporal gaps, OA values varied from 0.70 to 0.79. Considering that these maps were based solely on crop rotation statistics, accuracies were acceptable, but missed the target value. Additional image or land cover data of the current time step would be necessary to improve these maps. The spatial analysis of IRSeL outputs revealed that IRSeL interpolated spatial and temporal data gaps reasonably and preserved landscape structural patterns. Contrary to a standard post-classification or median filter, IRSeL preserved one pixel-wide narrow traffic routes and did not smooth field structures. Based on the results, we conclude that IRSeL is an efficient and easy-to-use approach to correct classification errors and to interpolate missing spatial and temporal data.

Some difficulties further exist such as the argument that the interpolated space-time pixels do not represent the true land cover reliably and therefore results and conclusions may be questioned; this challenge, however, is inherent to any interpolation technique (Wentz et al., 2010). Accuracy statistics obtained showed that interpolated values do not reduce the virtue of estimated pixels. IRSeL helps to acquire land cover data that provides the required spatial resolution and temporal availability. Future land cover related studies may use IRSeL improved data sets. The results presented, however, are limited to the case study; to confirm these findings, further studies should be carried out to evaluate the IRSeL approach in other ecosystems and landscapes.

5.6   Acknowledgements

Chapter 6

Assessment of the spatial and temporal representation of land use data on SWAT model performance

H. Rathjens and N. Oppelt

Abstract

The impact of land use changes on the hydrology of a watershed has been identified as a major future research issue. Models provide an efficient way to quantify these impacts, while the model performance is directly linked to the accuracy of land use representation in the model. In this study, the effect of the accuracy and temporal representation of land use data on hydrologic model results was evaluated with the Soil and Water Assessment Tool (SWAT). Comparisons were made between water balance results obtained using a single land use layer (i.e. static land use setup) and those obtained using more accurate individual land use layers for each simulation year (i.e. variable land use setup). The results suggest that highly accurate spatio-temporal land use input is less important when studying aggregated processes, but if the purpose of modeling is to replicate spatially distributed events, accurate land use data is necessary.

6.1   Introduction

Changes in land use may affect hydrological and ecological functions of a watershed. During the past decades the awareness of environmental issues has led to the idea of a sustainable management of landscapes. As a consequence, conservation practices are targeted on arable land to improve water quantity and quality issues. Land use can have a great impact on the water cycle (e.g., Franklin, 1992; Miller et al., 2002), on sediment transport (e.g., Bakker et al., 2008; Ouyang et al., 2010a) and on nutrient leaching caused by agrochemical losses (e.g., Allan et al., 1997; Turner and Rabalais, 2003). Chiang et al. (2010) even stated that land use changes may masks the water quality improvements from conservation practices implemented in the watershed. Thus, interactions between land use change and hydrologic processes have been identified as a major future research issue (DeFries and Eshleman, 2004). In the past, many studies have assessed the impact of historical and hypothetical changes in land use such as deforestation (e.g., Weber et al., 2001; Lorz et al., 2007), urbanization (e.g., Miller et al., 2002; Pai and Saraswat, 2011) and conversion of grasslands to croplands (e.g., Twine et al., 2004), while no attention was given to the impact of annual variability of land use proportions and distributions caused by crop rotations.

Watershed models provide a cost efficient way to quantify the impacts of land use at various spatial and temporal scales, and there are numerous studies where hydrological models are applied successfully for simulating the influence of land use on catchment hydrology. Hörmann et al. (2005) gave an overview of the prospects and limitations of eco-hydrological models for evaluation of land use options in mesoscale catchments. In this context, the SWAT (Soil and Water Assessment Tool, Arnold et al., 1998) model has proven to be a suitable tool to adequately represent general trends of catchment hydrology resulting from land use change (e.g., Volk et al., 2009). SWAT was developed to simulate the effects of management practices on the water cycle and has been applied in many studies evaluating the impact of land use changes on a watershed. Gassman et al. (2007), Krysanova and Arnold (2008), and Pai and Saraswat (2011) summarized many of these. Usually, land use layers are replaced by alternatives, which are based on assumptions of climatic change or the influence of political decisions, in the model to analyze the impact of land uses on water quantity and quality aspects by comparing model outputs. Pai and Saraswat (2011, 2013) stated that among various causes, accurate model predictions depend on how well the temporal status of land use in a watershed is represented in the model and that using a single land use layer for each scenario does not reflect temporal variation of land use in the catchment.

Usually, models represent annual variability of land use proportions in the watershed using crop rotations (i.e. changing fixed proportions of land uses in a catchment each

year). This method is simple and advantageous in data scarce areas, but leads to repetitive land use distributions and is not able to represent annual land use changes caused by economic factors. In addition, land use proportions within a catchment might be relatively constant, while its spatial distribution changes, which also cannot be reflected by crop rotations. Therefore, most studies that are applied to assess the influence of land use changes on hydrologic processes are based on conclusions drawn from catchment wide model results (e.g., water yield at the watershed outlet) with less attention to spatial results.

Due to the rapid development of GIS (Geographic Information System) and remote sensing systems, an increasing amount of land use data has become available. Remotely sensed land use data is often characterized by data gaps that are caused by clouds or classification thresholds (spatial data gaps) or by missing land use layers in a time series (temporal data gaps). Both kind of gaps hamper temporal as well as spatial representation of land use in a model. Conventional interpolation methods of spatial data gaps (e.g., nearest-neighbor method) produce poor results for larger data gaps and no recommended methods exist for interpolating temporal data gaps. Thus, land use data based on classification of remote sensing data seldom provides the requisite accuracy and temporal observational frequency for environmental studies (e.g., Foody, 2008). Recognizing these limitations, an advanced statistic approach developed to revise land use data was used in this study to represent the land use status of the study area as accurately as possible. The newly developed IRSeL-tool (**I**nterpolation and improvement of **R**emotely **Se**nsed **L**and cover, Rathjens et al., under review) corrects classification errors and interpolates missing land cover pixels in the temporal and spatial dimension. The approach leverages special properties known for agricultural areas such as crop rotations and temporally static land cover classes.

This study aims to demonstrate the impact of an accurate representation of land use data on SWAT model output. To perform this analysis, output of two SWAT setups for a ten-year simulation period from 2002 to 2011 were compared. One setup used a single land use layer, while for the second setup a series of ten IRSeL-improved land use layers for each year of simulation was taken. To ensure an accurate spatial distribution of land use data, both SWAT setups were based on grid cells; a sub-catchment of the River Elbe, the Bünzau catchment, served as a test site.
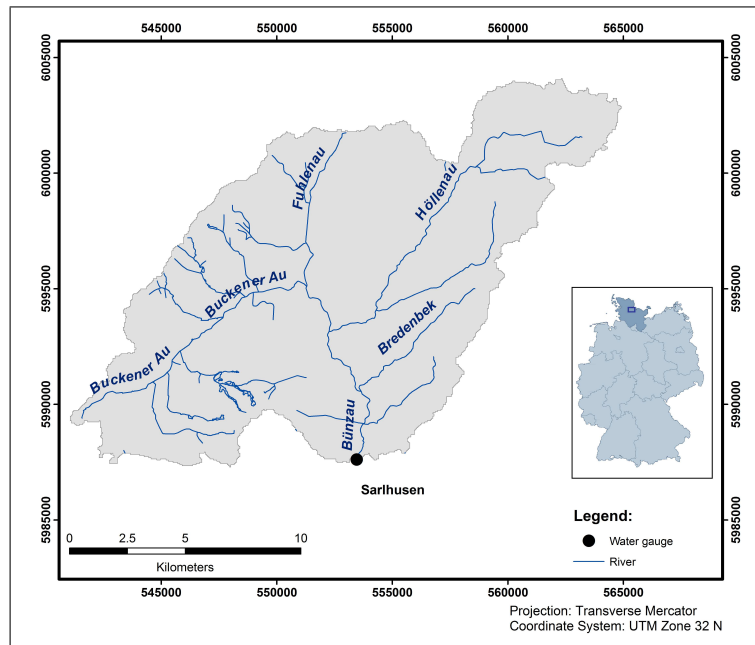
FIGURE 6.1: The Bünzau catchment and its location in Germany.

6.2 Materials and methods

6.2.1 Study area

The study area is the Bünzau catchment, located near the city of Neumünster in the federal state of Schleswig-Holstein in the Northern Germany lowlands (Figure 6.1). The catchment covers an area of 207 km^2 and is characterized by a flat topography and shallow groundwater levels. The rivers Buckener Au and Fuhlenau merge and form the origin of the river Bünzau; the rivers Höllenau and Bredenbek are two downstream tributaries. Several drainage pipes and ditches also flow into the Bünzau, which flows in a southern direction for 16 km before it drains into the Stör River. The gauge Sarlhusen, where an average discharge of 2.6 m^{3}s^{-1} was measured between 2002 and 2011 (LKN, 2012), is located at the catchment outlet.

The mean annual temperature is 9.5 °C and the mean annual precipitation is 863 mm (stations Neumünster and Padenstedt 2002 to 2011, DWD, 2012). On average, 136 days per year experience rainfall greater than 1 mm, and on 4 days rainfall is greater than 20 mm. Precipitation is evenly distributed throughout the year, with rare occurrences of convective thunderstorms and intense sudden rainfall.

In the Bünzau catchment the most prevalent land use types are pasture and arable land, indicating an intense agricultural use. Farmers plant corn monoculturally and cereals in a three-year rotation of winter wheat - winter wheat - rape (Oppelt et al., 2012). Dominant soil types are podzols and planosols; histosols are found in river valleys

Legend:

Land use classes (2007)
- Corn
- Rape
- Crop
- Grassland
- Decidious forest
- Evergreen forest
- Peat bog
- Sealed area
- Water
- Unclassified

Maximum likelihood classification of Landsat 5 scene (2007-04-25)
Overall accuracy: 86 %
Projection: Transverse Mercator
Coordinate System: UTM Zone 32N

Legend:

Soil types
- Gleyic Podzol
- Gleysol
- Histosol
- Luvisol
- Planosol
- Podzol
- Stagnic Podzol
- Water

Soil types according to World Reference Base for Soil Resources
Source: Finnern (1997) and LLUR (2010)
Projection: Transverse Mercator
Coordinate System: UTM Zone 32N

FIGURE 6.2: Land use (2007) and soil types in the Bünzau catchment.

and depressions. Figure 6.2 shows the distribution of land use in 2007 as well as the distribution of soil types.

6.2.2 The SWAT model

SWAT (Arnold et al., 1998) is a physically based catchment-scale model; it was developed to simulate the water cycle, the corresponding fluxes of energy and matter (e.g., sediment, nutrients, pesticides and bacteria) and the impact of management practices on these fluxes. The design of the model is modular and includes components for hydrology, weather, sediment transport, crop growth, nutrients and agricultural management. A detailed description of all components can be found in Arnold et al. (1998) and Neitsch et al. (2011b).

Calculation of surface runoff is performed using either the SCS curve number method (Soil Conservation Service Engineering Division, 1972) or the Green and Ampt infiltration equation (Green and Ampt, 1911). Lateral subsurface flow in the soil profile is calculated with a kinematic storage model estimated simultaneously with percolation. Groundwater flow from shallow aquifers to streams is simulated by creating a shallow aquifer storage using a linear tank storage model (Brutsaert, 2005). SWAT offers using either the Hargreaves (Hargreaves and Samani, 1985), the Priestley-Taylor (Priestley

TABLE 6.1: Overview of the land use data set (acquisition date, performance indexes, and unclassified area) based on classifications from Landsat 5 imagery.

Acquisition Date	Overall Accuracy [%]	Kappa	Unclassified [%]
Apr 2003	92.50	0.91	5.90
Jun 2006	92.92	0.92	10.62
Apr 2007	94.25	0.93	4.98
Jul 2009	83.84	0.81	2.62
Jun 2010	96.96	0.97	4.06
Aug 2011	96.64	0.96	13.50

and Taylor, 1972), or the Penman-Monteith (Monteith, 1965) method for estimating evapotranspiration. Further model components include snow melt, transmission losses from streams, and water storage and losses from ponds.

In this study the Curve Number (CN) method was used to calculate surface runoff, the Penman-Monteith method was applied to estimate evapotranspiration and the Muskingum river routing method served to route the water through the channel network.

6.2.3   Land use data

Simulations with SWAT were conducted for a ten-year period from 2002 to 2011. These years coincided with the availability of land use data (see Table 6.1). A comparison was made between SWAT output obtained using a static (SWAT STA) and a variable land use setup (SWAT VAR). In SWAT STA land use is represented by the 2007 land use layer with three-year crop rotations derived from statistics, while in SWAT VAR land use is updated yearly for each grid cell individually using IRSeL interpolated and revised land use maps.

For the ten-year simulation period, classifications obtained from six Landsat 5 images (see Table 6.1) were available. A detailed description of the land use classification data and a discussion about its characteristics and accuracies is given in Rathjens et al. (under review). To use the data for hydrological modeling, distinctions were made between classes that are expected to have a different hydrological behavior. The resulting nine classes are corn (CSIL), rape (RAPS), winter wheat (WWHT), pasture (PAST), deciduous forest (FRSD), evergreen forest (FRSE), wetlands (WETN), water (WATR), and urban areas (URBN). Land use (in the model setups) is represented by a single land use layer (SWAT STA) or by yearly updated land use maps (SWAT VAR).

Crop rotation WWHT - RAPS - WWHT and mono cultural CSIL, WWHT and PAST were defined for the agriculturally used areas in SWAT STA based on statistics provided

TABLE 6.2: Statistically most likely crop rotations and their probabilities (in parentheses) provided by IRSeL.

Land use class	Predecessor (probability)	Follower (probability)
CSIL	CSIL (0.56)	CSIL (0.54)
RAPS	WWHT (0.39)	WWHT (0.49)
WWHT	CSIL, WWHT (0.27, 0.25)	WWHT (0.31)
PAST	PAST (0.77)	PAST (0.70)
FRSD	FRSD (0.68)	FRSD (0.68)
FRSE	FRSE (0.64)	FRSE (0.77)
WETN	PAST (0.39)	PAST (0.39)
URBN	URBN (0.62)	URBN (0.52)
WATR	WATR (0.97)	WATR (0.95)

by IRSeL (see Table 6.2) to represent annual variabilites of land use. Forest, wetland, urban, and water areas are expected to be constant throughout the simulation period.

Figure 6.3 and Table 6.3 show land use proportions and distributions in the watershed. Some land use classes indicate a high variability, but no significantly increasing or decreasing trends could be identified. Simple three-year crop rotations as implemented in SWAT STA result in an annual redistribution of land use classes (e.g., all rape changes to winter wheat) and the proportions of land use classes in the catchment repeats every three years. Such crop rotations can not explain the variability of land use distributions in the study area. Table 6.1 demonstrates that some land use classes are temporally dynamic; e.g., the proportion of PAST ranges between 31 and 43 % without following steady state principles. Even if the proportions of land use classes are constant within a catchment, their locations might change. Crop rotations are not able to represent these spatial changes. This means that a yearly land use update would significantly improve both the temporal and spatial representation of land use in the watershed. Recognizing the variability in land use data, the IRSeL-tool was applied to represent land use in SWAT VAR as realistically as possible. A description of the specific IRSeL interpolation and revision technique, the data input requirements, data output structure, and an application study in the area of the Bünzau catchment can be found in Rathjens et al. (under review).

Figure 6.4 shows the 2011 land use classification result and the IRSeL-processed land use layer. There is a high proportion of unclassified cells in the original 2011 classification (13.5 %, see Table 6.1 and Figure 6.4a) mainly caused by clouds and cloud shadows. The land use interpolation tool was used to fill the data gaps and to revise the layer by correcting classification errors. The IRSeL revised land use layer reflects land use patterns realistically and provides a consistent land use layer without data gaps (see Figure 6.4b).
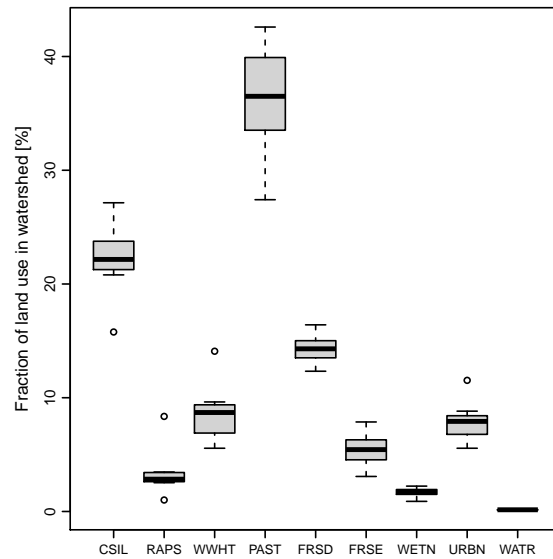
FIGURE 6.3: Box plots of yearly proportions of major land use types in the Bünzau catchment based on classifications of Landsat 5 imagery.

6.2.4   Modeling framework

SWAT STA and SWAT VAR results were compared to evaluate how the spatial and temporal representation of land use in the watershed affects simulated streamflow and water balance. Figure 6.5 shows the methodology. The ArcSWAT interface (Winchell et al., 2010) was used to carry out an initial sub-watershed model setup based on the 2009 land use map. Calibration was performed based upon comparison of simulated and observed discharge at gauge Sarlhusen in the Bünzau River from 2002 to 2006 (see Figure 6.1 and LKN, 2012). The calibrated parameter set was validated using the time period from 2007 to 2011. Hydrologic simulations in Northern Germany lowlands that included parameter sensitivity analysis were previously conducted by Dobslaff (2005), Schmalz and Fohrer (2009) and Kiesel et al. (2010). Their results showed a strong influence of groundwater parameters. Based upon their studies, nine parameters were included in

TABLE 6.3: Distribution of major land uses (corn CSIL, rape RAPS, winter wheat WWHT, pasture PAST, deciduous forest FRSD, evergreen forest FRSE, wetlands WETN, urban areas URBN and water WATR) in the Bünzau catchment based on classifications of Landsat 5 imagery (see Table 6.1).

Year	CSIL	RAPS	WWHT	PAST	FRSD	FRSE	WETN	URBN	WATR
2003	24.51	1.01	5.56	42.59	14.10	4.47	2.07	5.56	0.13
2006	15.78	2.84	9.63	41.65	16.41	6.30	1.34	5.92	0.13
2007	21.73	2.71	9.13	36.50	12.92	6.30	1.70	8.82	0.20
2009	27.14	2.53	14.09	30.85	12.33	3.08	1.79	8.02	0.15
2010	23.01	3.38	7.16	38.17	15.03	4.62	0.89	7.64	0.09
2011	20.80	8.36	6.63	27.41	15.00	7.87	2.23	11.53	0.18
2012	22.16	3.47	8.70	36.19	14.30	5.44	1.67	7.92	0.15
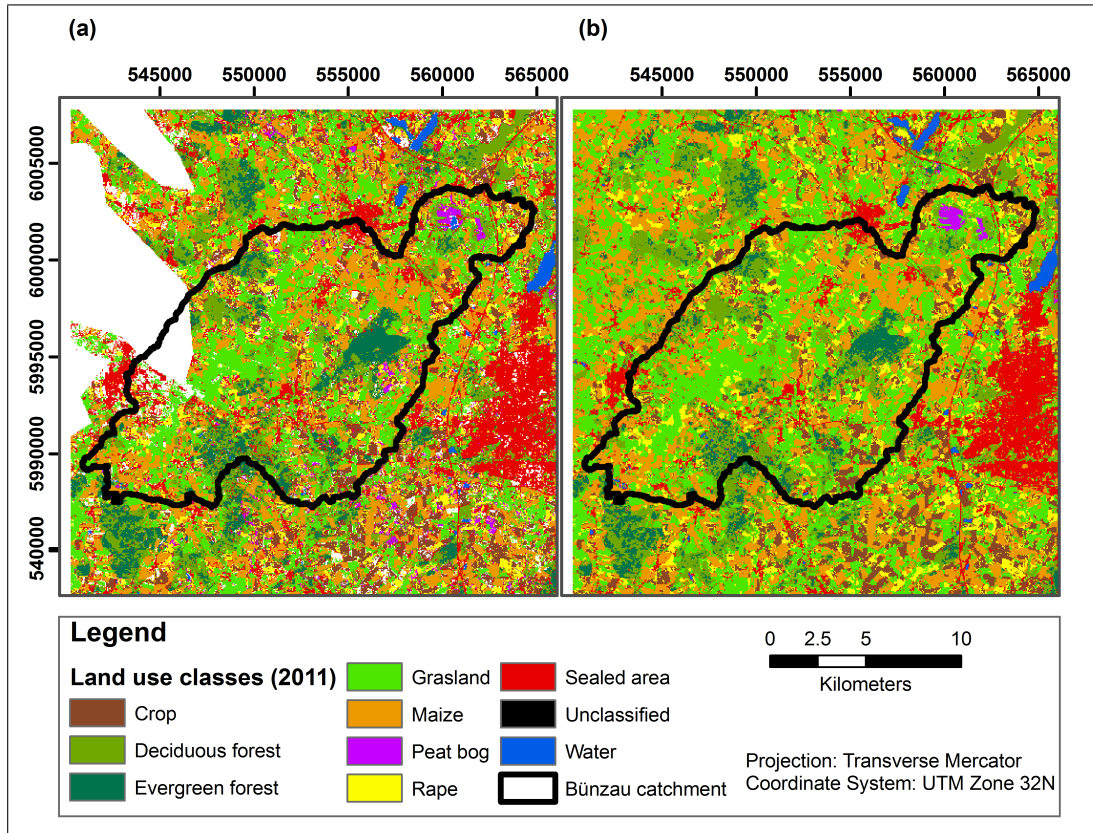
FIGURE 6.4: 2011 land use layer: (a) original classification results and (b) IRSeL interpolated and revised classification results.
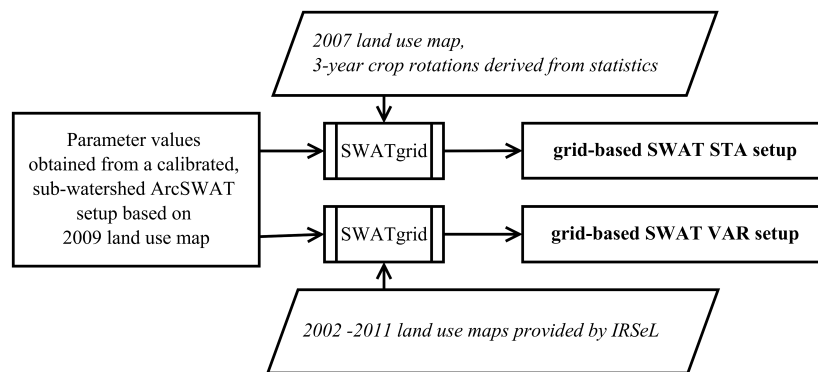
FIGURE 6.5: Flowchart of the SWAT STA and SWAT VAR model setups.

model calibration: runoff curve number (CNOP), soil evaporation compensation factor (ESCO), groundwater parameters (GW_DELAY, GWQMN, ALPHA_BF, GW_REVAP, REVAPMN), and hydraulic conductivity (CH_K, SOL_K). A detailed description of each parameter is provided by Arnold et al. (2013). The sub-watershed based setup performed well for both calibration and validation periods (NSE: 0.77, 0.67).

The interface SWATgrid (Rathjens and Oppelt, 2012b) was used to transfer the calibrated parameter set to the two grid setups without further parameter adjustments.

TABLE 6.4: Model input data sources.

Data type	Source	Data description
Topography (DEM)	LVA (2008)	Digital elevation model, 5 m × 5 m resolution
Soil map	Finnern (1997)	Physical properties of the soil, scale 1:100 000
	LLUR (2010)	Physical properties of the soil, scale 1:25 000
Land use maps	own classifications	Classifications based on Landsat 5 imagery, 30 m × 30 m resolution (see Table 6.1)
Climate data	DWD (2012)	Daily measured values of temperature, precipitation, wind speed, relative humidity (Neumünster station 2000-2007, Padenstedt station 2007-2011)
		Daily measured values of precipitation (Gnutz station 2000-2006)

This means that SWAT STA and SWAT VAR are the same except the land use data. In order to reduce the impact of model calibration (ArcSWAT setup) on the effects that different land use maps have on model output, different sets of land use data were taken for calibration and for the static setup; the ArcSWAT setup is based on 2009 land use data, while SWAT STA uses 2007 data (see Figure 6.5). SWATgrid generated grid-based SWAT model input using weather data and spatially distributed geographic datasets (Digital Elevation Model (DEM), soil and land use data). An overview of the essential input data sources is given in Table 6.4. Daily climate data obtained from three German weather service stations (DWD, 2012) from January 1st, 2002 to December 31st, 2011, including temperature, precipitation, wind speed and relative humidity, were integrated into the simulation. The Land Survey Office Schleswig-Holstein provided a DEM with a vertical resolution of 0.5 m and a horizontal resolution of 5 m (LVA, 2008). A soil layer as a composition of two soil type maps was obtained from the Agency for Nature and Environment Schleswig-Holstein (LLUR, 2010) and Finnern (1997).

SWATgrid divides the watershed into linked grids. Each grid has an individual combination of soil, land use and slope. Flow paths were determined from the DEM using the digital landscape analysis tool TOPAZ (Garbrecht and Martz, 2000), and runoff from a grid flows to one of the eight adjacent grids. A topographic analysis using TOPAZ and DEMs with different resolutions demonstrated that a small grid size of at least 50 m or 0.25 ha is necessary to ensure an accurate representation of the flat topography in the Bünzau catchment. A smaller grid size would lead to an increase of computation time and memory requirements of the model. As a compromise between a spatially accurate representation of landscape pattern and a timely manageable model, DEM, soil, and land use data were resampled to a resolution of 50 m. The Universal Transverse Mercator (UTM) projection is neither area nor distance accurate, so all layers were transformed to the Albers Equal Area projection.

6.2.5 Performance criteria

Standard test statistics recommended by Moriasi et al. (2007) as well as visual comparisons of observed and simulated data were used to evaluate daily, monthly and yearly streamflow SWAT simulations. Percent bias (PBIAS) was taken as a quantitative measure to compare observed and simulated total streamflow. PBIAS is calculated with equation (6.1):

$$\text{PBIAS } [\%] = \frac{\sum_{i=1}^{n} \left(Q_i^{obs} - Q_i^{sim} \right) 100}{\sum_{i=1}^{n} Q_i^{obs}}, \tag{6.1}$$

where Q_i^{obs} and Q_i^{sim} are the observed and simulated daily discharge for day $i = 1, \ldots, n$, and n is the number of observed values.

The RSR (RMSE-observations standard deviation ratio, Moriasi et al., 2007) was selected as an standardized error statistic. The RSR standardizes root mean square error (RMSE) values using the standard deviation of in-situ data and thus enables a comparison of error values of different studies. It is calculated with equation (6.2):

$$\text{RSR} = \frac{\sqrt{\sum_{i=1}^{n} \left(Q_i^{obs} - Q_i^{sim} \right)^2}}{\sqrt{\sum_{i=1}^{n} \left(Q_i^{obs} - Q_{mean}^{obs} \right)^2}}. \tag{6.2}$$

PBIAS as well as RSR are expected to reach 0 as the performance of the simulation improves.

The Nash-Sutcliffe efficiency (NSE, Nash and Sutcliffe, 1970) was selected as a normalized, correlation-related statistical index, which is often used to assess the quality of hydrological models. An NSE of 1 indicates a perfect match between observed and simulated data, while values lower than 0 indicate that the average of observed data is a better predictor than the simulated value. The NSE is calculated using equation (6.3):

$$\text{NSE} = 1 - \frac{\sum_{i=1}^{n} \left(Q_i^{obs} - Q_i^{sim} \right)^2}{\sum_{i=1}^{n} \left(Q_i^{obs} - Q_{mean}^{obs} \right)^2}. \tag{6.3}$$

Performance ratings published by Moriasi et al. (2007) were used for evaluating the simulation results for daily and monthly streamflow (see Table 6.5). The model was considered satisfactory if -25 % < PBIAS < 25 %, RSR < 0.7 (see also Singh et al., 2004) and NSE > 0.5 (see also Santhi et al., 2001). In addition, graphical techniques were used to identify trends and general differences between simulated and measured values.

TABLE 6.5: Model performance ratings for streamflow as established by Moriasi et al. (2007).

Performance rating	PBIAS [%]	RSR	NSE
Very good	|PBIAS| < 10	0.0 ≤ RSR ≤ 0.5	0.75 ≤ NSE ≤ 1.00
Good	10 ≤ |PBIAS| < 15	0.5 < RSR ≤ 0.6	0.65 < NSE ≤ 0.75
Satisfactory	15 ≤ |PBIAS| < 25	0.6 < RSR ≤ 0.7	0.50 < NSE ≤ 0.65
Unsatisfactory	|PBIAS| ≥ 25	RSR > 0.7	NSE ≤ 0.50

TABLE 6.6: Comparison of the ten-year average (2002 - 2011) of observed and simulated water balance components resulting from SWAT simulations with static (SWAT STA) and variable (SWAT VAR) land use data. Values in parentheses indicate the percentage of annual precipitation made up by the parameter.

Parameter [mm]	Observed	SWAT STA	SWAT VAR	Difference[a]
Precipitation	867.60	867.60	867.60	0.0
Surface Q	-	28.44 (3.3 %)	34.11 (3.9 %)	5.67
Lateral Q	-	19.35 (2.2 %)	18.99 (2.2 %)	-0.36
Groundwater Q	-	330.83 (38.1 %)	326.28 (37.6 %)	-4.55
Total water yield	389.19 (44.9 %)	378.38 (43.6 %)	379.08 (43.7 %)	0.70
GW recharge[b]	8.68 (1.0 %)	17.63 (2.0 %)	17.38 (2.0 %)	-0.25
ET[c]	469.73 (54.1 %)	465.70 (53.7 %)	465.50 (53.7 %)	-0.20

[a] Difference: SWAT VAR − SWAT STA
[b] Observed groundwater recharge calculated as 1 % of observed precipitation based on data from Preuss (1977).
[c] Observed evapotranspiration calculated by difference between precipitation (with 1 % groundwater recharge) and total water yield.

6.3   Results and Discussion

6.3.1   Evaluation of the annual water balance

Grid-based simulations were run for the period from 2002 to 2011 to assess the impact of land use data on SWAT model output. The 2007 land use layer was taken for the static setup and the IRSeL interpolated and revised land use data set was used for the variable setup. Table 6.6 shows annual means of the water balance components. For the observed data, total water yield was obtained from streamflow measurements, and evapotranspiration was calculated from the difference between precipitation and total water yield, assuming that storage components do not change between years and groundwater recharge was 1 % (Preuss, 1977) of annual precipitation. A shallow groundwater table, low hydraulic gradients, and high groundwater – stream water interactions characterize the Bünzau catchment. These interactions have been identified as the dominant processes (e.g., Schmalz and Fohrer, 2009) in the watershed. Groundwater contributes significantly to streamflow (approximately 38 % of the mean annual water balance), whereas hillslope surface runoff is very low (<4 %, e.g., Dobslaff, 2005).
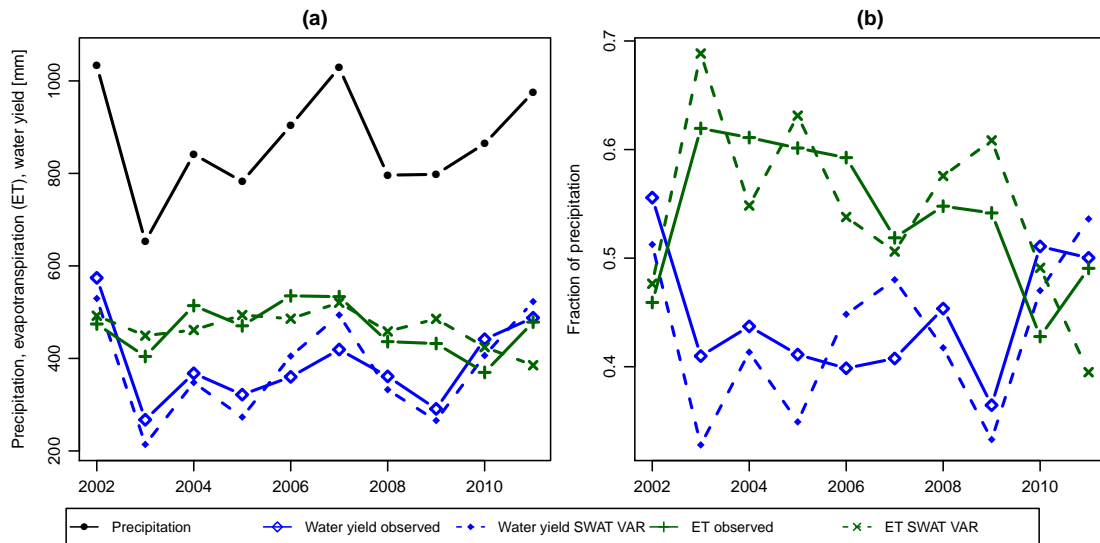
FIGURE 6.6: Comparison between the observed and simulated (SWAT VAR) water balance components for the Bünzau catchment from 2002 to 2011 (a) as absolute values [mm] and (b) as fraction of precipitation. Due to negligible differences between the results of the two setups, SWAT STA is not included in the figure.

For both model setups, results show a good agreement with the observed data. Differences between simulated and observed values were in a range of 1.2 percentage points (pp) of the mean annual water balance (see Table 6.6). Regarding total water yield and evapotranspiration, the model setups fit very well. The land use data seem to affect mainly surface and groundwater runoff. Mean annual surface runoff calculated by SWAT VAR was 5.67 mm higher than with SWAT STA, which is compensated by a lower amount of groundwater runoff (4.55 mm). Figure 6.6 shows annual values of total water yield and evapotranspiration from 2002 to 2011. In both setups, values are almost the same; differences between the the two setups for each year are smaller than 4.0 mm for water yield and 2.5 mm for evapotranspiration. For each year, simulated and observed total water yield were within a range of 8 pp of precipitation. The greatest difference was observed in the least humid year (2003), when observed and simulated water yield was 41 % and 33 % of precipitation, respectively (see Figure 6.6b). The greatest deviation in evapotranspiration was 10 pp, observed in 2011, where observed and simulated fraction of precipitation were 49 % and 39 %, respectively (see Figure 6.6b). Although observed data for flow components are not available, both model setups result in a sufficient representation of hydrological processes in the Bünzau catchment, as results are consistent and confirm previous studies by Jelinek (1999), Dobslaff (2005), and Schmalz and Fohrer (2009).

6.3.2   Evaluation of streamflow simulations

The hydrograph of daily streamflow (see Figure 6.7a for the ten-year period and Figure 6.8 for 2008) indicates that daily streamflow is accurately simulated in low flow conditions, while flow peaks are underestimated. Considering monthly streamflow, Figure 6.7b shows a good agreement between observed and simulated values in dry and wet months for both setups. The annual time series of observed and simulated total streamflow for the 2001 to 2011 period is shown in Figure 6.7c. Visual comparisons indicate good model agreement between observed and simulated daily, monthly and annual streamflow.

The main factors contributing to the errors between observed and simulated discharge were hydrograph timing and consistent underestimation of peak discharge (see Figure 6.7a). The simulated hydrograph peaks occurred approximately one day prior to the observed peaks. By shifting the calculated daily flows one day forward, performance statistics improved. Considering the period from 2002 to 2011, SWAT VAR NSE values increased from 0.61 to 0.64 and RSR values were reduced from 0.62 to 0.60. As groundwater flow is the predominant process in the Bünzau catchment, hydrograph timing and underestimation of peak discharge indicate that the streamflow simulations may be improved with better knowledge of groundwater conditions. SWAT simulates two aquifers, the shallow, unconfined aquifer causes return flow to streams within the watershed and the deep, confined aquifer contributes return flow to streams outside the watershed (Neitsch et al., 2011b). The model setups used in this study assume that groundwater parameters remain constant throughout the catchment. In addition, tile drains and depressions were neglected, although these landscape features heavily influence groundwater and streamflow processes in lowland catchments (Kiesel et al., 2010). Thus, model performance may be improved by using a multi-storage groundwater concept (e.g., Pfannerstill et al., 2013) and integrating tile drains, depressions, and spatially distributed groundwater conditions into the model. This paper, however, focuses on assessing the affect of land use data on model performance.

Test statistics (PBIAS, RSR, NSE) and visual comparison of the simulated and observed data at the watershed outlet were used to evaluate model performance. On a ten year basis the measurements summarized in Table 6.7 indicate that SWAT VAR performs slightly better than SWAT STA. According to Moriasi et al. (2007), model performance ratings for daily streamflow are within a satisfactory range for both setups and monthly ratings performed were very well, a trend typically observed in model applications (e.g., Moriasi et al., 2007).
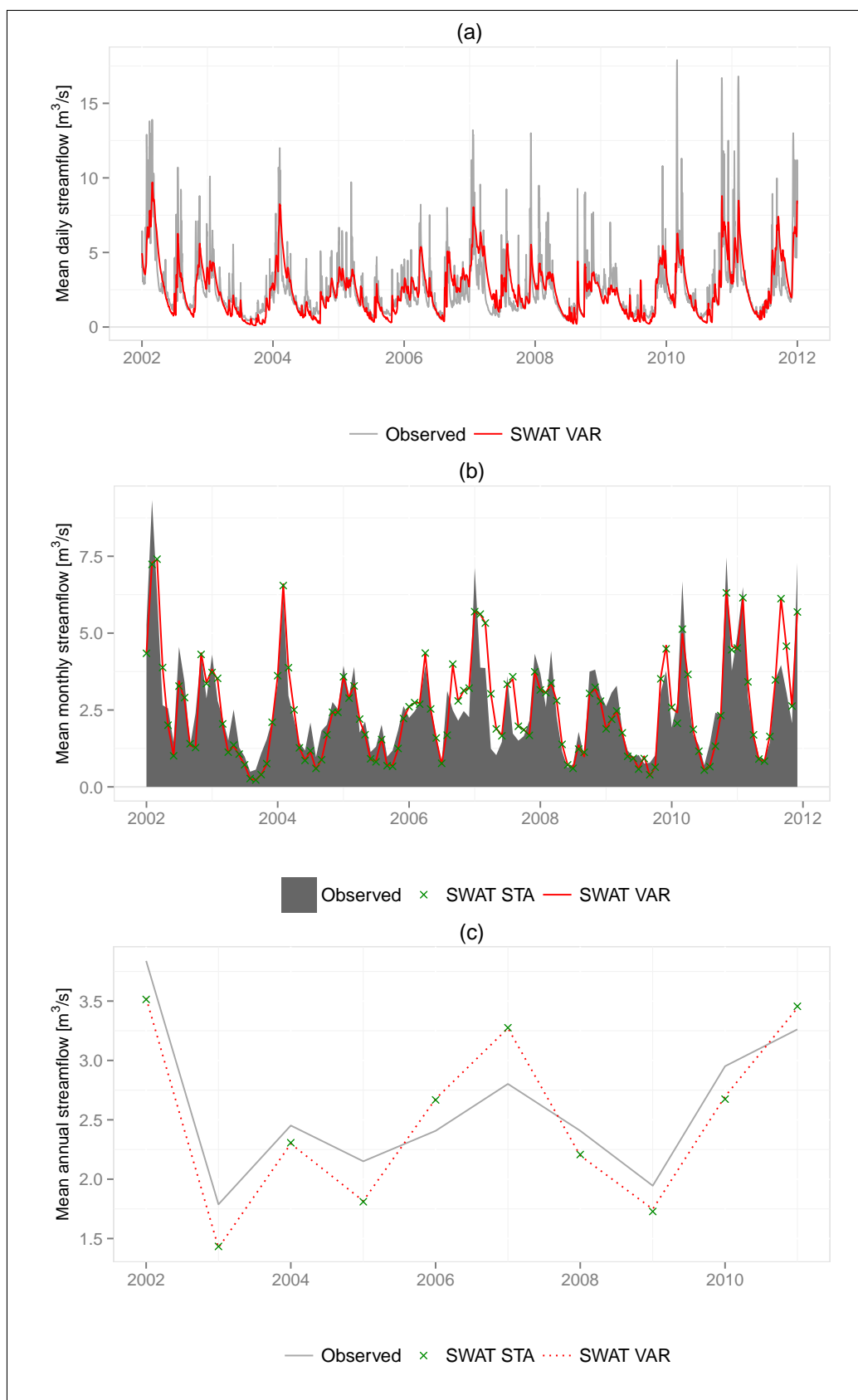
FIGURE 6.7: Observed and simulated (a) daily, (b) monthly, and (c) annual streamflow for the Bünzau catchment, 2002-2011.
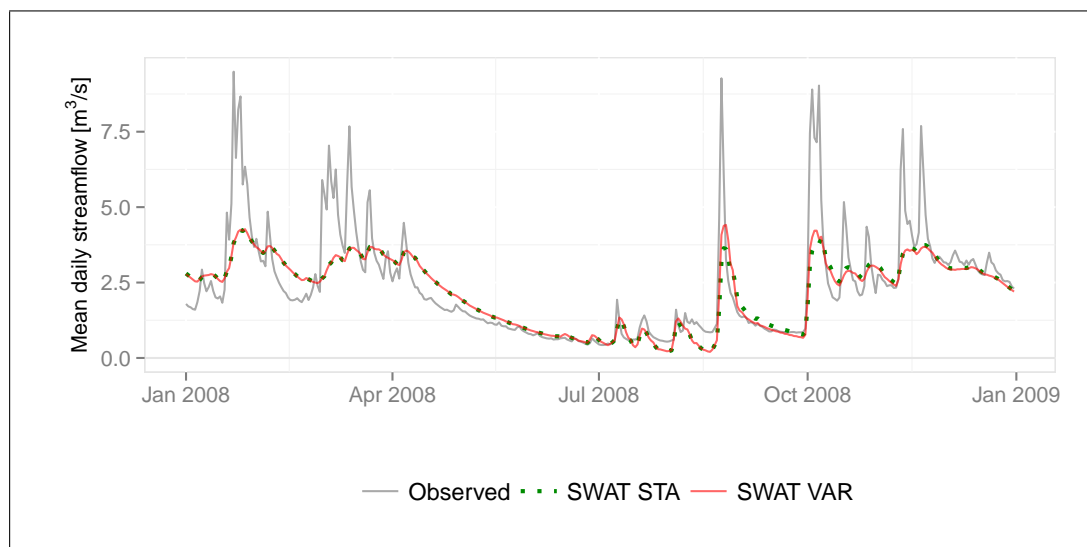
FIGURE 6.8: Observed and simulated daily streamflow for the Bünzau catchment, 2008.

TABLE 6.7: Accuracy measures of daily and monthly (in parentheses) simulated discharge for the SWAT STA and SWAT VAR results of the Bünzau catchment from 2002 to 2011.

Setup	PBIAS [%]	RSR	NSE	Performance rate	
SWAT STA	3.61	0.64 (0.46)	0.60 (0.79)	satis-	(very
SWAT VAR	3.45	0.62 (0.45)	0.61 (0.79)	factory	good)

Although SWAT VAR and SWAT STA performance measures are similar for the whole simulation period, larger differences occured on an annual scale. Figure 6.9 shows performance statistics of daily model output calculated for each year of the simulation period. Figure 6.9a shows similar percent bias values for both setups (differences are < 1.5 pp). These results indicate that annual differences of total water yield and evapotranspiration are negligible. Annual RSR and NSE values are shown in Figure 6.9b and c. The values indicate satisfactory model performances (RSR < 0.7, NSE ≥ 0.5) except for 2006 and 2007. In these years, the weak performance may be attributed to overprediction of flow volumes alongside underprediction of evapotranspiration (see Figure 6.6). SWAT VAR performs better than SWAT STA for each year of the ten-year simulation period, except 2009. However, no reasons (e.g., classification accuracy, varying streamflow characteristics, or particularly dry or wet year) were found for the better performance of SWAT STA in 2009. These results and the minor streamflow differences between the setups (see Figure 6.7 and 6.8) indicate that in the Bünzau catchment, other SWAT parameters (e.g., groundwater parameters) seem to be more important for model performance than land use data. However, a more accurate representation of land use patterns and its hydrologic properties in SWAT VAR leads to a better representation of the spatio-temporal land use status of the catchment, improves model performance and
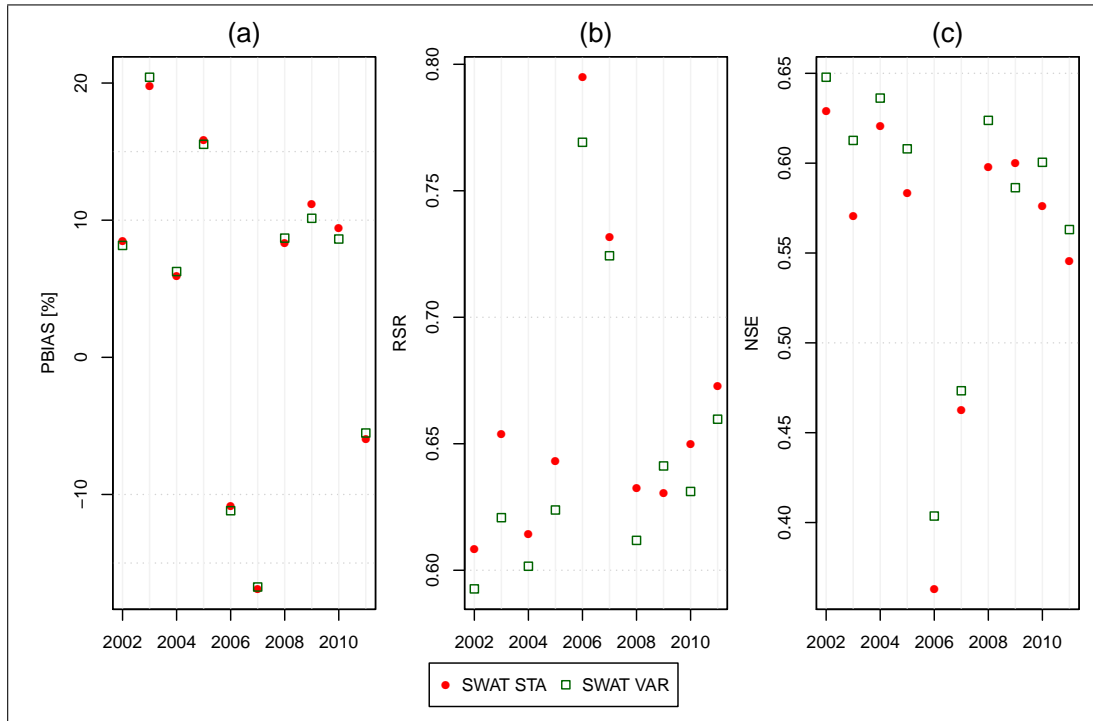
FIGURE 6.9: Annual performance measures (a) PBIAS, (b) RSR, and (c) NSE of daily
discharge from the static (SWAT STA) and variable (SWAT VAR) land use setups.

reduces uncertainties.

As SWAT STA is based on the 2007 land use data, this year is of particular interest.
SWAT STA uses classification results with an overall accuracy of 86 %, while SWAT VAR
simulations are based on the IRSeL revised land use data with an overall accuracy of 92 %
(Rathjens et al., under review). Differences between 2007 SWAT STA and SWAT VAR
daily streamflow performances are similar to differences observed for the rest of the
simulation period (see Figure 6.9). The highest difference in test statistics between the
setups was observed in 2003, the least humid year in the simulation period. The static
land use model seems to be less responsive to changes in weather conditions and tends
to require recalibration with changing weather conditions.

In general, varying performance measures indicate that there is a difference between
model results, but contain no information concerning the source of difference. Recog-
nizing this limitation, visual comparisons and a statistical analysis were applied. Visual
comparisons confirm a better performance of SWAT VAR, which can be explained by two
facts. First, simulation of peak discharge is better in SWAT VAR. Second, as indicated
by Figure 6.8, streamflow simulated by SWAT VAR rose and fell more realistically than
in the SWAT STA setup. Despite the differences observed at peak discharge and rising
and falling hydrographs, there is almost no difference between the two setups during low
flow conditions. Differences only occur if intense rainfall events cause rapidly rising and

falling streamflow hydrographs. Figure 6.10 visualizes the reason of differences between SWAT STA and SWAT VAR. Figure 6.10a shows the coherence between the absolute slope of measured discharge and differences between the setups. The higher the absolute slope in observed discharge, the higher the probability that there is a difference between the setups (solid line in Figure 6.10a); the higher the absolute slope of measured discharge, the higher the absolute difference between SWAT STA and SWAT VAR. Also, it was examined which proportion of differences between the setups were caused by a rapid change of measured discharge (i.e. a high absolute slope greater than two times its standard deviation of 3.2 m^3s^{-1}). Figure 6.10b shows the coherence between the absolute differences between the setups and the slopes of measured discharge. The higher the absolute differences between the setups, the higher the probability that the difference was caused by a rainfall event that led to rapidly rising or falling streamflow hydrograph (solid line); and the higher the absolute difference between the setups, the higher the absolute slope of observed discharge.

Overall, Figure 6.10 proves a strong correlation between the rate of rising and falling observed streamflow and the differences between the two setups; differences mainly occur if discharge changes rapidly. These events are often linked to more intense rainfall events which are expected to exceed the infiltration capacity of soil and therefore cause overland flow. SWAT uses the curve number equation to simulate surface runoff, which is parametrized by soil type, antecedent soil moisture, and land use. Each are associated with infiltration capacity, which imply infiltration excess runoff (e.g., Garen and Moore, 2005). Therefore, the effect of land use data on processes related to saturation excess flow or variable source area hydrology are hardly covered by this study. Plant characteristics affecting overall water yield or evapotranspiration seem to be negligible.

To sum up, flow components are the main hydrologic difference between SWAT STA and SWAT VAR, which can be confirmed by visual comparisons (see Figure 6.8), statistical analysis of the hydrographs (see Figure 6.10), and values of the average annual water balance (see Table 6.6). Flow components, especially surface runoff, are known to be extremely sensitive to CN values (Singh et al., 2004) that are associated to land use classes in the SWAT model. Due to the different proportions of land use distribution between the two setups (see Figure 6.3), CN values are updated each year in SWAT VAR or changed based on crop rotations in SWAT STA. A more accurate land use representation leads to more accurate CN values, which improves model performance and reduces model uncertainties.
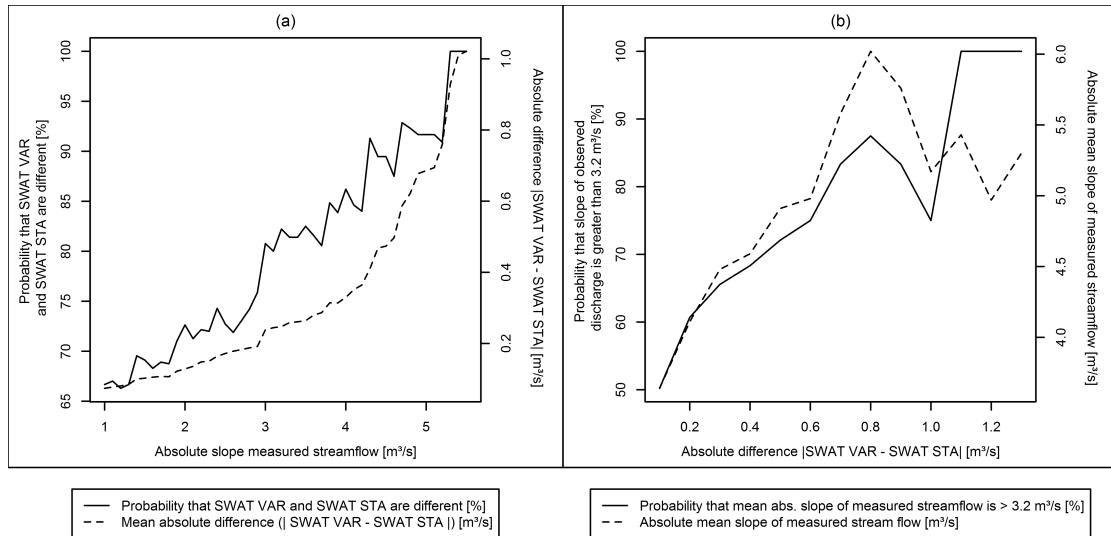
FIGURE 6.10: Coherence between rates of rising and falling streamflow and differences between SWAT STA and SWAT VAR. (a) The solid line shows the probability that slopes of observed streamflow (i.e. $|Q_i^{obs} - Q_{i+1}^{obs}|, i = 1, \ldots, n - 1$, n observed values) coincide with differences between SWAT VAR and SWAT STA. The dashed line shows the associated absolute mean difference between the two setups ($|$SWAT VAR $-$ SWAT STA$|$ [m³s⁻¹]). (b) The solid line shows the probability that absolute differences between the two setups ($|$SWAT VAR $-$ SWAT STA$|$ [m³s⁻¹]) coincide with changes in observed discharge greater 3.2 m³s⁻¹ (two times the standard deviation of measured discharge). The dashed line shows the associated absolute rate of observed discharge in m³s⁻¹.

6.4   Conclusion

In this study, the impact of the spatial and temporal representation of land use data on SWAT model output during a ten-year simulation period was examined. The Bünzau catchment, a sub-watershed of the Elbe River, served as a test site. A comparison was made between the simulation results obtained by using a single land use layer (SWAT STA), and the results obtained by updating the land use data each year (SWAT VAR). For this purpose, a land use interpolation and revision tool (IRSeL) was applied to obtain accurate land use data for each year of the simulation period.

Graphical comparisons and test statistics (PBIAS, RSR and NSE) were used to evaluate model performances. SWAT model results for the ten-year simulation period indicate that both setups yield reasonable estimates of daily, monthly and annual streamflow within the study area ($|$PBIAS$| \leq 25$ %, RSR < 0.7, and NSE > 0.5). Both setups, however, showed a one-day time lag between simulated and observed streamflow peaks, which may be an indication that the dominating interaction between groundwater and surface water is not well represented by the current model structure. Additionally, both setups underestimated peak discharge. It appears that additional model refinement may be necessary to better represent groundwater – surface water interactions. A satisfactory

output can, however, be obtained with both setups. Due to the better representation of land use distributions, slightly more accurate simulation results were obtained with SWAT VAR. In nine years of the ten-year simulation period, SWAT VAR provided better results than SWAT STA. Graphical and statistical comparisons between the setups indicate that SWAT VAR simulates flow components more realistically. With the results from this study we can conclude that an accurate spatial and temporal representation of land use data helps to reduce uncertainties in model predictions.

In general, models are evaluated based on their ability to simulate behavior at discrete locations (e.g., stream gages) because no spatially distributed data for model validation is available. Spatial heterogeneity becomes attenuated at the catchment scale and therefore differences observed between SWAT VAR and SWAT STA are hardly observable at the watershed outlet. These results confirm the findings of Volk (2010), which stated that only massive land use changes result in noteworthy shifts of the simulated water balances. However, even if no differences are observable at the catchment scale, there might be noteworthy spatial shifts within the catchment caused by land use changes. Such changes cannot be captured by using a single land use layer and crop rotations. Therefore, updating the land use data each year improves the model and leads to a spatially and temporally more accurate representation of spatial heterogeneity within the catchment, although the improvement is hardly observable at the catchment outlet.

Despite these difficulties, the impact of land use on SWAT output was evaluated based on the model's ability to correctly simulate flow hydrographs with less attention to spatial results. Almost negligible daily, monthly, and annual differences between SWAT STA and SWAT VAR observed at the catchment scale suggest that models using less accurate land use maps can be calibrated as well as models using high accuracy maps. This means that spatio-temporal accurate land use input is less important when studying aggregated (e.g., monthly values at the watershed outlet) behavior, but if the purpose of modeling is to replicate spatially distributed events (e.g., for identifying critical source areas of surface runoff, nutrients or pesticides) spatially accurate land use data is necessary.

The results presented are limited to the study area. With a generally shallow groundwater table, low temperatures and relatively evenly distributed rainfall, the Bünzau flow system is dominated by saturation excess (i.e. Hewlettian) overland flow (Stomph et al., 2002), while SWAT considers primarily infiltration excess runoff mechanisms (White et al., 2009). Thus, flow processes in the Bünzau catchment are expected to be more closely related to topography than to soils or land use. Smaller changes in land use data examined in this study (i.e. in the magnitude of its uncertainty and temporal variability) seem to be solely relevant for flow components. No significant differences in evapotranspiration or total water yield between the setups could be observed. This

means that in the Bünzau catchment, land use parameters affecting the infiltration capacity of the soil are more sensitive than parameters related to evapotranspiration or plant water consumption.

In order to verify the affects of the temporal representation of land use data on hydrologic model output, further studies in different watersheds using different models are necessary.

6.5   Acknowledgements

Chapter 7

Discussion and conclusion

7.1 Summarizing key achievements

The main objective of this dissertation is to improve the spatial representation of basin hydrology and flow processes in the SWAT model. This poses a particular challenge, as SWAT was originally designed as a semi-distributed model, operating at the sub-watershed scale, to predict agricultural management impacts on long-terms (i.e. decades) in relatively large watersheds (i.e. up to several thousand km^2). In the following, the results will be discussed with regard to the achievements of the research tasks, the answer to the main research question posed in Chapter 1 as well as the open questions and limitations of the developed model system.

> **Research Task 1**: Incorporating more spatial detail into SWAT by developing a model interface that setups SWAT in a grid-based discretization scheme.

This research task has been addressed in Chapters 2 and 3. Chapter 2 presents the interface SWATgrid that was developed to set up SWAT based on grid cells. A grid-based simulation allows the user to incorporate more spatial detail than the conventional sub-watershed approach. The primary goal of the grid-based setup is to simulate processes for every grid cell individually. Therefore, the model output can be directly linked to specific locations in a watershed (i.e. individual grid cells), making SWAT provide spatially distributed results. SWATgrid enables the modeler to incorporate spatially distributed information into a simulation. The functioning of SWATgrid is demonstrated in Chapter 3, in which a basic application of SWATgrid to a sub-catchment of the Elbe River, in Northern Germany, is presented. A comparison between SWATgrid and conventional sub-watershed-based results demonstrates that the two approaches agree well

at the watershed outlet, which proves the general functioning of the grid-based approach. Components of the water balance equation and streamflow at the watershed outlet temporally match well. Moreover, results suggest that the sub-watershed approach can be calibrated to a similar quality as the grid-based SWAT version but cannot provide spatially distributed results, and thus loses spatial information regarding flow paths. The grid-based SWAT version preserves the hierarchically organized structure of the model, i.e. its performance is as good as the well-established sub-watershed approach, and additionally, provides spatially distributed results. Taking spatially variable input data into account without information loss and obtaining spatial output data in the resolution of the applied DEM are the main advantages of the grid-based approach.

Chapter 3 also presents a time-efficient procedure to calibrate grid-based setups. To perform hydrological studies, a SWAT user first calibrates the model to fit it to the environmental and hydrological conditions of the catchment. Model output and in-situ data are compared to improve model input parameters iteratively. Compared to the sub-watershed approach, the grid-based setup significantly increases model computation time and, hence, aggravates calibration, according to established calibration guidelines.

> **Research Task 2**: Developing routing capabilities between grid cells and adapting the SWAT hydrologic algorithms from the sub-watershed to the hillslope scale.

This research task is the main focus of Chapter 4 , in which a grid-based version of the SWAT landscape model is presented. The newly developed model uses a new flow separation index that considers topographic features and soil properties to capture channel and landscape flow processes related to specific landscape positions. The resulting model includes surface, lateral, and groundwater fluxes in each grid cell of the watershed and is able to capture heterogeneously distributed flow and transport processes in a watershed. The model was calibrated and validated for the Little River Watershed (LRW, 334 km^2) near Tifton, Georgia, USA. The results suggest that the grid-based landscape model simulated the streamflow hydrograph at the outlet of the LRW satisfactorily. The new model predicts observed streamflow well and previously reported discrepancies between observed and simulated streamflow, for example, during zero-flow conditions (Bosch et al., 2004; Feyereisen et al., 2007) does not occur. Errors in the simulated streamflow can be attributed to an underestimation of streamflow peaks and an overestimation of streamflow during wetting-up periods. The results presented in Chapter 4 demonstrate that the grid-based SWAT version is generally able to simulate spatially distributed hydrological processes. However, the results also stress the importance of a model revision, specifically, the saturation excess concept, which has also been reported by White

et al. (2011) and Easton et al. (2011). The most important sources of uncertainty in the SWAT model are related to Variable Source Area (VSA) hydrology, soil moisture, and saturation excess overland flow at the hillslope scale. These uncertainties are discussed in a separate chapter (Chapter 7.3) below.

> **Research Task 3**: Improving SWAT input parameters by deriving input
> data from remotely sensed data.

Distributed modeling demands high quality spatial input data. Achieving this task is the central aim of Chapter 5, which presents a space-time interpolation and revision approach for remotely sensed land use data. The approach leverages special properties known for agricultural areas, such as crop rotations or temporally static land cover classes. The newly developed IRSeL-tool (**I**nterpolation and improvement of **R**emotely **Se**nsed **L**and cover) corrects classification errors and interpolates missing land cover pixels in the temporal or spatial dimension. Afterwards, Chapter 6 presents an application study, which assesses the impact of the accuracy and temporal representation of land use data on SWAT model performance. Comparisons were made between SWAT results obtained using a single land use layer and those obtained using more accurate IRSeL-modified individual land use layer for each simulation year. The results suggest that models using less accurate land use maps can be calibrated to make them as good as models using high accuracy maps, but they cannot represent the impact of the annual variability of land use data on model output. Chapter 6 demonstrates that an accurate temporal representation of land use data helps to reduce uncertainties in model predictions. The requirements of distributed models on spatial input data and its effects on model uncertainties are discussed in a separate chapter (Chapter 7.2) below.

> **Central research question**: Does the incorporation of more spatial detail
> into a SWAT model help to fulfill the requirements of integrated water basin
> management?

Most decisions on water policy are addressed at larger watersheds (Beven and Freer, 2001). Integrated water basin management, however, requires spatially detailed model results for the identification of critical source areas within a watershed, where the implementation of the best management practice need to be focused on. As SWAT was developed to assist water resource managers to assess the impact of management on water supplies on the watershed scale (Arnold et al., 1998) a model revision seems necessary. This dissertation achieved spatial enhancement of the SWAT model by incorporating a grid-based discretization scheme, revising the spatial representation of

hydrologic processes, and improving the quality of input land use data. Results indicate that the performance of the grid-based model is as good as the conventionally used sub-watershed approach at the watershed-outlet (i.e. on the catchment scale), and reduces model uncertainties at the hillslope scale.

However, the quality and spatial resolution of input data as well as physical representation of processes create barriers to the use of SWAT for river basin management. The recurring problem in its use for watershed management is the discretization of the watershed to best represent watershed processes without exceeding the limitation of available data and computational time requirements. For this reason, SWAT is based on assumptions for up-scaling processes that exist at the hillslope scale. The model aggregates processes acting at different scale levels by combining empirically derived functions with physically based ones. Of course, the applicability of SWAT for distributed modeling is also restricted by a lack of suitable data for the different scales. A review of scale-specific data requirements and processes, as well as process representation in the SWAT model is crucial to assess model uncertainty at specific scales. If it is known which scale is important for watershed management, which processes act at which scale, and how they are represented in the model, uncertainties can be assessed and future research needs can be pointed out (Blöschl and Sivapalan, 1995; Volk et al., 2008).

7.2   Spatial input data and distributed modeling

The need to precisely describe the characteristics of a watershed is well-known in environmental modeling. Spatial input data (such as climate, topography, land use, and soil type) are time-consuming and costly to obtain, especially when large areas are considered. The quality of the spatial input data is assumed to directly affect the simulation results of hydrologic models (e.g., Quinn et al., 1991; Chaplot, 2005). Therefore, the analysis of the sensitivity of models to the accuracy of these relatively expensive and difficult-to-obtain data has become a challenging issue in environmental modeling (e.g., Beven, 1993; Chaplot, 2013). Chaplot (2013) recently stated that a consensus on the sensitivity of models to the whole range of spatial input data and different environmental conditions has not been reached. Modelers are still challenged by the question concerning how to weigh the level of investment to be made in generating spatial input data; i.e. decisions about the resolution and the precision of input maps (e.g., soil type and land use) have to be made.

By using SWAT, Chaplot (2005) demonstrated that hydrology is hardly affected by the resolution of land use maps. They explained these results by slight differences in the proportion of the different crops between the low and high resolution maps. Lower

soil map resolution, however, greatly degrades the prediction quality (e.g., Geza and McCray, 2008). Chaplot (2013) stated that the minimum spatial input data resolution needed to achieve accurate modeling results could be predicted from a watershed's relief and mean annual precipitation. These studies evaluated model performance, based on the model's ability to correctly predict flow hydrographs with lesser attention to spatial results. The process of calibrating a model at discrete locations (e.g., streamgages) does not necessarily improve the spatial accuracy of the model (White et al., 2009). In this context, Arnold et al. (2010) showed that aggregated datasets and models can be calibrated to be as good as more detailed catchment representations but cannot account for spatial heterogeneity within a catchment. Therefore, the appropriate precision and resolution of spatial input strongly depends on the modeling purpose and the ability of the model to capture small-scale processes. If the model is developed to replicate spatially distributed events, high resolution spatial data is necessary, but if it is more important to simulate aggregated behavior at the watershed outlet, lower resolution data may be appropriate.

Chapters 5 and 6 demonstrate that the lack of high quality and accurate long-term series of model input data having the desired spatial resolution limits the capacity to perform distributed water basin simulations. This issue represents a general problem in environmental modeling and results in uncertainty. As shown in Chapter 6, modelers can help to reduce uncertainty by analyzing and improving existing datasets statistically as well as developing appropriate monitoring and data sampling strategies (e.g., Ullrich et al., 2008). Generally, remote sensing has the potential to become a useful tool to provide environmental information needed for water basin management and for deriving spatially detailed model input parameters. This includes information about topography (DEM), climate data (e.g., Yan et al., 2010), land use patterns (e.g., Ouyang et al., 2010b; Pandey et al., 2005; Xue et al., 2008), vegetation parameters and vitality (e.g., Strauch and Volk, 2013), or soil parameters (e.g., Pause et al., 2008). Besides, remote sensing data has shown a high potential for spatial model validation e.g., evapotranspiration (e.g., Glenn et al., 2010; Vinukollu et al., 2011) or soil moisture (e.g., Cashion et al., 2005; Pierdicca et al., 2010).

7.3 Hydrological processes and their representation in the SWAT model across spatial scales

The role of models in reflecting our understanding of hydrologic systems is important to the establishment of the best management practice in integrated management plans. A review of the underlying drivers that control hydrology at scale levels relevant for spatial
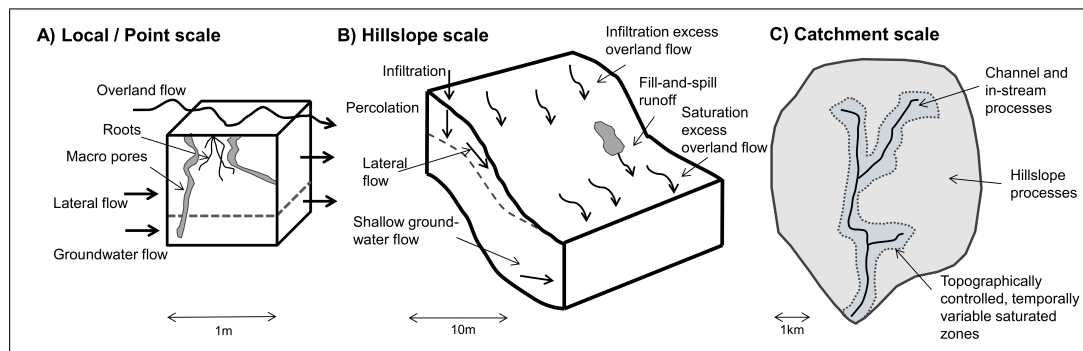
FIGURE 7.1: Processes and scale (adapted from Quinn, 2004; Garen and Moore, 2005). (A) A typical $1\,m^2$ soil column where hydrologic processes are dominated by soil conductivity, roots and macroporosity. (B) Water fluxes and streamflow generating processes on a typical hillslope section terminating at a stream channel. Ground water table is shown as a dashed line. (C) Schematic representation of saturated zones (variable source areas) under relatively dry conditions (dashed line), where dominant land use, soil type, topography and rainfall gradients dominate hydrologic processes.

planning should be carried out before any model is applied. Ideally, processes should be modeled at the scale that is relevant for planning and river basin management. Generally, process representation is the most fundamental problem of model development. As scale increases, processes integrate to yield responses requiring data sets and simulation strategies that differ markedly from those appropriate for smaller scales (e.g., Quinn, 2004). This underscores the importance for modeling strategies and stresses the need for multi-scale catchment models that operate at all scale levels relevant for spatial planning. By showing the processes at each scale, it is possible to look at some problems of process simulation and measurement. Figure 7.1 (inspired by Quinn (2004), and Garen and Moore (2005)) is an attempt to demonstrate how hydrological processes change with scale, helping to identify key factors that influence hydrology. It is then possible to check at which scales the SWAT model is appropriate. The following review focuses on the processes, while the problem of actual availability of data needed for describing these processes still remains.

7.3.1   Point scale

In Figure 7.1A, $1\,m^2$ of soil is assumed to be the plot scale or 'point' scale where soil type, crop type, and leaching processes are dominant. The soil, roots and macropores are shown, all of which control the soil moisture (Quinn, 2004). Once water infiltrates into the soil, it is still affected by gravity and either infiltrates to the water table or travels downslope (e.g., Selby, 1993); capillary pressure and gravity thresholds dictate hydraulic conductivity in the unsaturated soil matrix (Spence, 2010). As water drains from the soil, a larger number of voids become empty, leaving a more circuitous route for the remaining water (Knapp, 1978), which results in asymptotic drainage. Void

heterogeneity dictates that saturation is not a complete reversal of drainage. The result is the non-linearity and hysteresis between water content and hydraulic conductivity (Spence, 2010). The hysteresis is, however, neglected in many applications and models because of its complicated nature (Spence, 2010) although its importance for processes acting at larger scales (e.g., hillslope runoff) has been noted (Sloan et al., 1983; Quinton et al., 2008).

The frequency at which macropores conduct pipe flow is controlled by macropore storage thresholds and the ability of the soil matrix to receive and conduct water. The rate of transfer from the soil matrix needs to equal or exceed infiltration losses from the macropore to the soil matrix in order to fill the macropore and initiate and sustain pipe flow (Spence, 2010). Furthermore, macropores have different thresholds of response, which is due to two controls. First, the area contributing flow to the macropore may be different. Second, the number, size and connectivity of macropores within the soil profile can differ (McDonnell, 1990). Already saturated macropores do not require upslope water or filling by the soil matrix. Thus, they react more quickly to rainfall events. This means that the moisture status of the soil matrix and its moisture-characteristic curves determine how, when, and where the soil and macropore network become saturated in response to a given input of water (Spence, 2010).

SWAT's soil moisture routine greatly simplifies processes that govern water movement through porous media in partly-saturated regions. It represents soil moisture dynamics with a volume-balance equation applied over the root zone of a plant. Guswa et al. (2002) demonstrated that the use of such a simple routine to predict soil moisture is not appropriate if the plant lacks the ability to compensate for spatial variation in saturation of the soil profile. Saturation excess flow is a dominant streamflow-generating process during most storms of ordinary intensity. Soil column scale hysteresis has a significant impact on soil saturation, which determines saturation excess flow that originates only in certain areas, not over the entire watershed. As a consequence, SWAT considers primarily infiltration excess runoff mechanisms (e.g., White et al., 2009), while saturation excess flow may also be an important factor (Garen and Moore, 2005). Analyzing hydrological processes at the plot scale demonstrates that storage thresholds occurring at this scale must be necessarily breached to initiate the transfer of surface or subsurface downslope flow. Therefore, processes acting at the plot scale affect hillslope scale runoff processes (Torres et al., 1998; Spence, 2010). Chapter 4 of this dissertation demonstrates that SWAT is not able to adequately simulate saturation excess overland flow, which might be related to the soil moisture equations implemented in the SWAT model. The saturation status of the watershed is not well represented by the model. Streamflow during wetting-up periods is generally overpredicted, while peak streamflow is underestimated if the watershed is saturated. The results presented in Chapter 4

clearly indicate that model performance strongly depends on the saturation status of the watershed.

7.3.2   Hillslope

Figure 1B shows that many differing flow processes are in operation at the hillslope scale. In general, hydrological processes tend to vary greatly between the catchment divide and the main channel, reflecting a change in landscape. The dynamics of both the unsaturated and saturated flow processes are spatially and temporarily complex (Quinn, 2004).

Once a soil column becomes saturated, hydraulic conductivity across that section of the hillslope increases exponentially (Spence, 2010), making different processes important. These processes transmit water through the hillslope and include infiltration and saturation excess overland flow, subsurface flow, and fill-and-spill runoff. The importance of each process in different landscapes is well discussed in the literature (e.g., Beven, 2012). Depending on the landscape features, each runoff generation process is dictated by its own inherent thresholds. The spatial distribution of infiltration excess runoff is controlled by where infiltration capacity is exceeded (Betson, 1964), saturation overland flow is generated at the topographic surface when the rate at which water is supplied to the soil column is higher than the hydraulic conductivity (Hewlett and Hibert, 1967), and fill-and-spill runoff occurs if spatially variable key stores across the hillslope are satisfied (Tromp van Meerveld and McDonnell, 2006). Accurate estimates of soil thickness, soil type, slope, relief shape, potential contributing area and local hydrometeorology are needed to adequately describe these processes (e.g., Spence, 2010). Dunne and Black (1970), for example, analyzed the impact of soil thickness and convex and concave slopes on runoff. All these mechanisms result in dynamic contributing areas on hillslopes over space and time (McNamara et al., 2005; Tromp van Meerveld and McDonnell, 2006). Different surface and subsurface flow processes have been observed on the same hillslopes under different saturation conditions (Montgomery and Dietrich, 1995; Spence, 2010). The potential exists for any runoff mechanisms to occur on any hillslope, but it is the interplay between inputs and storage thresholds that defines when and how frequently each process' thresholds will be breached (Spence, 2010).

The grid-based SWAT landscape model (based on the versions of Volk et al. (2007) and Arnold et al. (2010)) presented in Chapter 4, computes surface runoff for each grid cell with the curve number method. Run-on to an adjacent downslope landscape unit is estimated using an individual coefficient to partition the amount of flow that is channelized before leaving the grid cell and the amount that is direct surface run-on.

The curve number varies non-linearly with the moisture content of the soil (that is calculated using a simple volume-balance equation). It drops as the soil approaches the wilting point and increases as the soil approaches saturation. Due to the curve number method, SWAT primarily considers infiltration excess runoff mechanisms (White et al., 2009). Arnold et al. (1998) explained their choice of curve number instead of an infiltration equation for use in the SWAT model with data availability issues (rainfall and soil data), computation time, and the model application scale. The curve number procedure was, however, designed to predict streamflow (i.e. total water yield) on the catchment scale (Soil Conservation Service Engineering Division, 1972). Applying the equation to the hillslope scale means that the calculated values are interpreted to be overland flow (i.e. unchannelized water flowing over the surface into the next channel); assuming equivalence between streamflow and overland flow implies, in terms of the curve number equation, that only overland flow is responsible for streamflow generation (Garen and Moore, 2005). In the SWAT model (and in this dissertation), the curve number procedure is applied to the hillslope scale, although the equation seems unable to capture the variety of runoff generating processes and its associated thresholds. There are a few applications and studies that analyzed SWAT model results qualitatively at the hillslope scale (e.g., Chapter 4 of this dissertation; Bosch et al., 2007a; Volk et al., 2007; Arnold et al., 2010) and only Bosch et al. (2010) evaluated SWAT model performance quantitatively. They stated that there was a relatively poor fit to the monthly surface runoff observations (negative monthly Nash-Sutcliffe efficiency), but the trends in general were correct. Results were considered 'encouraging', while additional calibration and testing of the SWAT landscape model was necessary. In particular, the model requires additional detail to properly describe interactions between the soil surface, the vadose zone, and groundwater (Bosch et al., 2010). In this context, the empirical curve number equation seems to be a key weakness of the SWAT model. Observations made in Chapter 4 of this dissertation demonstrate that SWAT is not able to adequately simulate saturation excess runoff mechanisms. SWAT can be calibrated to an average saturation condition of the watershed, but model performance significantly decreases as the watershed saturation differs from its average. Streamflow is underestimated when the watershed is saturated and overestimated during low-flow conditions. Spatial results obtained with the curve number, however, are reasonable. Highest surface runoff values occur in urban areas, and the model simulates more surface runoff in upland areas than in flat floodplain areas. Hence, the curve number method is able to account for spatial heterogeneities related to topography (i.e. slope), soil type, and land use, but is not able to simulate the temporal, dynamic nature of saturation excess runoff in the floodplains. Alternative concepts should be considered to overcome the difficulties inherent in the curve number method. Agnew et al. (2006) stated that there are several physically based distributed hydrologic models that consider variable source area hydrology,

requiring large amounts of input data and/or substantial calibration and yielding mixed results (e.g., Bernier, 1985; Beven, 1989; Wigmosta et al., 1994), making their application to ungaged watersheds and data-scarce catchments uncertain (Grayson et al., 1992; Beven, 2012). Grayson et al. (1992) stated that complex, process-based models are useful in research, but models used for river basin management should be simple, with few data requirements and clearly stated assumptions. TOPMODEL (e.g., Beven and Kirkby, 1979) and the Soil Moisture Routing model (SMR, e.g., Frankenberger et al., 1999; SWL, 2003) are two physically-based, simple watershed-based models (Agnew et al., 2006). Both models are able to capture Variable Source Area (VSA) hydrology and have been shown to successfully identify saturated areas (e.g., Mehta et al. (2004), for SMR; Holko and Lepistö (1997), for TOPMODEL). TOPMODEL is based on the assumption that a catchment-wide water table intersects the landscape to predict saturated runoff generating areas. It uses a topographic index that implies steady-state assumptions and requires some calibration. In contrast, SMR assumes that saturated areas are controlled by transient interflow, perched on a shallow restricting layer. The model uses a simple physically-based water budget equation that requires virtually no calibration (e.g., Agnew et al., 2006). It is fully distributed, runs on a daily time step, and predicts daily saturation-excess overland flow occurring at any point in a watershed. SMR's input requirements include digital elevation data, soil parameters, and land use data (Frankenberger et al., 1999); data that is needed for SWAT simulations anyway. Both TOPMODEL and SMR are watershed-based models that operate on a daily time step. Their concepts are thus considered to have strong potential to improve spatial distribution of hydrologic processes in the SWAT model that are related to VSA hydrology, particularly to soil moisture and saturation excess runoff. In Chapter 4, parts of the TOMPODEL framework are integrated into SWAT, and the results obtained demonstrate that using a modified version of the topographic TOPMODEL index improved spatial representation of basin hydrology. Data requirements, spatial scale, and time step of SWAT and SMR are similar and SMR's methods are simple, but physically based and fully distributed. Therefore, incorporating the well-evaluated hydrological algorithms used in SMR into SWAT seems to be a promising task for future studies.

Lateral soil flow volumes are simulated using a kinematic storage model with multiple soil layers as a function of saturated hydrological conductivity, slope, slope length, and porosity (Arnold et al., 1998). SWAT represents associated soil moisture dynamics with a volume-balance equation. Guswa et al. (2002), however, demonstrated that the use of such a simple routine may not be appropriate for predicting vertical soil moisture distribution. Furthermore, the curve number method used for calculating surface runoff is unable to directly model infiltration (Neitsch et al., 2011b). The amount of water entering the soil profile is calculated as the difference between the volume of precipitation

and the volume of surface runoff. The Green & Ampt infiltration method (Green and Ampt, 1911), which is also integrated in the SWAT model, models infiltration directly but requires precipitation data in smaller time increments that are often not available.

Groundwater flow is calculated as routing through a series of linear storage elements (often named tank model, see Brutsaert, 2005) that may be influenced by groundwater evaporation or seepage to the deep aquifer (Arnold et al., 2010). Pfannerstill et al. (2013) demonstrated recently that an extended groundwater concept, using multiple storage components, can significantly improve the representation of groundwater processes in the SWAT model. Streamflow results of the SWATgrid application study performed in Chapter 4 of this dissertation indicate systematic differences between the observed and simulated baseflow component. The model generally overpredicts baseflow during wetting-up periods; the observed baseflow component increases slowly, while the simulated baseflow rises too rapidly. The opposite happens during drying periods, when the observed streamflow decreases slowly, while the simulated streamflow falls too rapidly. The model, however, performs well during average saturation conditions. These results indicate an underestimation of the available groundwater storage at wetting-up and drying periods. A multiple groundwater storage concept will be able to consider a greater groundwater storage capacity during these periods, leading to a slower filling in the wetting-up period and a longer hydrograph on the falling side.

SWAT greatly simplifies both surface and subsurface hillslope runoff processes. Review of SWAT's hydrological algorithms leads to the conclusion that SWAT seems unable to capture the interplay among multiple storage thresholds that define when surface or subsurface hillslope runoff will occur; results presented in previous studies (e.g., Bosch et al., 2010) and in Chapter 4 confirm this finding. Hydrological runoff processes acting at the hillslope scale (i.e. infiltration and saturation excess overland flow, subsurface flow, fill-and-spill runoff) heavily rely on the spatial distribution of soil thickness and soil moisture (e.g., Guswa et al., 2002; Zehe et al., 2005; Spence, 2010), water table height (e.g., McCaig, 1983), and topography (e.g., Dunne and Black, 1970). Hence, hillslope runoff process is hysteric, highly non-linear, its occurrence is not static, it does not follow steady state principles, and is threshold-mediated (McGlynn and McDonnell, 2003; Spence, 2010). The suitability of the SWAT model for analyzing how different landscape units interact over time to produce a catchment runoff signal can be questioned. However, the role of topography, soil, and human influences are at their greatest at the hillslope scale (Quinn, 2004). Integrated models should reflect impacts of hillslope scale conservation measures and landscape features (e.g., wetlands, hedgerows, and buffer zones) and capture the impact of the dominant hillslope flow path on the channel. The temporal dynamics of saturated areas and the surface and subsurface flow connectivity of these areas to the receiving channels need to be addressed in future studies.

7.3.3   Catchment

Many water resource management problems occur at the catchment scale, and it is often accepted that, as catchment size increases, complex local patterns become attenuated. Hewlett and Hibert (1967) and Dunne and Black (1970), however, demonstrated how storage thresholds associated with different hydrologic processes at the hillslope scale dictate catchment runoff response (see also Spence, 2010). The most profound effect at the catchment scale is that the area contributing to surface and subsurface runoff is diverse and variable. This phenomenon showed how the distribution of landscapes features and associated storage thresholds determine the organization of the stream network, the flow contributing areas overtime, and thus runoff response at the catchment outlet (e.g., Spence et al., 2010).

However, the superimposition of processes is accepted as the scale increases, and SWAT has proven to be a suitable model at the catchment scale. The use of the curve number method for catchment runoff, as well as simple soil storage, groundwater, and lateral flow equations is appropriate. Numerous applications use the outlet gauge discharge data for validation purposes. Results presented in Chapters 2, 3, 4, and 6 of this dissertation confirm the good model performance at the catchment scale. The model still performs well even if model calculations are made at a finer spatial scale. Up-scaling processes from smaller scales to the catchment scale and superimposing smaller scale runoff processes produces a non-linear relationship between inputs and runoff, reflecting a catchment runoff response. The use of these methods in non-point source water quantity and quality models for answering complex questions on detailed spatial and temporal scales is, however, questionable.

7.4   Conclusions and further research needs

A broad re-classification of the landscape at the hillslope scale is needed for river basin management to reflect the hydrologically dominant processes, including both natural and man-made factors (Quinn, 2004; Volk, 2010). In the light of the relatively simple hydrologic algorithms and equations used in the SWAT model, the question arises whether SWAT represents an adequate choice of model for simulating such complex, spatially and heterogeneously distributed processes at the hillslope scale. Environmental modeling generally involves the challenge of finding a balance between an adequate representation of crucial processes in a model and its data requirements. Empirical models like the curve number method are still used because of their ease of application and low data requirements (Arnold et al., 1998). However, empirical models are not able

to simulate physical processes, and the reliability of results should be carefully verified. In contrast, physically based models provide an accurate and detailed representation of processes, but are computationally intensive and require a large amount of data. SWAT combines empirically derived algorithms with physically based ones. To use models for integrated watershed management it is necessary that they provide information on a wide range of abiotic and biotic aspects of hydrology (Seppelt et al., 2009). Among the numerous hydrological and water quality models that have been recently developed, SWAT is one of the most suitable models for simulating water quantity and quality under various environmental conditions (e.g., Behera and Panda, 2006). SWAT simulations performed in this dissertation yielded promising results, demonstrating the general applicability and suitability of the model for river basin management, while additional development is necessary to improve representation of processes that are spatially heterogeneously distributed throughout the catchment. For this purpose, the use of the freely available, open-source model SWAT is advantageous, as users can easily modify the model if desired.

Spatial modeling requires a framework that includes a clear idea of the modeling purpose and the associated selection of an appropriate model and data scale. Processes relevant to river basin management act at the catchment and at the hillslope scale level. The key influence of hydrology at the catchment scale is the large-scale variability of soil type, land use, rainfall, and topography. Any integrated river basin model should try to reflect this variability. As conservation measures need to focus on critical source areas affecting processes that act at the hillslope scale, integrated river basin models should also provide a spatially distributed representation of basin hydrology and transport processes. Spatial results obtained from distributed models can only be as good as the quality of the input data. This means that the performance of distributed hydrological models depend on both the quality of the model (i.e. representation of processes) and the quality of the input data (i.e. accuracy and resolution issues).

Hence, fulfilling the demand for distributed data is a major challenge in distributed hydrological modeling (Shrestha et al., 2006). Chapter 6 analyzes the hydrologic predictive uncertainty associated with the gap between the need, on the one hand, and the availability and quality of land use input data, on the other. Results indicate that overall basin hydrology and model performance is only slightly affected by variations in land use data. Model calibration seems to be much more important for model performance than land use representation. However, modeling small-scale processes (e.g., infiltration and overland flow processes) requires high quality and high resolution input data. Therefore, accurate land use representation helps to reduce uncertainties in spatial model predictions. Chapter 5 of this dissertation suggests a method that shows how existing land

use data sets can be used to improve land use input data in the spatial and temporal dimension.

A landscape with defined ranges is close to both the local and the national decision-making levels (Briassoulis, 1999) and represents a suitable scale for water basin management (Volk, 2010). The landscape (or land phase) components implemented in SWAT can be divided into hydrology, weather, sedimentation, soil, crop growth, nutrients, pesticides, and agricultural management. SWAT combines concepts and modules of several models (Neitsch et al., 2011b) to simulate processes on a wide range of abiotic and biotic aspects of hydrology. Some models that contributed to the development of SWAT are CREAMS (Chemicals, Runoff, and Erosion from Agricultural Management Systems, Knisel, 1980), GLEAMS (Groundwater Loading Effects on Agricultural Management Systems, Leonard et al., 1987), SCS-CN (Soil Conservation Service Engineering Division, 1972), and EPIC (Erosion-Productivity Impact Calculator, Williams et al., 1984). Each of them was developed and tested for specific applications and scales. CREAMS and EPIC are field scale models that simulate the impact of land management on water, sediment, nutrients, pesticides (CREAMS), and erosion (EPIC), while the SCS curve number model was designed to predict stream flow generated by large rain storms at the catchment scale. Generally, SWAT was developed as a long-term water yield model operating on a daily time step (Arnold et al., 1998). Hence, process representation of the model should be checked carefully at the relevant scales before conclusions are drawn, based on model results. In this context, reviewing hydrologic processes across scales and analyzing their representation in the SWAT model lead to the conclusion that results provided at the hillslope scale are questionable.

There are numerous SWAT applications that use the outlet gauge discharge data for validation purposes, i.e. validating the model at the catchment scale. This turns out to be one of the most serious shortcomings of current watershed simulations using models like SWAT (Agnew et al., 2006); the models are mostly evaluated on the basis of their ability to correctly predict flow hydrographs with lesser attention to the locations of runoff producing areas. Integrated models should, however, preserve geographically distributed information and capture VSA processes for identifying saturated source areas in the landscape. In this context, the empirical curve number equation seems to be another key weakness of the SWAT model. Daily precipitation is input to the model and the empirical curve number equation is applied to daily rainfall without accounting for intensity to calculate surface runoff. The curve number equation implemented in SWAT is parameterized by soil type, antecedent soil moisture, and land use, each of which is associated with infiltration capacity, thus, implying infiltration excess runoff. Gburek et al. (2002), however, proposed a method for identifying potential saturated areas based on curve numbers and the assumption that saturated areas concentrate

around perennial waterways. Integrated hydrological models demand a more physically based, robust alternative for saturated variable source area hydrology (e.g., Agnew et al., 2006). To sum up, spatial distributed simulations as well as estimating hydrological processes at the hillslope scale seem to require a revision of the SWAT model.

In general, SWAT has proven to be a very useful tool and has shown its capability to adequately represent general trends of water quantity and quality changes resulting from various measures based on land use and management change at the catchment scale (Fohrer et al., 2005; Gassman et al., 2007). The model helped to obtain a working knowledge of hydrological systems and the processes occurring on a wide scale of watersheds and environmental conditions. However, spatially detailed simulations at the hillslope scale seem to touch the boundary of the model; in its current status, a revision of the hydrological processes seems to be needed. This dissertation is a first step in the development of a spatially distributed SWAT model that helps to fulfill the requirements of river basin management. This was achieved by improving the spatial representation of processes in the SWAT model and providing more accurate input data. The research conducted in this dissertation has created new options for spatial modeling. Depending on the purpose of modeling and the data available, the user can choose between a grid-based version, with limited routing capabilities (see Chapters 2 and 3), and a version that includes landscape processes (see Chapter 4). Each model version can be run using either conventional land use maps or land use data with an improved spatial accuracy and temporal availability (i.e. IRSeL-modified land use data, see Chapters 5 and 6). Therefore, the groundwork for distributed hydrological modeling with the SWAT model has been laid successfully.

As testing and development of the model is expanded, the full utility of the model will be realized. However, reviewing the processes at the hillslope scale and its representation in the SWAT model increases the importance of analyzing whether models based on simple, empirical equations (e.g., the curve number method) can appropriately represent complex hydrological runoff processes at the hillslope scale. Of course, the problem whether data needed for more sophisticated models are actually available still remains. As stated by Garen and Moore (2005), "complex questions will require complex models, which are data- and resource-intensive; there are no short cuts." This seems to be true for spatially detailed, fully distributed hydrological simulations.

References

Abbaspour, K.C., 2007. User Manual for SWAT-CUP, SWAT Calibration and Uncertainty Analysis Programs. Swiss Federal Institute of Aquatic Science and Technology, EAWAG. Dübendorf, Switzerland.

Agnew, L.J., Lyon, S., Gerard-Marchant, P., Collins, V.B., Lembo, A.J., Steenhuis, T.S., Walter, M.T., 2006. Identifying hydrologically sensitive areas: bridging the gap between science and application. Journal of Environmental Management 78, 63–76.

Agresti, A., 2007. An Introduction to Categorical Data Analysis (Wiley Series in Probability and Statistics). Wiley-Interscience.

Allan, J., Erickson, D., Fay, J., 1997. The influence of catchment land use on stream integrity across multiple spatial scales. Freshwater Biology 37, 149–161.

Arabi, M., Govindaraju, R.S., Hantush, M.M., Engel, B.A., 2006. Role of watershed subdivision on modeling the effectiveness of best management practices with SWAT. JAWRA Journal of the American Water Resources Association 42, 513–528.

Arnold, J., Allen, P., Volk, M., Williams, J., Bosch, D., 2010. Assessment of different representations of spatial variability on SWAT model performance. Transactions of the ASABE 53, 1433–1443.

Arnold, J.G., Fohrer, N., 2005. SWAT2000: current capabilities and research opportunities in applied watershed modelling. Hydrological Processes 19, 563–572.

Arnold, J.G., Kiniry, J.R., Srinivasan, R., Williams, J.R., Haney, E., Neitsch, S.L., 2013. Soil and Water Assessment Tool – Input/Output File Documentation: Version 2012. TR-439. Texas Water Resources Institute.

Arnold, J.G., Srinivasan, R., Engel, B., 1994. Flexible watershed configurations for simulation models. Hydrological Science and Technology 10, 1–9.

Arnold, J.G., Srinivasan, R., Muttiah, R.S., Williams, J.R., 1998. Large area hydrologic modeling and assessment part I: model development. JAWRA Journal of the American Water Resources Association 34, 73–89.

Bakker, M.M., Govers, G., van Doorn, A., Quetier, F., Chouvardas, D., Rounsevell, M., 2008. The response of soil erosion and sediment export to land-use change in four areas of Europe: the importance of landscape pattern. Geomorphology 98, 213–226.

Barling, R.D., Moore, I.D., Grayson, R.B., 1994. A quasi-dynamic wetness index for characterizing the spatial distribution of zones of surface saturation and soil water content. Water Resources Research 30, 1029–1044.

Behera, S., Panda, R., 2006. Evaluation of management alternatives for an agricultural watershed in a sub-humid subtropical region using a physical process based model. Agriculture, Ecosystems & Environment 113, 62 – 72.

Bennett, N.D., Croke, B.F., Guariso, G., Guillaume, J.H., Hamilton, S.H., Jakeman, A.J., Marsili-Libelli, S., Newham, L.T., Norton, J.P., Perrin, C., Pierce, S.A., Robson, B., Seppelt, R., Voinov, A.A., Fath, B.D., Andreassian, V., 2013. Characterising performance of environmental models. Environmental Modelling & Software 40, 1 – 20.

Bernier, P., 1985. Variable source areas and storm-flow generation: an update of the concept and a simulation effort. Journal of Hydrology 79, 195 – 213.

Betson, R.P., 1964. What is watershed runoff? Journal of Geophysical Research 69, 1541–1552.

Beven, K., 1989. Changing ideas in hydrology – the case of physically-based models. Journal of Hydrology 105, 157 – 172.

Beven, K., 1993. Prophecy, reality and uncertainty in distributed hydrological modelling. Advances in Water Resources 16, 41 – 51.

Beven, K., Freer, J., 2001. A dynamic TOPMODEL. Hydrological Processes 15, 1993–2011.

Beven, K.J., 2012. Rainfall-Runoff Modelling: The Primer. Wiley-Blackwell.

Beven, K.J., Kirkby, M.J., 1979. A physically based, variable contributing area model of basin hydrology. Hydrological Sciences Bulletin 24, 43–69.

Bicknell, B., Imhoff, J., Jr., K., J.L., Jobes, T., Donigan Jr., A., 1996. Hydrological Simulation Program: Fortran User's Manual for Release 11. Technical Report. AQUA TERRA Consultants Mountain View, California (USA).

Bingner, R., Garbrecht, J., Arnold, J., Srinivasan, R., 1997. Effect of watershed subdivision on simulation runoff and fine sediment yield. Transactions of the American Society of Agricultural Engineers 40, 1329–1335.

Blöschl, G., Sivapalan, M., 1995. Scale issues in hydrological modelling: a review. Hydrological Processes 9, 251–290.

Born, S., Sonzogni, W., 1995. Integrated environmental management: strengthening the conceptualization. Environmental Management 19, 167–181.

Bosch, D.D., Arnold, J.G., Volk, M., 2007a. SWAT revisions for simulating landscape components and buffer systems, in: 2007 ASABE Annual International Meeting, Minneapolis, Minnesota, USA. pp. 1–9.

Bosch, D.D., Arnold, J.G., Volk, M., Allen, P.M., 2010. Simulation of a low-gradient coastal plain watershed using the SWAT landscape model. Transactions of the ASABE 53, 1445–1456.

Bosch, D.D., Sheridan, J.M., 2007. Stream discharge database, Little River Experimental Watershed, Georgia, United States. Water Resources Research 43, 1–4.

Bosch, D.D., Sheridan, J.M., Batten, H.L., Arnold, J.G., 2004. Evaluation of the SWAT model on a coastal plain agricultural watershed. Transactions of the ASAE 47, 1493–1506.

Bosch, D.D., Sheridan, J.M., Davis, F.M., 1999. Rainfall characteristics and spatial correlation for the Georgia Coastal Plain. Transactions of the ASABE 42, 1637–1644.

Bosch, D.D., Sheridan, J.M., Marshall, L.K., 2007b. Precipitation, soil moisture, and climate database, Little River Experimental Watershed, Georgia, United States. Water Resources Research 43, 1–5.

Briassoulis, H., 1999. Who plans whose sustainability? Alternative roles for planners. Journal of Environmental Planning and Management 42, 889–902.

Brutsaert, W., 2005. Hydrology: An Introduction. Cambridge University Press, Cambridge, U.K.

Burkhard, B., Kroll, F., Nedkov, S., Müller, F., 2012. Mapping ecosystem service supply, demand and budgets. Ecological Indicators 21, 17–29.

Campbell, J.B., Wynne, R.H., 2011. Introduction to Remote Sensing, Fifth Edition. The Guilford Press.

Carpenter, S.R., Caraco, N.F., Correll, D.L., Howarth, R. W. Sharpley, A.N., Smith, V.H., 1998. Nonpoint pollution of surface waters with phosphorus and nitrogen. Ecological Applications 8, 559–568.

Cashion, J., Lakshmi, V., Bosch, D., Jackson, T.J., 2005. Microwave remote sensing of soil moisture: evaluation of the TRMM microwave imager (TMI) satellite for the Little River Watershed Tifton, Georgia. Journal of Hydrology 307, 242–253.

Chaplot, V., 2005. Impact of DEM mesh size and soil map scale on SWAT runoff, sediment, and NO_3-N loads predictions. Journal of Hydrology 312, 207 – 222.

Chaplot, V., 2013. Impact of spatial input data resolution on hydrological and erosion modeling: recommendations from a global assessment. Physics and Chemistry of the Earth, Parts A/B/C (in press).

Chaubey, I., Cotter, A.S., Costello, T.A., Soerens, T.S., 2005. Effect of DEM data resolution on SWAT output uncertainty. Hydrological Processes 19, 621–628.

Chen, E., Mackay, D.S., 2004. Effects of distribution-based parameter aggregation on a spatially distributed agricultural nonpoint source pollution model. Journal of Hydrology 295, 211 – 224.

Chiang, L., Chaubey, I., Gitau, M., Arnold, J., 2010. Differentiating impacts of land use changes from pasture management in a CEAP watershed using the SWAT model. Transactions of the ASABE 53, 1569–1584.

Cho, J., Bosch, D., Lowrance, R., Strickland, T., Vellidis, G., 2009. Effect of spatial distribution of rainfall on temporal and spatial uncertainty of SWAT output. Transactions of the ASABE 52, 1545–1555.

Cho, J., Bosch, D., Vellidis, G., Lowrance, R., Strickland, T., 2013. Multi-site evaluation of hydrology component of SWAT in the coastal plain of southwest Georgia. Hydrological Processes 27, 1691–1700.

Cho, J., Lowrance, R.R., Bosch, D.D., Strickland, T.C., Her, Y., Vellidis, G., 2010. Effect of watershed subdivision and filter width on SWAT simulation of a coastal plain watershed. JAWRA Journal of the American Water Resources Association 46, 586–602.

Clarke, K., Hoppen, S., 1997. A self-modifying cellular automaton model of historical urbanization in the San Francisco Bay area. Environment and Planning B: Planning and Design 24, 247–261.

Clarke, K.C., Gaydos, L.J., 1998. Loose-coupling a cellular automaton model and GIS: long-term urban growth prediction for San Francisco and Washington/Baltimore. International Journal of Geographical Information Science 12, 699–714.

Cohen, J., 1960. A coefficient of agreement for nominal scales. Educational and Psychological Measurement 20, 37–46.

Congalton, R.G., 1991. A review of assessing the accuracy of classifications of remotely sensed data. Remote Sensing of Environment 37, 35–46.

Copeland, C., 2010. Clean Water Act: A Summary of the Law. CRS Report RL30030. Congressional Research Service.

Copeland, C., 2012. Water Quality Issues in the 112th Congress: Oversight and Implementation. CRS Report R41594. Congressional Research Service.

DeFries, R., Eshleman, K.N., 2004. Land-use change and hydrologic processes: a major focus for the future. Hydrological Processes 18, 2183–2186.

Dixon, B., Earls, J., 2009. Resample or not?! Effects of resolution of DEMs in watershed modeling. Hydrological Processes 23, 1714–1724.

Dobslaff, N., 2005. GIS-basierte Modellierung von Wasserhaushalt und Abflussbildung am Beispiel des Einzugsgebietes der oberen Stör. Diplomarbeit. Kiel University.

D'Odorico, P., Rigon, R., 2003. Hillslope and channel contributions to the hydrologic response. Water Resources Research 39, n/a–n/a.

Dooge, J.C.I., 1986. Looking for hydrologic laws. Water Resources Research 22, 46S–58S.

Douglas, D.H., 1986. Experiments to locate ridges and channels to create a new type of digital elevation model. Cartographica 23, 29–61.

Drewry, J.J., Newham, L.T.H., Greene, R.S.B., Jakeman, A.J., Croke, B.F.W., 2006. A review of nitrogen and phosphorus export to waterways: context for catchment modelling. Marine and Freshwater Research 57, 757–774.

Dunne, T., Black, R.D., 1970. Partial area contributions to storm runoff in a small New England watershed. Water Resources Research 6, 1296–1311.

Dunne, T., Moore, T., Taylor, C., 1975. Recognition and prediction of runoff-producing zones in humid regions. Hydrological Sciences Bulletin 20, 305–327.

DWD, 2011. Weather and climate data from the German Weather Service – station Gnutz (1997-2006), Neumünster (1997-2007), and Padenstedt (2007-2010). Deutscher Wetterdienst.

DWD, 2012. Weather and climate data from the German Weather Service – station Gnutz (1997-2006), Neumünster (1997-2007), and Padenstedt (2007-2011). Deutscher Wetterdienst.

Easton, Z.M., Walter, M.T., Fuka, D.R., White, E.D., Steenhuis, T.S., 2011. A simple concept for calibrating runoff thresholds in quasi-distributed variable source area watershed models. Hydrological Processes 25, 3131–3143.

Fairfield, J., Leymarie, P., 1991. Drainage networks from grid digital elevation models. Water Resources Research 27, 709–717.

FAO, 1997. State of the World's Forests. Technical Report. Food and Agriculture Organization. Rome, Italy.

FAO/UNEP, 1999. Terminology for Integrated Resources Planning and Management. Technical Report. Food and Agriculture Organization/United Nations Environmental Programme. Rome, Italy and Nairobi, Kenya.

Feyereisen, G., Strickland, T., Bosch, D., Sullivan, D., 2007. Evaluation of SWAT manual calibration and input parameter sensitivity in the Little River Watershed. Transactions of the ASABE 50, 843–855.

Finnern, J., 1997. Böden und Leitbodengesellschaften des Störeinzugsgebietes in Schleswig-Holstein – Vergesellschaftung und Stoffaustragsprognose (K, Ca, Mg) mittels GIS. Dissertation. Institut für Pflanzenernährung und Bodenkunde der Universität Kiel – Kiel University.

FitzHugh, T.W., Mackay, D.S., 2000. Impacts of input parameter spatial aggregation on an agricultural nonpoint source pollution model. Journal of Hydrology 236, 35 – 53.

Fohrer, N., Haverkamp, S., Frede, H.G., 2005. Assessment of the effects of land use patterns on hydrologic landscape functions: development of sustainable land use concepts for low mountain range areas. Hydrological Processes 19, 659–672.

Foody, G.M., 2002. Status of land cover classification accuracy assessment. Remote Sensing of Environment 80, 185 – 201.

Foody, G.M., 2004. Thematic map comparison: evaluating the statistical significance of differences in classification accuracy. Photogrammetric Engineering & Remote Sensing 5, 627–633.

Foody, G.M., 2008. Harshness in image classification accuracy assessment. International Journal of Remote Sensing 29, 3137–3158.

Frankenberger, J.R., Brooks, E.S., Walter, M.T., Walter, M.F., Steenhuis, T.S., 1999. A GIS-based variable source area hydrology model. Hydrological Processes 13, 805–822.

Franklin, J.F., 1992. Scientific basis for new perspectives in forests and streams, in: Naiman, R.J. (Ed.), Watershed management – balancing sustainability and environmental change, Springer-Verlag, New York. pp. 25–72.

Gallego, F.J., 2004. Remote sensing and land cover area estimation. International Journal of Remote Sensing 25, 3019–3047.

Garbrecht, J., Martz, L., 2000. TOPAZ User Manual: Version 3.1. Technical Report. Grazinglands Research Laboratory, USDA, Agricultural Research Service. El Reno (Oklahoma).

Garen, D.C., Moore, D.S., 2005. Curve number hydrology in water quality modeling: uses, abuses, and future directions. JAWRA Journal of the American Water Resources Association 41, 377–388.

Gassman, P.W., Reyes, M.R., Green, C.H., Arnold, J.G., 2007. The Soil and Water Assessment Tool: historical development, applications, and future research directions. Transactions of the ASABE 50, 1211–1250.

Gburek, W.J., Drungil, C.C., Srinivasan, M.S., Needelman, B.A., Woodward, D.E., 2002. Variable-source-area controls on phosphorus transport: Bridging the gap between research and design. Journal of Soil and Water Conservation 57, 534–543.

Geological Survey (U.S.), 1998. Landsat 7 science data users handbook. USGS Unnumbered Series, General Interest Publication, revised edition.

Geza, M., McCray, J.E., 2008. Effects of soil data resolution on SWAT model stream flow and water quality predictions. Journal of Environmental Management 88, 393 – 406.

Glenn, E.P., Nagler, P.L., Huete, A.R., 2010. Vegetation index methods for estimating evapotranspiration by remote sensing. Surveys in Geophysics 31, 531–555.

Goldstein, N.C., Candau, J., Clarke, K., 2004. Approaches to simulating the "march of bricks and mortar". Computers, Environment and Urban Systems 28, 125 – 147.

Grayson, R.B., Moore, I.D., McMahon, T.A., 1992. Physically based hydrologic modeling 2. Is the concept realistic? Water Resources Research 28, 2659–2666.

Green, W.H., Ampt, G.A., 1911. Studies on soil phyics. The Journal of Agricultural Science 4, 1–24.

Gregory, K.J., Walling, D.E., 1968. The variation of drainage density within a catchment. International Association of Scientific Hydrology. Bulletin 13, 61–68.

Guo, L.B., Gifford, R.M., 2002. Soil carbon stocks and land use change: a meta analysis. Global Change Biology 8, 345–360.

Gupta, H.V., Sorooshian, S., Yapo, P.O., 1999. Status of automatic calibration for hydrologic models: comparison with multilevel expert calibration. Journal of Hydrologic Engineering 4, 135–143.

Guswa, A.J., Celia, M.A., Rodriguez-Iturbe, I., 2002. Models of soil moisture dynamics in ecohydrology: a comparative study. Water Resources Research 38, 5–1–5–15.

Haith, D.A., Shoenaker, L.L., 1987. Generalized watershed loading functions for stream flow nutrients. JAWRA Journal of the American Water Resources Association 23, 471–478.

Hargreaves, G.H., Samani, Z.A., 1985. Reference crop evapotranspiration from temperature. Applied Engineering in Agriculture 1, 69–99.

Haverkamp, S., Fohrer, N., Frede, H.G., 2005. Assessment of the effect of land use patterns on hydrologic landscape functions: a comprehensive GIS-based tool to minimize model uncertainty resulting from spatial aggregation. Hydrological Processes 19, 715–727.

Hering, D., Borja, A., Carstensen, J., Carvalho, L., Elliott, M., Feld, C.K., Heiskanen, A.S., Johnson, R.K., Moe, J., Pont, D., Solheim, A.L., van de Bund, W., 2010. The European Water Framework Directive at the age of 10: a critical review of the achievements with recommendations for the future. Science of The Total Environment 408, 4007 – 4019.

Hering, D., Borja, A., Carvalho, L., Feld, C., 2013. Assessment and recovery of European water bodies: key messages from the WISER project. Hydrobiologia 704, 1–9.

Hewlett, J., Nutter, W., 1970. The varying source area of streamflow from upland basins, in: Proceedings of the Symposium on Interdisciplinary Aspects of Watershed Management, ASCE, New York, Bozeman, MT (USA). pp. 65–83.

Hewlett, J.D., Hibert, A.R., 1967. Factors affecting the response of small watersheds to precipitation in humid areas, in: Sopper, W., Lull, H. (Eds.), Forest hydrology, Pergamon Press, New York. pp. 275–90.

Holko, L., Lepistö, A., 1997. Modelling the hydrological behaviour of a mountain catchment using TOPMODEL. Journal of Hydrology 196, 361–377.

Hörmann, G., Horn, A., Fohrer, N., 2005. The evaluation of land-use options in mesoscale catchments: prospects and limitations of eco-hydrological models. Ecological Modelling 187, 3 – 14.

Horn, A.L., Rueda, F.J., Hörmann, G., Fohrer, N., 2004. Implementing river water quality modelling issues in mesoscale watershed models for water policy demands – an overview on current concepts, deficits, and future tasks. Physics and Chemistry of the Earth, Parts A/B/C 29, 725 – 737.

Horton, R.E., 1945. Erosional development of streams and their drainage basins; hydrophysical approach to quantitative morphology. Geological Society of America Bulletin 56, 275–370.

Immerzeel, W., Droogers, P., 2008. Calibration of a distributed hydrological model based on satellite evapotranspiration. Journal of Hydrology 349, 411 – 424.

ITTVIS, 2006. ENVI, version 4.2.

Jaeger, K.L., Montgomery, D.R., Bolton, S.M., 2007. Channel and perennial flow initiation in headwater streams: management implications of variability in source-area size. Environmental Management 40, 775–786.

Jelinek, S., 1999. Über das Abflußverhalten kleiner Einzugsgebiete in Norddeutschland am Beispiel der oberen Stör in Schleswig-Holstein. Hydrologie und Wasserwirtschaft 43, 3–16.

Jenerette, G., Wu, J., 2001. Analysis and simulation of land-use change in the central Arizona – Phoenix region, USA. Landscape Ecology 16, 611–626.

Jha, M., Gassman, P., Secchi, S., Gu, R., Arnold, J., 2004. Effect of watershed subdivision on SWAT flow, sediment, and nutrient predictions. Journal of the American Water Resources Association 40, 811–825.

Kiesel, J., Fohrer, N., Schmalz, B., White, M.J., 2010. Incorporating landscape depressions and tile drainages of a northern German lowland catchment into a semi-distributed model. Hydrological Processes 24, 1472–1486.

Klemeš, V., 1983. Conceptualization and scale in hydrology. Journal of Hydrology 65, 1 – 23.

Knapp, B.J., 1978. Infiltration and storage of soil water, in: Kirkby, M.J. (Ed.), Hillslope Hydrology (Landscape Systems: A Series in Geomorphology), Wiley. pp. 43–72.

Knisel, W.G., 1980. CREAMS: a field scale model for Chemicals, Runoff, and Erosion from Agricultural Management Systems. USDA Conservation Research Rept. 26. U.S. Department of Agriculture.

Krause, S., Jacobs, J., Voss, A., Bronstert, A., Zehe, E., 2008. Assessing the impact of changes in landuse and management practices on the diffuse pollution and retention of nitrate in a riparian floodplain. Science of The Total Environment 389, 149–164.

Kroll, F., Müller, F., Haase, D., Fohrer, N., 2012. Rural-urban gradient analysis of ecosystem services supply and demand dynamics. Land Use Policy 29, 521 – 535.

Krysanova, V., Arnold, J.G., 2008. Advances in ecohydrological modelling with SWAT – a review. Hydrological Sciences Journal 53, 939–947.

Krysanova, V., Haberlandt, U., 2002. Assessment of nitrogen leaching from arable land in large river basins: part I. Simulation experiments using a process-based model. Ecological Modelling 150, 255 – 275.

Krysanova, V., Hattermann, F., Wechsung, F., 2005. Development of the ecohydrological model SWIM for regional impact studies and vulnerability assessment. Hydrological Processes 19, 763–783.

Kumar, R., Samaniego, L., Attinger, S., 2013. Implications of distributed hydrologic model parameterization on water fluxes at multiple scales and locations. Water Resources Research 49, 360–379.

Leonard, R.A., Knisel, W., Still, D.A., 1987. GLEAMS: Groundwater loading effects on agricultural management systems. Transactions of the ASAE 30, 1403–1428.

Linsley, R.K., Paulhus, J.L., Kohler, M.A., 1982. Hydrology for Engineers. McGraw-Hill Companies.

LKN, 2011. Daily discharge data for gauging station Sarlhusen (114131). Landesbetrieb für Küstenschutz, Nationalpark und Meeresschutz Schleswig-Holstein – State office for coastal protection, national park and marine protection.

LKN, 2012. Daily discharge data for gauging station Sarlhusen (114131). Landesbetrieb für Küstenschutz, Nationalpark und Meeresschutz Schleswig-Holstein – State office for coastal protection, national park and marine protection.

LLUR, 2010. Bodenkarte im Maßstab 1:25.000 des Landes Schleswig-Holstein. Landesamt für Landwirtschaft, Umwelt und ländliche Räume des Landes Schleswig-Holstein – Agency for Nature and Environment Schleswig-Holstein.

Lorz, C., Volk, M., Schmidt, G., 2007. Considering spatial distribution and functionality of forests in a modeling framework for river basin management. Forest Ecology and Management 248, 17 – 25.

LVA, 2007. ATKIS (official topographical cartographic information system). Landesamt für Vermessung und Geoinformation Schleswig-Holstein – Land survey office Schleswig-Holstein.

LVA, 2008. ATKIS-DEM 5 m grid size derived from LiDAR data. Landesamt für Vermessung und Geoinformation Schleswig-Holstein – Land survey office Schleswig-Holstein.

Lyon, S.W., Walter, M.T., Gérard-Marchant, P., Steenhuis, T.S., 2004. Using a topographic index to distribute variable source area runoff predicted with the SCS curve-number equation. Hydrological Processes 18, 2757–2771.

Manguerra, H.B., Engel, B.A., 1998. Hydrologic parameterization of watersheds for runoff prediction using SWAT. JAWRA Journal of the American Water Resources Association 34, 1149–1162.

Mausbach, M.J., Dedrick, A.R., 2004. The length we go: measuring environmental benefits of conservation practices. Journal of Soil and Water Conservation 59, 96A–103A.

McCaig, M., 1983. Contributions to storm quickflow in a small headwater catchment – the role of natural pipes and soil macropores. Earth Surface Processes and Landforms 8, 239–252.

McDonnell, J.J., 1990. A rationale for old water discharge through macropores in a steep, humid catchment. Water Resources Research 26, 2821–2832.

McGlynn, B.L., McDonnell, J.J., 2003. Quantifying the relative contributions of riparian and hillslope zones to catchment runoff. Water Resources Research 39, n/a–n/a.

McNamara, J.P., Chandler, D., Seyfried, M., Achet, S., 2005. Soil moisture states, lateral flow, and streamflow generation in a semi-arid, snowmelt-driven catchment. Hydrological Processes 19, 4023–4038.

Tromp van Meerveld, H.J., McDonnell, J.J., 2006. Threshold relations in subsurface stormflow: 2. the fill and spill hypothesis. Water Resources Research 42, n/a–n/a.

Mehta, V.K., Walter, M.T., Brooks, E.S., Steenhuis, T.S., Walter, M.F., Johnson, M., Boll, J., Thongs, D., 2004. Application of SMR to modeling watersheds in the Catskill Mountains. Environmental Modeling & Assessment 9, 77–89.

Miller, S.N., Kepner, W.G., Mehaffey, M.H., Hernandez, M., Miller, R.C., Goodrich, D.C., Kim Devonald, K., Heggem, D.T., Miller, W.P., 2002. Integrating landscape assessment and hydrologic modeling for land cover change analysis. JAWRA Journal of the American Water Resources Association 38, 915–929.

MLUR, 2010. IACS (Integrated Administration and Control System) land use data. Ministerium für Energiewende, Landwirtschaft, Umwelt und ländliche Räume des Landes Schleswig-Holstein – Ministry for Nature and Environment Schleswig-Holstein.

Moglen, G.E., Eltahir, E.A.B., Bras, R.L., 1998. On the sensitivity of drainage density to climate change. Water Resources Research 34, 855–862.

Monteith, J., 1965. Evaporation and environment, in: The state and movement of water in living organisms, Cambridge University Press, London, UK. pp. 205–234.

Montgomery, D.R., Dietrich, W.E., 1988. Where do channels begin? Nature 336, 232 – 234.

Montgomery, D.R., Dietrich, W.E., 1989. Source areas, drainage density, and channel initiation. Water Resources Research 25, 1907–1918.

Montgomery, D.R., Dietrich, W.E., 1994. Landscape dissection and drainage area-slope thresholds, in: Kirkby, M.J. (Ed.), Models and Theoretical Geomorphology, John Wiley, New York. pp. 221–246.

Montgomery, D.R., Dietrich, W.E., 1995. Hydrologic processes in a low-gradient source area. Water Resources Research 31, 1–10.

Moriasi, D.N., Arnold, J.G., Liew, M.W.V., Bingner, R.L., Harmel, R.D., Veith, T.L., 2007. Model evaluation guidelines for systematic quantification of accuracy in watershed simulations. Transactions of the ASABE 50, 885–900.

Nash, J., Sutcliffe, J., 1970. River flow forecasting through conceptual models part I – a discussion of principles. Journal of Hydrology 10, 282 – 290.

Neitsch, S.L., Arnold, J.G., Kiniry, J.R., Srinivasan, R., Williams, J.R., 2010. Soil and Water Assessment Tool Input/Output File Documentation: Version 2009. Technical Report 365. Texas Water Resources Institute (Texas).

Neitsch, S.L., Arnold, J.G., Kiniry, J.R., Srinivasan, R., Williams, J.R., 2011a. Soil and Water Assessment Tool Input/Output File Documentation: Version 2009. Texas Water Ressources Institute Technical Report 365. Texas A&M University System. College Statation (Texas).

Neitsch, S.L., Arnold, J.G., Kiniry, J.R., Williams, J.R., 2005. Soil and Water Assessment Tool Theoretical Documentation: Version 2005. Texas Agricultural Experiment Station (Texas) and USDA Agricultural Research Service (Texas). Temple (Texas).

Neitsch, S.L., Arnold, J.G., Kiniry, J.R., Williams, J.R., 2011b. Soil and Water Assessment Tool Theoretical Documentation Version 2009. Technical Report 406. Texas Water Resources Institute. Temple (Texas).

O'Loughlin, E.M., 1986. Prediction of surface saturation zones in natural catchments by topographic analysis. Water Resources Research 22, 794–804.

Oppelt, N., Rathjens, H., Dörnhöfer, K., 2012. Integration of land cover data into the open source model SWAT, in: Proceedings of the First Sentinel-2 Preparatory Symposium held on 23-27 April 2012 in ESA-ESRIN, Frascati, Italy. DVD Publication.

Ouyang, W., Skidmore, A.K., Hao, F., Wang, T., 2010a. Soil erosion dynamics response to landscape pattern. Science of The Total Environment 408, 1358–1366.

Ouyang, W., Skidmore, A.K., Toxopeus, A., Hao, F., 2010b. Long-term vegetation landscape pattern with non-point source nutrient pollution in upper stream of Yellow River basin. Journal of Hydrology 389, 373 – 380.

Pai, N., Saraswat, D., 2011. SWAT2009_luc: a tool to activate the land use change module in SWAT 2009. Transactions of the ASABE 54, 1649–1658.

Pai, N., Saraswat, D., 2013. Impact of land use and land cover categorical uncertainty on SWAT hydrologic modeling. Transactions of the ASABE 56, 1387–1397.

Pandey, V., Panda, S.N., Sudhakar, S., 2005. Modelling of an agricultural watershed using remote sensing and a geographic information system. Biosystems Engineering 90, 331 – 347.

Pause, M., Volk, M., Schulz, K., 2008. Radar-based surface soil moisture retrieval over agricultural used sites – a multi-sensor approach, in: Sànchez-Marrè, M., Béjar, J., Comas, J., Rizzoli, A., Guariso, G. (Eds.), Proceedings of the iEMSs Fourth Biennial Meeting: International Congress on Environmental Modelling and Software (iEMSs 2008), peer reviewed, Barcelona, Catalonia. pp. 415–421.

Pfannerstill, M., Guse, B., Fohrer, N., 2013. A multi-storage groundwater concept for the SWAT model to emphasize nonlinear groundwater dynamics in lowland catchments. Hydrological Processes (in press).

Pierdicca, N., Pulvirenti, L., Bignami, C., 2010. Soil moisture estimation over vegetated terrains using multitemporal remote sensing data. Remote Sensing of Environment 114, 440 – 448.

Pinol, J., Beven, K., Freer, J., 1997. Modelling the hydrological response of mediterranean catchments, prades, catalonia. The use of distributed models as aids to hypothesis formulation. Hydrological Processes 11, 1287–1306.

Preuss, E.F., 1977. Ermittlung der Grundwasserneubildung in Schleswig-Holstein mit Hilfe des USDAHL-Modells. Schr. Naturwiss. Ver. Schlesw.-Holst. 47, 57–62.

Priestley, C.H.B., Taylor, R.J., 1972. On the assessment of surface heat flux and evaporation using large-scale parameters. Monthly Weather Review 100, 81–92.

Prodanovic, P., Simonovic, S., 2010. An operational model for support of integrated watershed management. Water Resources Management 24, 1161–1194.

Quansah, J.E., Engel, B.A., Chaubey, I., 2008. Tillage practices usage in early warning prediction of atrazine pollution. Transactions of the ASABE 51, 1311–1321.

Quinn, P., 2004. Scale appropriate modelling: representing cause-and-effect relationships in nitrate pollution at the catchment scale for the purpose of catchment scale planning. Journal of Hydrology 291, 197 – 217.

Quinn, P., Beven, K., Chevallier, P., Planchon, O., 1991. The prediction of hillslope flow paths for distributed hydrological modelling using digital terrain models. Hydrological Processes 5, 59–79.

Quinton, W.L., Hayashi, M., Carey, S.K., 2008. Peat hydraulic conductivity in cold regions and its relation to pore size and geometry. Hydrological Processes 22, 2829–2837.

Rathjens, H., Dörnhöfer, K., Oppelt, N., under review. An interpolation and improvement approach for remotely sensed land cover data. International Journal of Applied Earth Observation and Geoinformation n/a.

Rathjens, H., Oppelt, N., 2012a. SWAT model calibration of a grid-based setup. Advances in Geosciences 32, 55–61.

Rathjens, H., Oppelt, N., 2012b. SWATgrid: an interface for setting up SWAT in a grid-based discretization scheme. Computers & Geosciences 45, 161–167.

Reed, B.C., Brown, J.F., VanderZee, D., Loveland, T.R., Merchant, J.W., Ohlen, D.O., 1994. Measuring phenological variability from satellite imagery. Journal of Vegetation Science 5, 703–714.

Refsgaard, J., Storm, B., 1995. MIKE SHE, in: Singh, V.P. (Ed.), Computer Models of Watershed Hydrology, Water Resources Publications, Colorado, USA. pp. 809–846.

Refsgaard, J.C., 1997. Parameterisation, calibration and validation of distributed hydrological models. Journal of Hydrology 198, 69 – 97.

Rinaldo, A., Marani, A., Rigon, R., 1991. Geomorphological dispersion. Water Resources Research 27, 513–525.

Rinaldo, A., Vogel, G.K., Rigon, R., Rodriguez-Iturbe, I., 1995. Can one gauge the shape of a basin? Water Resources Research 31, 1119–1127.

Robinson, J.S., Sivapalan, M., Snell, J.D., 1995. On the relative roles of hillslope processes, channel routing, and network geomorphology in the hydrologic response of natural catchments. Water Resources Research 31, 3089–3101.

Romanowicz, A., Vanclooster, M., Rounsevell, M., Junesse, I.L., 2005. Sensitivity of the SWAT model to the soil and land use data parametrisation: a case study in the Thyle catchment, Belgium. Ecological Modelling 187, 27–39.

Sabatier, P.A., Focht, W., Lubell, M., Trachtenberg, Z., Vedlitz, A., Matlock, M., 2005. Collaborative Approaches to Watershed Management. The MIT Press.

Saco, P.M., Kumar, P., 2002. Kinematic dispersion in stream networks 1. Coupling hydraulic and network geometry. Water Resources Research 38, 26–1–26–14.

Santhi, C., Arnold, J.G., Williams, J.R., Dugas, W.A., Srinivasan, R., Hauck, L.M., 2001. Validation of the SWAT model on a large river basin with point and nonpoint sources. Journal of the American Water Resources Association 37, 1169–1188.

Schmalz, B., Fohrer, N., 2009. Comparing model sensitivities of different landscapes using the ecohydrological SWAT model. Advances in Geosciences 21, 91–98.

Schulla, J., 1997. Hydrologische Modellierung von Flussgebieten zur Abschätzung der Folgen von Klimaänderungen. Ph.D. thesis. Geographisches Institut – Departement of Geography, ETH Zürich.

Schulla, J., 2012. Model Description WaSiM (Water balance Simulation Model). Technical report. Hydrology Software Consulting J. Schulla. Regensdorferstrasse 162, 8049 Zürich, CH.

Schulz, K., Seppelt, R., Zehe, E., Vogel, H.J., Attinger, S., 2006. Importance of spatial structures in advancing hydrological sciences. Water Resources Research 42, n/a–n/a.

Selby, M.J., 1993. Hillslope Materials and Processes. Oxford University Press, USA.

Seppelt, R., Müller, F., Schröder, B., Volk, M., 2009. Challenges of simulating complex environmental systems at the landscape scale: a controversial dialogue between two cups of espresso. Ecological Modelling 220, 3481 – 3489.

Sheridan, J.M., 1997. Rainfall-streamflow relations for coastal plain watersheds. Applied Engineering in Agriculture 13, 333–344.

Shirmohammadi, A., Sheridan, J.M., Asmussen, L.E., 1986. Hydrology of alluvial stream channels in southern coastal plain watersheds. Transactions of 29, 135–142.

Shrestha, R., Tachikawa, Y., Takara, K., 2006. Input data resolution analysis for distributed hydrological modeling. Journal of Hydrology 319, 36 – 50.

Singh, J., Knapp, H.V., Demissie, M., 2004. Hydrologic Modeling of the Iroquois River Watershed Using HSPF and SWAT. Illinois State Water Survey Contract Report 2004-08. Illinois Department of Natural Resources and Illinois State Geological Survey.

Sloan, P.G., Moore, I.D., Coltharp, G.B., Eigel, J.D., 1983. Modeling Surface and Subsurface Stormflow on Steeply-sloping Forested Watersheds. Water Resouces Inst. Report 142. Water Resources Research Institute, University of Kentucky. Lexington, Kentucky, USA.

Soil Conservation Service Engineering Division, 1972. Section 4: Hydrology, in: National Engineering Handbook, pp. 10–1 – 10–22.

Spence, C., 2010. A paradigm shift in hydrology: storage thresholds across scales influence catchment runoff generation. Geography Compass 4, 819–833.

Spence, C., Guan, X.J., Phillips, R., Hedstrom, N., Granger, R., Reid, B., 2010. Storage dynamics and streamflow in a catchment with a variable contributing area. Hydrological Processes 24, 2209–2221.

Steinhardt, U., Volk, M., 2001. Scales and spatio-temporal dimensions in landscape ecology, in: Krönert, R., Steinhardt, U., Volk, M. (Eds.), Landscape balance and landscape assessment, Springer, Berlin Heidelberg-New York. pp. 137–162.

Stomph, T.J., de Ridder, N., Steenhuis, T.S., Van de Giesen, N.C., 2002. Scale effects of Hortonian overland flow and rainfall-runoff dynamics: laboratory validation of a process-based model. Earth Surface Processes and Landforms 27, 847–855.

Strahler, A.N., 1952. Hypsometric (area-altitude) analysis of erosional topography. Geological Society of America Bulletin 63, 1117–1142.

Strauch, M., Volk, M., 2013. SWAT plant growth modification for improved modeling of perennial vegetation in the tropics. Ecological Modelling 269, 98 – 112.

Sullivan, D.G., Batten, H.L., Bosch, D., Sheridan, J., Strickland, T., 2007. Little River Experimental Watershed, Tifton, Georgia, United States: a geographic database. Water Resources Research 43, 1–4.

SWL, 2003. SMDR – The Soil Moisture Distribution and Routing Model. Soil and Water Laboratory – Biological and Environmental Engineering Dept. Cornell University. Ithaca, NY 14853, USA.

van der Tak, L.D., Bras, R.L., 1990. Incorporating hillslope effects into the geomorphologic instantaneous unit hydrograph. Water Resources Research 26, 2393–2400.

Torres, R., Dietrich, W.E., Montgomery, D.R., Anderson, S.P., Loague, K., 1998. Unsaturated zone processes and the hydrologic response of a steep, unchanneled catchment. Water Resources Research 34, 1865–1879.

Townshend, J.R.G., 1992. Land cover. International Journal of Remote Sensing 13, 1319–1328.

Turner, R.E., Rabalais, N.N., 2003. Linking landscape and water quality in the Mississippi River Basin for 200 years. BioScience 53, 563–572.

Twine, T., Kucharik, C., Foley, J., 2004. Effects of land cover change on the energy and water balance of the Mississippi River Basin. Journal of Hydrometeorology 5, 640–655.

Ullrich, A., Volk, M., Schmidt, G., 2008. Influence of the uncertainties of monitoring data on model calibration and evaluation, in: Sànchez-Marrè, M., Béjar, J., Comas, J., Rizzoli, A., Guariso, G. (Eds.), Proceedings of the iEMSs Fourth Biennial Meeting: International

Congress on Environmental Modelling and Software (iEMSs 2008), peer reviewed, Barcelona, Catalonia. pp. 544–552.

U.S. Environmental Protection Agency, 2006. Wadeable Streams Assessment: A Collaborative Survey of the Nation's Streams. EPA 841-B-06-002. United States Environmental Protection Agency Office of Water. Washington, DC 20460.

Vinukollu, R.K., Wood, E.F., Ferguson, C.R., Fisher, J.B., 2011. Global estimates of evapotranspiration for climate studies using multi-sensor remote sensing data: evaluation of three process-based approaches. Remote Sensing of Environment 115, 801 – 823.

Volk, M., 2010. Scale appropriate analysis, assessment and management of landscape water and matter dynamics. Habilitationsschrift. Halle, Univ., Naturwissenschaftliche Fakultät III.

Volk, M., Arnold, J., Bosch, D., Allen, P., Green, C., 2007. Watershed configuration and simulation of landscape processes with the SWAT model, in: Oxley, L., Kulasiri, D. (Eds.), MODSIM 2007 International Congress on Modelling and Simulation, Modeling and Simulation Society of Australia and New Zealand. pp. 2383–2389.

Volk, M., Herzog, F., Schmidt, T., Geyler, S., 2001. Der Einfluss von Landnutzungsänderungen auf die Grundwasserneubildung, in: H., H., Ring, I., Herzog, F. (Eds.), Nachhaltige Wasserbewirtschaftung und Landnutzung – Methoden und Instrumente der Entscheidungsfindung und -umsetzung, Marburg, Germany. pp. 147–164.

Volk, M., Hirschfeld, J., Dehnhardt, A., Schmidt, G., Bohn, C., Liersch, S., Gassman, P.W., 2008. Integrated ecological-economic modelling of water pollution abatement management options in the Upper Ems River Basin. Ecological Economics 66, 66 – 76.

Volk, M., Liersch, S., Schmidt, G., 2009. Towards the implementation of the European Water Framework Directive? Lessons learned from water quality simulations in an agricultural watershed. Land Use Policy 26, 580 – 588.

Volk, M., Steinhardt, U., 2001. Landscape balance, in: Krönert, Rönert, R., Steinhardt, U., Volk, M. (Eds.), Landscape Balance and Landscape Assessment, Springer. pp. 163–202.

Walter, M.T., Walter, M.F., Brooks, E.S., Steenhuis, T.S., Boll, J., Weiler, K., 2000. Hydrologically sensitive areas: variable source area hydrology implications for water quality risk assessment. Journal of Soil and Water Conservation 55, 277–284.

Weber, A., Fohrer, N., Möller, D., 2001. Long-term land use changes in a mesoscale watershed due to socio-economic factors – effects on landscape structures and functions. Ecological Modelling 140, 125–140.

Wentz, E.A., Peuquet, D.J., Anderson, S., 2010. An ensemble approach to space-time interpolation. International Journal of Geographical Information Science 24, 1309–1325.

White, E.D., Easton, Z.M., Fuka, D.R., Collick, A.S., Adgo, E., McCartney, M., Awulachew, S.B., Selassie, Y.G., Steenhuis, T.S., 2011. Development and application of a physically based landscape water balance in the swat model. Hydrological Processes 25, 915–925.

White, M., Storm, D., Busteed, P., Stoodley, S., Phillips, S., 2009. Evaluating nonpoint-source critical source area contributions at the watershed scale. Journal of Environmental Quality 38, 1654–1663.

White, M., Storm, D., Busteed, P., Stoodley, S., Phillips, S., 2010. Evaluating conservation program success with Landsat and SWAT. Environmental Management 45, 1164–1174.

Wigmosta, M.S., Vail, L.W., Lettenmaier, D.P., 1994. A distributed hydrology-vegetation model for complex terrain. Water Resources Research 30, 1665–1679.

Wilkinson, G., 2005. Results and implications of a study of fifteen years of satellite image classification experiments. IEEE Transactions on Geoscience and Remote Sensing 43, 433–440.

Williams, J., Jones, C., Dyke, P., 1984. A modeling approach to determining the relationship between erosion and soil productivity. Transactions of the ASAE 27, 129–144.

Williams, J.R., 1969. Flood routing with variable travel time or variable storage coefficients. Transactions of the ASAE 12, 100–103.

Winchell, M., Srinivasan, R., Di Luzio, M., Arnold, J.G., 2010. ArcSWAT Interface for SWAT 2009 – User's Guide. Texas Agricultural Experiment Station and USDA Agricultural Research Service. Temple (Texas).

Xie, X., Zhang, D., 2010. Data assimilation for distributed hydrological catchment modeling via ensemble Kalman filter. Advances in Water Resources 33, 678 – 690.

Xue, B., Keming, M., Liu, Y., Jieyu, Z., Xiaolei, Z., 2008. Differences of ecological functions inside and outside the wetland nature reserves in Sanjiang Plain, China. Acta Ecologica Sinica 28, 620 – 626.

Yan, E., Milewski, A., Sultan, M., Abdeldayerm, A., Soliman, F., Gelil, K.A., 2010. Remote-sensing based approach to improve regional estimation of renewable water resources for sustainable development, in: US-Egypt Workshop on Space Technology and Geoinformation for Sustainable Development, Cairo, Egypt. pp. 1–7.

Young, R.A., Onstad, C.A., Bosch, D.D., Anderson, W.P., 1989. AGNPS: a nonpoint-source pollution model for evaluating agricultural watersheds. Journal of Soil and Water Conservation 44, 168–173.

Zehe, E., Becker, R., Bárdossy, A., Plate, E., 2005. Uncertainty of simulated catchment runoff response in the presence of threshold processes: role of initial soil moisture and precipitation. Journal of Hydrology 315, 183 – 202.

Acknowledgements

Declaration of Authorship

Hiermit erkläre ich, dass ich die vorliegende Dissertation, abgesehen von der Beratung durch meine Betreuer, selbständig verfasst habe und keine weiteren Quellen und Hilfsmittel als die hier angegebenen verwendet habe. Diese Arbeit hat weder ganz noch in Teilen bereits an anderer Stelle einer Prüfungskommission zur Erlangung des Doktorgrades vorgelegen. Ich erkläre, dass die vorliegende Arbeit gemäß der Grundsätze zur Sicherung guter wissenschaftlicher Praxis der Deutschen Forschungsgemeinschaft erstellt wurde.

Kiel, 5.2.2014

Hendrik Rathjens